

**A STUDY OF THE MECHANICAL PROPERTIES AND THE EQUILIBRIUM NATURE OF
THE BLEND OF THERMOTROPIC LIQUID CRYSTALLINE COPOLYESTERS**

by

Rajeev Mehta

Thesis submitted to the Faculty of the
Virginia Polytechnic Institute and State University
in partial fulfillment of the requirements for the degree of
Master Of Science
in
Chemical Engineering

APPROVED:

Donald G. Baird, Chairman

Garth L. Wilkes

Wolfgang G. Glasser

May, 1989

Blacksburg, Virginia

A STUDY OF THE MECHANICAL PROPERTIES AND THE EQUILIBRIUM NATURE OF THE BLEND OF THERMOTROPIC LIQUID CRYSTALLINE COPOLYESTERS

by

Rajeev Mehta

Donald G. Baird, Chairman

Chemical Engineering

(ABSTRACT)

This work deals with the melt blend of 60/40 PHB/PET (p-hydroxybenzoic acid and polyethylene terephthalate) and 80/20 PHB/PET copolyesters in a 50:50 weight% ratio. Specifically, the interest was to determine as to how do the mechanical properties of the injection-molded parts from the blend compare with that of 70/30 PHB/PET composition and to find out if the melt blend obtained after a single extrusion pass represents an equilibrium composition blend.

To determine the anisotropic mechanical properties, injection-molded plaques were obtained by injection-molding the blend at different temperatures. It was found that the tensile properties (tensile strength, modulus and elongation at break in the machine direction) of the blend increase with the increase in the injection-molding temperature (from 300 to 320°C) and then decrease. The flexural modulus of the injection-molded plaques (at an injection-molding temperature of 330°C) of a 50:50 blend of 60/40 PHB/PET and 80/20 PHB/PET mixed only in the injection-molded unit was 2.2×10^6 psi which is 40% higher than that reported for the 60/40 PHB/PET, 100% higher than reported for either 80/20 PHB/PET or 70/30 PHB/PET.

To determine the equilibrium nature of the blend, samples with different residence time in the extruder and the 70/30 PHB/PET samples were analyzed by means of Differential Scanning Calorimeter (DSC), Dynamic Mechanical Analysis (DMA), Thermal Mechanical Analysis (TMA), Scanning Electron Microscope (SEM) and Rheometrics Mechanical Spectrometer (RMS), and the mechanical properties of the injection-molded plaques were also determined. The DSC thermogram of the four extrusion pass blend showed multiple melting endotherms. Similar behavior was observed for a number of samples which had been annealed above the melt temperatures for different lengths of time. The formation of multiple peaks was attributed to the the incomplete

transesterification reaction in the extruder. The DMA results also indicated a substantial decrease in the melting temperatures with the increase in the number of extruder passes. A similar decrease in the melting temperatures has been reported in the literature for various polyesters undergoing transesterification reaction. The TMA results showed that the modulus versus temperature profiles (softening profiles) of one, two and three extrusion pass samples were the same but that of the four extrusion pass film was different and was closer to the softening profile of the 70/30 PHB/PET film. The softening profile of the four extrusion pass sample indicated the presence of crystallites of varying degrees of development, which corresponds well with the splitting peak phenomenon observed in the corresponding DSC thermograms. Thus, it is clear that a chemical reaction is occurring in the extruder. It is suspected that the observed decrease in the flexural properties with the increase in the number of extruder passes is due the transesterification reaction occurring in the extruder.

Transesterification studies were also carried out in a cone & plate geometry in the RMS in a no-shear (simple melt annealing) and shearing environment on a larger time scale. From a comparison of the thermal behavior of the blend (as a function of the reaction time) in different environments, it was concluded that the transesterification reaction proceeds faster in the presence of deformation such as occurs in the extruder or in a simple shear flow and with an increase in temperature.

Finally, to compare the rheological properties of the multiple extrusion pass and the 70/30 PHB/PET samples, dynamic frequency sweeps were performed in the RMS at different temperatures. At a given frequency, the complex viscosity, storage modulus and loss modulus increased with an increase in the number of extrusion passes. This increase is unexpected. A number of explanations have been proposed to account for this increase in the rheological properties.

Acknowledgements

The author wishes to express his sincere appreciation to his advisor, Professor Donald G. Baird, for his advice, criticism, understanding and encouragement in the course of this study. The use of Professor Wilkes and Professor Glasser's laboratory for part of the experimental work is greatly appreciated.

Sincere thanks go to Dr. Sun. He was always there to discuss the basic concepts. The author would like to apologize for bothering him an innumerable number of times during his lunch hour. Deep appreciation goes to Dr. Done and _____ for their help, especially in solving the problems concerned with the VM1 main frame system. Special thanks go to _____ for his help in learning the DSC instrument and to _____ for her help with the optical microscope. Also to Dr. Hao Shing for his help in taking the electron micrographs and to _____ for doing the DMA and TMA analysis. The author would also like to express his appreciation for the patience and understanding of his other colleagues -

and

Finally, the author would like to extend his deepest appreciation to his parents and his brother, _____. Though they were thousands of miles away, it is doubtful whether this work would have been completed without their encouragement and love.

Table of Contents

| | |
|--|-----------|
| 1. Introduction | 1 |
| 2. Literature review | 5 |
| 2.0 Introduction | 6 |
| 2.1 Evidence for the mesophase character of PHB/PET copolyesters | 6 |
| 2.2 Mechanical properties of PHB/PET copolyesters | 10 |
| 2.3 Thermal transitions of the PHB/PET copolyesters | 19 |
| 2.4 Interchange reactions (Transesterification) in Polyesters | 32 |
| 2.4.1 Evidence for occurrence of interchange reactions | 33 |
| 2.4.2 Kinetics of Interchange | 41 |
| 2.5 Crystallization near melt temperature | 42 |
| 2.6 Summary | 44 |
| 3. Experimental | 46 |
| 3.1 Plan of investigation | 46 |
| 3.2 Materials | 47 |
| 3.3 Sample preparation | 48 |

| | | |
|-----------|---|-----------|
| 3.3.1 | Injection molded plaques | 48 |
| 3.3.2 | Compression molded films | 48 |
| 3.3.3 | Samples for SEM and optical microscope | 49 |
| 3.4 | Processing Equipment | 50 |
| 3.4.1 | Extruder | 50 |
| 3.4.2 | Injection molder | 51 |
| 3.5 | Characterization Techniques | 51 |
| 3.5.1 | Mechanical testing | 51 |
| 3.5.2 | Differential Scanning Calorimetry (DSC) | 52 |
| 5.5.3 | Dynamic mechanical analysis (DMA) and Thermal mechanical analysis (TMA) | 56 |
| 5.5.4 | Rheometrics Mechanical Spectrometer (RMS) | 56 |
| 4. | Results and Discussion | 58 |
| 4.1 | Mechanical properties | 59 |
| 4.1.1 | Zero extrusion pass material | 59 |
| 4.1.2 | Tensile properties of the 'multiple extrusion pass' blend | 71 |
| 4.1.3 | Flexural properties of the 'multiple extrusion pass' blend | 71 |
| 4.2 | DSC results | 73 |
| 4.2.1 | Low temperature annealing results | 74 |
| 4.2.2 | Pure 60/40 PHB/PET and 80/20 PHB/PET | 77 |
| 4.2.3 | 'Multiple extrusion pass' blends and 70/30 PHB/PET | 80 |
| 4.2.4 | DSC results of the samples annealed in RMS | 89 |
| 4.2.5 | DSC results of the samples sheared in RMS | 96 |
| 4.3 | DMA and TMA results | 102 |
| 4.4 | SEM results | 106 |
| 4.5 | RMS results | 106 |
| 4.6 | Optical microscopy results | 133 |

| | |
|---|------------|
| 5. Conclusions and Recommendations | 135 |
| 5.1 Mechanical properties | 135 |
| 5.2 Equilibrium nature of the blend | 137 |
| 5.3 Recommendations | 139 |
| | |
| Bibliography | 142 |
| | |
| Appendix A. The rheological data of 'multiple extrusion pass' blends And 70/30 PHB/PET copolyester | 146 |
| | |
| Appendix B. Source listing of the Fortran Program | 159 |
| | |
| Vita | 161 |

List of Illustrations

| | | |
|------------|--|----|
| Figure 1. | Melt viscosity of PHB/PET copolyesters as a function of PHB content | 8 |
| Figure 2. | Melt viscosity of PHB/PET copolyesters as function of shear rate | 9 |
| Figure 3. | Effect of thickness on along- and across- the flow flexural modulus of 60/40 PHB/PET copolyester | 14 |
| Figure 4. | Effect of thickness on along- and across- the flow flexural strength of 60/40 PHB/PET copolyester | 15 |
| Figure 5. | Flexural modulus distribution of the liquid crystal polymer, poly(butylene terephthalate) (PBT), and glass filled PBT | 17 |
| Figure 6. | Glass transition temperatures of PHB/PET copolyesters as a function of the composition | 24 |
| Figure 7. | Melting temperatures of PHB/PET copolyesters as a function of the composition | 25 |
| Figure 8. | Simplified molecular model at (a) low levels of PHB, (b) high levels of PHB | 28 |
| Figure 9. | Phase diagram for PHB/PET copolyesters at 280°C | 29 |
| Figure 10. | Schematic of the three point bend apparatus used for the flexural tests in conjunction with the Instron mechanical tester | 53 |
| Figure 11. | Schematic of a typical DSC scan of a semicrystalline polymer | 55 |
| Figure 12. | Plot of tensile strength in the machine direction versus the injection-molding temperature for the multiple extrusion pass blends | 61 |
| Figure 13. | Plot of tensile strength in the transverse direction versus the injection-molding temperature for the multiple extrusion pass blends | 62 |
| Figure 14. | Plot of tensile modulus in the machine direction versus the injection-molding temperature for the multiple extrusion pass blends | 63 |
| Figure 15. | Plot of tensile modulus in the transverse direction versus the injection-molding temperature for the multiple extrusion pass blends | 64 |
| Figure 16. | Plot of elongation at break in the machine direction versus the injection-molding temperature for the multiple extrusion pass blends | 65 |

| | |
|---|-----|
| Figure 17. Plot of elongation at the midpoint of the maximum stress point and the break point in the transverse direction versus the injection-molding temperature for the multiple extrusion pass blends | 66 |
| Figure 18. Differential scanning calorimetric results for the one extrusion pass samples annealed at 150°C for different lengths of time | 75 |
| Figure 19. Differential Scanning Calorimetric Results For Unextruded 60 HBA/PET And Unextruded 80 HBA/PET Annealed AT T = 120 °C | 78 |
| Figure 20. Differential Scanning Calorimetric Results For Multiple Extrusion Passes Of The Blend Of 60% & 80% PHB/PET And For The Unextruded 70% HBA/PET Annealed At T = 120°C | 82 |
| Figure 21. Differential Scanning Calorimetric Results For The Multiple Extrusion Pass Blend Of 60% & 80% PHB/PET And For The Unextruded 70% HBA/PET Annealed At T = 120°C | 84 |
| Figure 22. Differential Scanning Calorimetric Results For The Multiple Extrusion Pass Blend Of 60% And 80% PHB/PET And For Unextruded 70% HBA/PET Annealed At T = 150°C | 86 |
| Figure 23. Differential Scanning Calorimetric Results For The One Extrusion Pass Samples Annealed In RMS At T = 310 °C For Different Lengths Of Time | 92 |
| Figure 24. Differential Scanning Calorimetric Results For The One Extrusion Pass Samples Annealed In RMS AT T = 300c °C For Different Lengths Of Time | 94 |
| Figure 25. Differential Scanning Calorimetric Results For The One Extrusion Pass Samples Sheared In RMS (Parallel Plate, Steady Mode, 10 1/Sec) At T = 310 °C For Different Time | 97 |
| Figure 26. Differential Scanning Calorimetric Results For The One Extrusion Pass Samples Sheared In RMS (Parallel Plate, Steady Mode, 10 1/Sec) At T = 300 °C For Different Time | 99 |
| Figure 27. Thermal Mechanical Analysis Results For The Multiple Extrusion Pass Blend And 70/30 PHB/PET Films Annealed At 120°C | 105 |
| Figure 28. SEM of the 'one extruder pass' blend | 107 |
| Figure 29. SEM of the 'two extruder pass' blend | 108 |
| Figure 30. SEM of the 'three extruder pass' blend | 109 |
| Figure 31. SEM of the 'four extruder pass' blend | 110 |
| Figure 32. SEM of the 70/30 PHB/PET composition | 111 |
| Figure 33. Strain sweep of the one extrusion pass blend at 290°C (cone & plate geometry, frequency = 10 rad/sec) | 113 |
| Figure 34. Strain sweep of the one extrusion pass blend at 290°C after the material had been subjected to a time sweep (frequency = 10 rad/sec, strain = 2%, time = 60 sec., 290°C) | 114 |

| | |
|--|-----|
| Figure 35. Frequency Sweeps Of One Extruder Pass Blend Of 60% & 80% HBA/PET AT T = 300°C (cone & plate geometry, strain = 10%, frequency = 10 rad/sec) .. | 115 |
| Figure 36. Frequency Sweeps Of two Extruder Pass Blend Of 60% & 80% HBA/PET AT T = 300°C (cone & plate geometry, strain = 10%, frequency = 10 rad/sec) .. | 116 |
| Figure 37. Frequency Sweeps Of Three Extruder Pass Blend Of 60% & 80% HBA/PET AT T = 300°C (cone & plate geometry, strain = 10%, frequency = 10 rad/sec) .. | 117 |
| Figure 38. Frequency Sweeps Of Four Extruder Pass Blend Of 60% & 80% HBA/PET AT T = 300°C (cone & plate geometry, strain = 10%, frequency = 10 rad/sec) .. | 118 |
| Figure 39. Frequency Sweeps Of 70/30 PHB/PET AT T = 300°C (cone & plate geometry, strain = 10%, frequency = 10 rad/sec) | 119 |
| Figure 40. Frequency Sweeps Of One Extruder Pass Blend Of 60% & 80% HBA/PET AT T = 290°C (cone & plate geometry, strain = 10%, frequency = 10 rad/sec) .. | 120 |
| Figure 41. Frequency Sweeps Of Two Extruder Pass Blend Of 60% & 80% HBA/PET AT T = 290°C (cone & plate geometry, strain = 10%, frequency = 10 rad/sec) .. | 121 |
| Figure 42. Frequency Sweeps Of Three Extruder Pass Blend Of 60% & 80% HBA/PET AT T = 290°C (cone & plate geometry, strain = 10%, frequency = 10 rad/sec) .. | 122 |
| Figure 43. Frequency Sweeps Of Four Extruder Pass Blend Of 60% & 80% HBA/PET AT T = 290°C (cone & plate geometry, strain = 10%, frequency = 10 rad/sec) .. | 123 |
| Figure 44. Frequency Sweeps Of 70/30 PHB/PET AT T = 290°C (cone & plate geometry, strain = 10%, frequency = 10 rad/sec) | 124 |
| Figure 45. Dynamic Viscosity Of The Multiple Extrusion Pass Blends And 70/30 PHB/PET AT T = 300°C (cone & plate geometry, strain = 10%, frequency = 10 rad/sec) | 125 |
| Figure 46. Storage Modulus Of The Multiple Extrusion Pass Blends And 70/30 PHB/PET AT T = 300°C (cone & plate geometry, strain = 10%, frequency = 10 rad/sec) | 126 |
| Figure 47. Loss Modulus Of The Multiple Extrusion Pass Blends And 70/30 PHB/PET AT T = 300°C (cone & plate geometry, strain = 10%, frequency = 10 rad/sec) .. | 127 |
| Figure 48. Dynamic Viscosity Of The Multiple Extrusion Pass Blends And 70/30 PHB/PET AT T = 290°C (cone & plate geometry, strain = 10%, frequency = 10 rad/sec) | 128 |
| Figure 49. Storage Modulus Of The Multiple Extrusion Pass Blends And 70/30 PHB/PET AT T = 290°C (cone & plate geometry, strain = 10%, frequency = 10 rad/sec) | 129 |
| Figure 50. Loss modulus Of The Multiple Extrusion Pass Blends And 70/30 PHB/PET AT T = 290°C (cone & plate geometry, strain = 10%, frequency = 10 rad /sec) | 130 |
| Figure 51. Optical Microstructure Of The 'One Extrusion Pass' blend (Magnification = 350) between the cross polars at 305°C | 134 |

List of Tables

| | | |
|-----------|---|----|
| Table 1. | Properties of injection-molded PHB/PET copolyesters (directly injection-molded bars) | 11 |
| Table 2. | Properties of injection-molded plaques of PHB/PET copolyesters | 12 |
| Table 3. | Intrinsic viscosity, glass transition, melting temperature and solubility of PHB/PET copolyesters | 21 |
| Table 4. | Ester-interchange reaction in a PET film containing 30 wt% of Bz-T-E-T-DE-T-E-T-Bz | 39 |
| Table 5. | Ester-interchange reaction in the melt | 40 |
| Table 6. | Anisotropic tensile properties of the injection-molded plaques of the 'zero extrusion pass' blend as a function of the cylinder temperature of the injection-molder | 60 |
| Table 7. | Anisotropic flexural properties of the blend as a function of the number of extrusion passes (injection-molding temperature = 330 °c) | 68 |
| Table 8. | Anisotropic flexural properties of the 'zero extrusion pass' and 'one extrusion pass' pure 60/40 PHB/PET (at 260°c) and pure 80/20 PHB/PET (at 340°c) | 70 |
| Table 9. | Anisotropic tensile properties of the blend as a function of the number of extrusion passes (injection-molding temperature = 330°c) | 72 |
| Table 10. | Differential scanning calorimetric results for the one extrusion pass samples annealed at 150°c for different lengths of time | 76 |
| Table 11. | Differential Scanning Calorimetric Results For Unextruded 60 HBA/PET And Unextruded 80 HBA/PET Annealed AT T = 120 °C | 79 |
| Table 12. | Differential Scanning Calorimetric Results For Multiple Extrusion Passes Of The Blend Of 60% & 80% PHB/PET And For The Unextruded 70% HBA/PET Annealed At T = 120°C | 83 |
| Table 13. | Differential Scanning Calorimetric Results For The Multiple Extrusion Pass Blend Of 60% & 80% PHB/PET And For The Unextruded 70% HBA/PET Annealed At T = 120°C | 85 |

| | | |
|------------|--|-----|
| Table 14. | Differential Scanning Calorimetric Results For The Multiple Extrusion Pass Blend Of 60% And 80% PHB/PET And For Unextruded 70% HBA/PET Annealed At T = 150°C. | 87 |
| Table 15. | Average residence time of the blend in the extruder as a function of the extruder speed | 90 |
| Table 16. | Differential Scanning Calorimetric Results For The One Extrusion Pass Samples Annealed In RMS At T = 310 °C For Different Lengths Of Time | 93 |
| Table 17. | Differential Scanning Calorimetric Results For The One Extrusion Pass Samples Annealed In RMS AT T = 300c °C For Different Lengths Of Time | 95 |
| Table 18. | Differential Scanning Calorimetric Results For The One Extrusion Pass Samples Sheared In RMS (Parallel Plate, Steady Mode, 10 1/Sec) At T = 310 °C For Different Time | 98 |
| Table 19. | Differential Scanning Calorimetric Results For The One Extrusion Pass Samples Sheared In RMS (Parallel Plate, Steady Mode, 10 1/Sec) At T = 300 °C For Different Time | 100 |
| Table 20. | Dynamic Mechanical Analysis Results For the Multiple Extrusion Pass Blend And The 70/30 PHB/PET Films Annealed At 120°C | 104 |
| Table A1. | Strain sweep of the one extrusion pass blend at 290°C (cone & plate geometry, frequency = 10 rad/sec) | 147 |
| Table A2. | Strain sweep of the one extrusion pass blend at 290°C after the material had been subjected to a time sweep (frequency = 10 rad/sec, strain = 2%, time = 60 sec., 290°C) | 148 |
| Table A3. | Frequency Sweeps Of One Extruder Pass Blend Of 60% & 80% HBA/PET AT T = 300°C (cone & plate geometry, strain = 10%, frequency = 10 rad/sec) ... | 149 |
| Table A4. | Frequency Sweeps Of two Extruder Pass Blend Of 60% & 80% HBA/PET AT T = 300°C (cone & plate geometry, strain = 10%, frequency = 10 rad/sec) ... | 150 |
| Table A5. | Frequency Sweeps Of Three Extruder Pass Blend Of 60% & 80% HBA/PET AT T = 300°C (cone & plate geometry, strain = 10%, frequency = 10 rad/sec) ... | 151 |
| Table A6. | Frequency Sweeps Of Four Extruder Pass Blend Of 60% & 80% HBA/PET AT T = 300°C (cone & plate geometry, strain = 10%, frequency = 10 rad/sec) ... | 152 |
| Table A7. | Frequency Sweeps Of 70/30 PHB/PET AT T = 300°C (cone & plate geometry, strain = 10%, frequency = 10 rad/sec) | 153 |
| Table A8. | Frequency Sweeps Of One Extruder Pass Blend Of 60% & 80% HBA/PET AT T = 290°C (cone & plate geometry, strain = 10%, frequency = 10 rad/sec) ... | 154 |
| Table A9. | Frequency Sweeps Of Two Extruder Pass Blend Of 60% & 80% HBA/PET AT T = 290°C (cone & plate geometry, strain = 10%, frequency = 10 rad/sec) ... | 155 |
| Table A10. | Frequency Sweeps Of Three Extruder Pass Blend Of 60% & 80% HBA/PET AT T = 290°C (cone & plate geometry, strain = 10%, frequency = 10 rad/sec) | 156 |
| Table A11. | Frequency Sweeps Of Four Extruder Pass Blend Of 60% & 80% HBA/PET AT T = 290°C (cone & plate geometry, strain = 10%, frequency = 10 rad/sec) | 157 |

| | |
|---|-----|
| Table A12. Frequency Sweeps Of 70/30 PHB/PET AT T = 290°C (cone & plate geometry, strain = 10%, frequency = 10 rad/sec) | 158 |
| Table B1. Source listing of a Fortran program which calculates the tensile properties from the raw Instron data | 160 |

1. Introduction

In recent years, a new class of polymeric materials has been developed through molecular engineering. The liquid crystalline polymers or mesomorphic polymers have a semirigid conformation, in which the chains have an inherent tendency to align along the flow direction compared to the flexible chain conformation. Perhaps the most widely studied liquid crystalline polymers in this decade are the copolyesters of p-hydroxybenzoic acid and polyethylene terephthalate (PHB/PET), the copolyesters of 60/40 PHB/PET (60 mole% p-hydroxybenzoic acid and 40 mole% polyethylene terephthalate) and 80/20 PHB/PET, in particular, have received most attention. Apart from the scientific curiosity to discern the structure of these unique polymers (which, to this day is controversial), the main interest in their study stems from their high mechanical properties, relatively high melting temperatures and their ease of processing.

The processing behavior of thermotropic liquid crystalline polymers depends on the rheological properties of the melt, the melting temperature, the degree of supercooling, and the crystallization kinetics. In this respect, both 60 and 80 mole% PHB/PET have certain advantages and limitations. For example, 60 mole% PHB/PET is known to exhibit a weak "melting point" at about 230-260°C and supercools by as much as 50-60°C (36). 80 mole% PHB/PET, on the other hand, has a "melting point" of about 300°C and supercools only about 15°C (36). This higher melting point and lower degree of supercooling limits the processing options available for the 80

mole% PHB/PET. Yet, because of the higher degree of crystallization this system has certain physical properties which are more desirable such as a higher heat distortion temperature (i.e. 154°C (1)), in contrast to 60 mole% PHB/PET which only has a heat distortion temperature of 64°C (1). Also, in contrast to 60/40 PHB/PET, blending of 80/20 HBA/PET with polyphenylene sulfide (PPS) does not result in an in-situ fibril formation (18). An interesting question then arises as to what will happen if 60 and 80 mole% PHB/PET are melt blended. The motivation for this work is based on a study done in our laboratory on the blending of 60/40 and 80/20 HBA/PET to match the rheology of PPS for the in-situ formation of reinforced thermoplastic composite (18). Once, it was observed that the rheology (i.e. degree of supercooling) of the blend is affected, we needed to know as to how does the properties of the blend compares with those of 60/40 and 80/20 PHB/PET copolyesters. Initial indications (37) were that the heat distortion temperatures of the blend improved (compared to 60/40 PHB/PET composition). There were, however, a number of questions to be answered. These were:

1. Does a single pass through the extruder give us an equilibrium composition blend?
2. How do the mechanical properties of the injection-molded parts from the blend compare with that of 70/30 PHB/PET composition.

The first objective of this study was to determine the mechanical properties of the injection-molded parts of the melt blend of 60/40 and 80/20 PHB/PET (in a 50:50 weight% ratio). The temperature at which the injection-molding is carried out is also significant. Thus, a whole spectrum of tensile and flexural properties with respect to temperature, was generated. The next logical question would be as to how this blend or its properties compares with 70 mole% PHB/PET copolyester, which has rather poor mechanical properties (1). Let us call the 70 mole% PHB/PET composition as the equilibrium composition (though, as has been pointed out later, this would not be the true equilibrium state which the blend should theoretically approach). In other words, if the blend is passed through the extruder again and again, would it approach the equilibrium composition (which represents poor properties) and if so, why? If the blend indeed approaches the equilibrium composition as a function of residence time in the extruder, how will the mechanical properties change? The search for an answer to these questions constituted the second objective

of this research. To accomplish this, the materials which had been passed through the extruder a different number of times were analyzed for the differences in their mechanical properties and in their thermal transitions, rheology and morphology. These results were then compared to those of the 70/30 PHB/PET composition.

It was suspected that this system will undergo a chemical reaction in the extruder, which might serve as a driving force to lead it towards equilibrium. The reason for this is the presence of ester bonds in both the copolyesters constituting the blend. It is widely recognized that ester bonds in polyesters undergo transesterification reaction. The possibility of the occurrence of transesterification reaction in the extruder for our system has been investigated. This would help in answering the important question as to whether melt blending of 60 & 80 mole% PHB/PET results in a simple mechanical blend or a chemically reactive blend. The residence time in the extruder is quite short (compared to the reported time periods for the completion of transesterification for other polyesters which range from an hour to a few days). Thus, it was suspected that transesterification reaction might not have occurred to an appreciable extent even for the four extrusion pass material (i.e., for the material whose residence time in the extruder is four times that of the single extrusion pass material). And for this reason, the trend in the changing of the chosen parameters (which would be expected to be sensitive to the transesterification reaction), for the materials which have been passed through the extruder different number of times, might not be very distinct. Therefore, transesterification studies were carried out outside the extruder, on a larger time-scale, in a no-shear (simple annealing above melt temperatures) and a shearing environment, to gain further insight. Additionally, an attempt was made to qualitatively predict the effect of temperature and shear on the rate of transesterification reaction in the blend.

This work has been organized in five chapters. Following the introduction, the literature review covering the mechanical properties and thermal transitions of PHB/PET copolyesters, along with a discussion of crystallization near melt temperature and the transesterification phenomenon is given in chapter 2. In chapter 3, the experimental techniques that were used to obtain measurements are described. Furthermore the limitations and the problems which arise due to the nature of the research (extremely short residence time in the extruder) in relation to the experimental tools

at our disposal, have been discussed. In chapter 4, there is a discussion of the above questions based on the experimental results in conjunction with the results of the other investigators. Finally, chapter 5 includes a summary of the conclusions and the recommendations for future work.

2. Literature review

In this chapter, a literature review of the studies which address the various aspects of PHB/PET copolyesters has been presented. Following a brief introduction about the PHB/PET copolyesters, the evidence for the mesophase character of 60/40, 70/30 and 80/20 PHB/PET copolyesters has been briefly discussed in section 2.1. In section 2.2, the mechanical properties of the injection-molded as well as those of the drawn fibers of 60/40, 70/30 and 80/20 PHB/PET compositions have been presented. The review of these studies is important for two reasons. First, since enough of the 70/30 PHB/PET composition was not available to be injection-molded, a knowledge of results from the literature, which pertains to 70/30 as well as 60/40 and 80/20 PHB/PET compositions is necessary. Second, these studies bring out some important structure - processing - property relationships for PHB/PET copolyesters. Following this, a review of the studies which deal with the thermal transitions, segmental composition uniformity and the morphology of PHB/PET copolyesters is given in section 2.3. An understanding of the crystallization behavior of these copolyesters is essential to the interpretation of the DSC thermograms of the blend. In section 2.4, the nature of the transesterification reaction has been discussed. Due to the presence of ester bonds in the 60/40 and 80/20 HBA/PET copolyesters, it was expected that this reaction will occur during extrusion. The methods of monitoring transesterification have been especially discussed in some detail. Finally, since we are interested in

the changes occurring in the melt state, the important phenomenon of crystallization near the melt temperature for the PHB/PET and some other systems have been discussed in section 2.5.

2.0 Introduction

It is widely recognized that liquid crystalline properties can be generated in a polymer by the incorporation of suitable rigid mesogenic groups into the molecule. The series of copolyesters based on poly(ethylene terephthalate)(PET) that has been copolymerized with p-acetoxybenzoic acid were prepared by Jackson and Kuhfuss (1) in 1976. When the basic PHB (p-hydroxybenzoic acid) structure is modified with PET, the ethylene glycol units introduce flexibility into the polymer chain, and the melting point is reduced. Some of these copolyesters have been shown to exhibit liquid crystallinity (1). The mesogenic group, in general, is responsible for the occurrence of liquid crystallinity and in determining the phase and the temperature range of the mesophase. The copolyesters of PHB/PET form main chain thermotropic systems. A thermotropic polymer shows liquid crystalline properties over a particular temperature range in the melt state, in contrast to a lyotropic system, where, in addition to the thermal effects, increasing the solution concentration can transform the system from an isotropic to a liquid crystalline one. A main chain liquid crystalline polymer has the mesogenic groups in the polymer backbone.

2.1 Evidence for the mesophase character of PHB/PET copolyesters

Jackson and Kuhfuss (1) reported that at or above 35 mole% PHB content, liquid crystalline order in the melt state is observed for the PHB/PET copolyesters. This was deduced from the unique low melt viscosities and the observance of opaque melts. The molten polyester as well as the pressed films were opaque when at least 35 mole % PHB was present. This can be explained on the basis of liquid crystallinity. Also, it was observed that as the HBA content in the

copolyesters increase to about 30 mole%, a reduction in melt viscosity occurs. The effect of HBA content on the melt viscosity at 275°C is shown in Fig. 1 (1). The melt viscosity increased as the HBA content in the copolyester increased to about 30 mole % and then decreased as the HBA content was increased further to 60 mole %. The higher value for 80 mole % PHB/PET is due to the fact that measurements were taken at 275°C which is lower than melting point of 80 mole % PHB/PET which is reported to be about 300°C (2,4,5,6). The effect of shear on the melt viscosities of these copolyesters at 275°C is shown in Fig. 2. As the HBA content increases the polymer becomes shear-sensitive at lower shear rates. These observations i.e. the lowering of the viscosity and the early onset of shear thinning behavior, can be explained on the basis of liquid-crystal formation. Similar results have been reported for various liquid crystalline systems (7, 8, 9, 10, 12, 13). However, it might not be fair to interpret the results in Figs. 1 & 2 to indicate that a lower viscosity is indicative of liquid crystalline order. First, we do not know if the molecular weights of the various compositions are same. Second, all the melt viscosities have been determined at 275°C even though the melting points of the various compositions of HBA/PET copolyesters are vastly different. For example, the viscosity of 60/40 PHB/PET is higher than that of 80/20 PHB/PET above about 300°C and is lower below this temperature (36).

Lastly, HBA/PET copolyesters have been shown to exhibit characteristic microstructures under cross-polarizers, which are associated with regions of local molecular alignment (11). The typical schlieren textures observed indicate the presence of dark brushes which correspond to the extinction positions of the mesophase. For the liquid crystalline polymers, it has been observed that at certain points two dark brushes meet, at other points there are four brushes meeting. These points indicate singularities i.e. disclinations in the structure. From the observation of the points at which only two dark brushes meet, the mesophase can be identified unambiguously as a nematic mesophase since these singularities occur nowhere else (67) However, it is also possible to observe the points at which four brushes meet for the nematic mesophase. Mesophase character as determined from optical microscopy has been reported by several researchers for these copolyesters (2, 3, 17, 28, 30). There is a near consensus in the literature about the type of mesomorphic transition the copolyesters of PHB/PET containing more than about 30 mole% undergoes. It is believed that

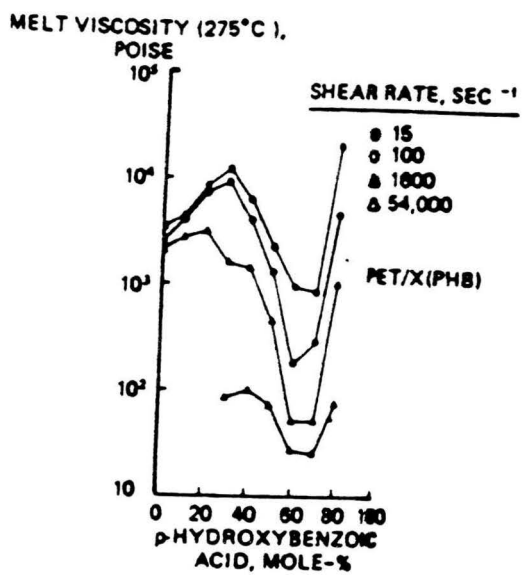


Figure 1. Melt viscosity of PHB/PET copolyesters as a function of PHB content (ref. 1)

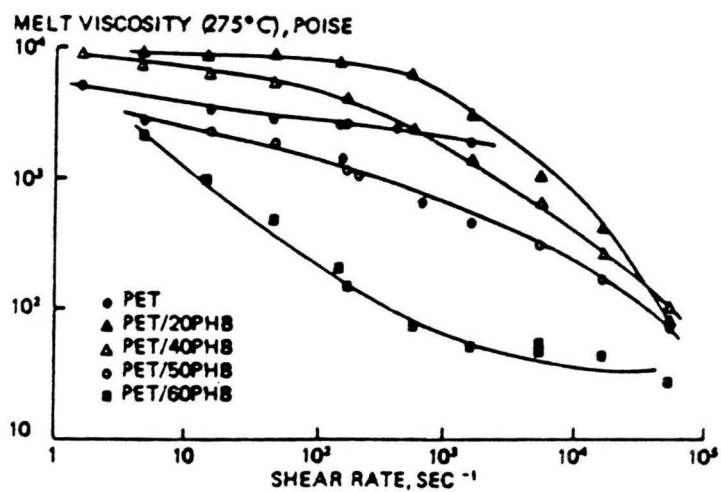


Figure 2. Melt viscosity of PHB/PET copolyesters as function of shear rate (ref. 1)

increasing the temperature leads to a semi-crystalline to nematic transition. An exception to this is the smectic texture reported for the 60 mole % PHB/PET by Viney and Windle (3). However, they also report the transition from smectic to nematic state on further increase in temperature. At still higher temperatures, the two-dimensional order of clusters of parallel molecules within the fluid is broken down and the molecules have enough energy to rotate. The fluid is then isotropic and clear. However, it is not always possible to observe the liquid crystalline state to isotropic transition because of thermal instability of the polymer at such high temperatures. Thus, this transition has never been reported for x PHB/PET where x is greater than or equal to 60 mole %. We can conclude that 60/40, 70/30 and 80/20 HBA/PET copolyesters exhibit mesophase character in the melt state. It is believed that the ability of these copolyesters to maintain a two dimensional mesophase order is responsible for their higher mechanical properties in comparison to those of pure PET. The mechanical properties of PHB/PET copolyesters are discussed in the following section.

2.2 Mechanical properties of PHB/PET copolyesters

Jackson and Kuhfuss (1) reported that mechanical properties of the injection-molded copolyesters containing 40-90 mole % PHB were highly anisotropic and dependent upon the HBA content, injection-molding temperature, and specimen thickness. Table 1 shows the effect of HBA content on a number of the properties of injection-molded copolyesters. In comparison to the PET homopolymer, the tensile strengths and flexural moduli of the PHB/PET copolyesters are significantly high. The maximum flexural modulus is shown for the 60 mole % PHB/PET. The heat deflection temperature for the compositions containing less than or equal to 70 mole % PHB is quite low compared to the value for 80/20 PHB/PET copolyester. Particularly noteworthy is the absence of mold shrinkage in compositions containing 40-80 mole % PHB.

The temperature at which the PHB copolyesters are injection-molded affects the orientation of the polymer chains and, therefore, affects the mechanical properties. The tensile strength,

Table 1. Properties of injection-molded PHB/PET copolyesters (directly injection-molded bars) (ref. 1)

| Property | PHB content, | | | | | | |
|--|--------------|--------|--------|--------|--------|--------|--------|
| | 0 | 30 | 40 | 50 | 60 | 70 | 80 |
| | | mole-% | mole-% | mole-% | mole-% | mole-% | mole-% |
| Cylinder temperature, °C | 275 | 250 | 250 | 260 | 260 | 280 | 340 |
| Tensile strength, 10 ³ psi | 8.0 | 17.0 | 28.6 | 32.5 | 33.7 | 26.1 | 34.8 |
| Elongation to break, % | 240 | 12 | 10 | 26 | 20 | 10 | 24 |
| Flexural modulus, 10 ³ psi | 3.3 | 5.8 | 11.1 | 14.1 | 18.1 | 14.5 | 14.0 |
| Izod impact strength | | | | | | | |
| Notched, ft-lb/in. | 0.3 | 1.0 | 1.2 | 1.6 | 7.8 | 2.3 | 2.2 |
| Unnotched, ft-lb/in. | 9.5 | 18.0 | 31.9 | 27.5 | 27.7 | 14.7 | 14.1 |
| Heat-deflection temperature, °C | 66 | 73 | 71 | 66 | 64 | 74 | 154 |
| Mold shrinkage, % | 0.6 | 0.1 | 0.0 | 0.0 | 0.0 | 0.0 | 0.0 |

Table 2. Properties of injection-molded plaques of PHB/PET copolyesters (ref. 1)

| Property | 40 PHB ^{a,b} | | 60 PHB ^{a,c} | | 80 PHB ^d | |
|---|-----------------------|-------------|-----------------------|-------------|---------------------|----------------|
| | Along Flow | Across Flow | Along Flow | Across Flow | Along Flow | Across Flow |
| Tensile strength, 10 ³ psi | 17.6 | 7.6 | 15.5 | 4.2 | 14.9 | 5.4 |
| Elongation, % | 2 | 5 | 8 | 10 | 12 | 28 |
| Flexural modulus, 10 ⁵ psi | 11.7 | 3.2 | 17.1 | 2.3 | 8.5 | 2.3 |
| Flexural strength, 10 ³ psi | 19.4 | 8.7 | 15.9 | 4.9 | 15.9 | 6.2 |
| Notched Izod impact strength, ft-lb/in. | 1.0 | 1.7 | 6.1 | 0.6 | 4.0 | 2.3 |
| Heat-deflection temperature, °C | 77 | 62 | 66 | 55 | — ^e | — ^e |
| Mold shrinkage, % | 0.0 | 0.7 | 0.0 | 0.3 | 0.07 | 0.8 |

^a 4 1/2 x 4 1/2 x 1/8 in. plaques, gated along one edge and injection-molded in 6-oz New Britain 175-TP machine (cylinder temperature 260°C, mold temperature 23°C), were cut into 0.5-in. wide specimens; these specimens were milled into the standard tensile bar shape for tensile measurements.

^b Inherent viscosity 0.59 before molding, 0.57 after molding.

^c Inherent viscosity 0.64 before molding, 0.61 after molding.

^d 3 x 3 x 1/8 in. plaques, gated along one edge and molded in 1-oz Newbury HV1-25T machine (cylinder temperature 340°C, mold temperature 23°C), were cut and formed into specimens as above. Melt flow 5.1 g/10 min at 325°C (0.04-in. capillary).

^e Specimens not long enough to determine this property.

elongation, stiffness, and impact strength for the 60 mole % PHB/PET tended to increase as the cylinder temperature of the injection molder was increased from 210°C to 260°C (1). However, somewhat lower level of properties were obtained when the temperature was 280°C, which was ascribed to possible loss of some orientation because of the relaxation of the polymer chains in the melt before the polymer solidified. For the 80/20 PHB/PET, the tensile strength, stiffness, impact strength, and the heat deflection temperature increased dramatically and also monotonically with the increase in the injection-molder cylinder temperature (1).

Jackson and Kuhfuss also showed that the type of injection-molding machine used to mold the copolyesters affects the mechanical properties. Also, in order to compare the "along-the-flow"(machine direction) properties with the "across-the-flow" (transverse direction) properties, the 40/60, 60/40 and 80/20 PHB/PET compositions were injection-molded and the plaques (gated along one edge) were then cut along and across the flow direction to give specimens for testing. Table 2 shows that the mechanical properties are highly anisotropic. Also significant is the fact that plaques have lower along-the-flow tensile strength, flexural moduli, and impact strength than the tensile and flexural specimen bars of the same compositions and thickness molded on the same machine. The effect of the specimen thickness on along and across-the-flow flexural modulus and flexural strength of 60% is shown in Figs. 3 & 4. The thinnest specimens had the most anisotropic properties (the stiffness and strength were highest in the machine direction and lowest in the transverse direction). These properties were almost isotropic when the thickness approached 1/2 in..

The cause of this very high anisotropy and its decrease with increase in plaque thickness may be due to the differences in the relative amounts of skin and core orientation. To explore this further, a study on end gated injection-molded plaques of the 60 mole % and 80 mole % PHB/PET copolyesters was done by Joseph et al. (14). This study indicated the presence of a highly oriented "HBA rich" skin region and a less oriented "PET rich" core region. The rationale of the proposed explanation (14) for the origin of anisotropy and its decrease with increase in the specimen thickness is as follows. A higher amount of orientation can be caused by extensional flow field that is present at the flow front during the mold filling process. This is due to the "fountain flow" process described by Tadmor (15). Also, it is recognized that the higher shear stresses generated near the

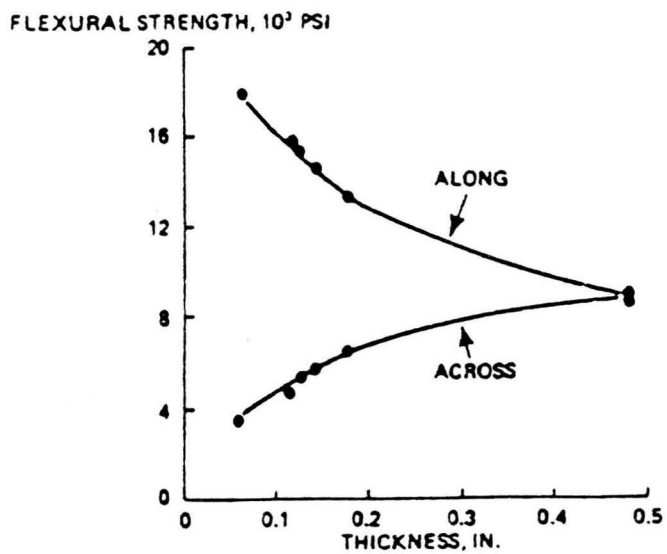


Figure 3. Effect of thickness on along- and across- the flow flexural modulus of 60/40 PHB/PET copolyester (ref. 1)

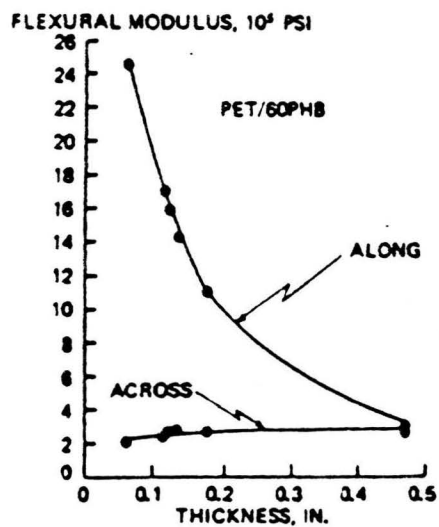


Figure 4. Effect of thickness on along- and across- the flow flexural strength of 60/40 PHB/PET copolyester (ref. 1)

mold wall and the relatively lower shear stresses present in the center of the mold may lead to the difference in skin and core orientation. Similarly, the anisotropy might arise due to greater thermal relaxation (loss of orientation) in the core region (less heat transfer). It is speculated that regions somewhat richer in HBA, and hence less viscous, will be at the flow front. This combined with the presence of extensional flow at the front due to the "fountain flow" phenomena causes the HBA rich melt to end up at the mold wall in a highly oriented state. The separation of HBA rich regions is possible because of the suspected non uniform texture (33) (HBA rich and PET rich regions) present in the melt.

The marked anisotropy of the properties has also been observed for an all aromatic copolyester of 60 mole % p-acetoxybenzoic acid, 20 mole % terephthalic acid and 20 mole % naphthalene diacetate (16). The flexural modulus of the injection molded disc was measured in different directions (Fig. 5) and it is evident that the modulus decreases significantly with the increase in the angle at which the samples are cut relative to the flow direction.

Mechanical properties of the filaments of 30/70 and 60/40 PHB/PET obtained by melt spinning at temperatures between 225 and 285°C have been studied by Acierno, La Mentia, Polizzotti, Cifferi, and Valenti (17). The 60/40 PHB/PET filaments showed the highest modulus values of 32 GPa at 225°C whereas 30/70 PHB/PET yielded a maximum modulus of the order of 3 GPa. Mesophase formation was observed at 265°C for 60/40 PHB/PET. The higher modulus value for 60 mole % extruded at lower temperatures was attributed to the presence of HBA crystals. It was suggested that the small amount of HBA crystals present at such low temperatures act as reinforcing contacts in maintaining the orientation of the chain segments not in the crystalline state. However, these results are in conflict with those reported by Jackson and Kuhfuss (1), where the modulus was reported to increase from 210 to 260°C; and also the results of a few others as discussed below.

Diametrically opposite results have been reported by Muramatsu and Krigbaum (19,20,21). Studies were carried out on two samples of 60/40 PHB/PET. The first sample was non random, and showed non-Newtonian flow behavior at all temperatures, in addition to exhibiting a thermal history effect. A similar thermal history effect has been reported for the thermotropic 60/40 PHB/PET by Viola, Done, and Baird (22), Cogswell(23) and Wissbrun(24). Also the modulus of

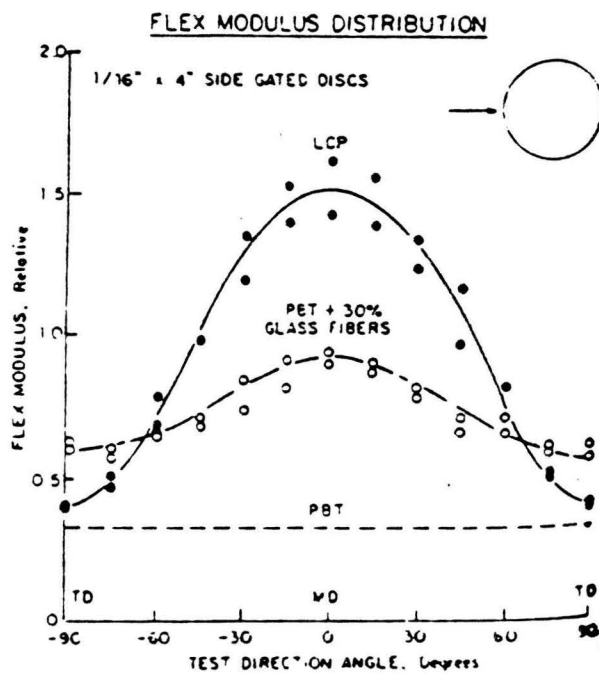


Figure 5. Flexural modulus distribution of the liquid crystal polymer, poly(butylene terephthalate) (PBT), and glass filled PBT (ref. 16)

the spun fibres increased as the spinning temperature was raised. Preheating was also found to increase the modulus values to the value expected for spinning at the higher preheating temperature. The second sample exhibited little HBA crystallinity and for this reason has been considered to be more random by the authors. However, a lower degree of HBA crystallinity might not be indicative of a more random structure. It is known that the as received samples with different histories, i.e. flakes versus pellets, will have different amount of initial crystallinity. Nothing has been said about the annealing and drying of the as received samples. The second sample showed Newtonian flow behavior above the melting temperature; the melt exhibited no thermal history effects. The modulus exhibited no dependence upon the spinning temperature. These differences (i.e., flow behavior, thermal effects, preheating effects and also DSC results) were ascribed to the lower amount of HBA crystallinity in the second sample. Specifically, the increasing of modulus with temperature and with preheating were ascribed to the melting of HBA crystallites. Additional support for this was provided when chips of the more random sample were heated for one hour at 235°C, the melt viscosity was found to increase and the modulus of the fibres decreased (the same property-temperature dependence had been observed for the more crystalline sample). Thus, even though the proposition that the two different samples of 60/40 PHB/PET had vastly different degrees of randomness is debatable, it can probably be concluded that lowering of PHB crystallinity would result in a higher modulus value.

In another study on the 60/40 PHB/PET, Sugiyama, Lewis, White, and Fellers (27) reported that the level of crystalline orientation in melt spun fibres does not vary significantly with drawdown ratio. Muramatsu and Krigbaum found in agreement with Acierno that the fiber emerging from the capillary is not well oriented and that some spin draw is essential to obtain good orientation and high modulus. They suggested that there appears to be two spinning regimes for thermotropic nematic polymers. If orientation is introduced by shear in the capillary (supplemented by the required amount of spin draw), better orientation is achieved at higher spinning temperatures. If essentially all the orientation is introduced by spin draw, which was the procedure used by Acierno, better orientation is achieved at lower spinning temperatures.

Thus, the decrease in modulus with increasing temperature for the drawn fibres as reported by Acierno is not in conflict with the increase in modulus with increasing temperature effect for the injection-molded plaques as reported by Jackson and Kuhfuss (1). We can conclude that in the case of injection molded parts, the lowering of HBA crystallinity and the increasing of the temperature of the injection-molding would result in the development of better orientation and therefore better mechanical anisotropic properties. However, increasing the temperature would not necessarily increase the properties monotonically because at some high temperature, the availability of the large thermal energy might result in the loss of orientation (due to the relaxation of the polymer chains in the melt, before solidification), as was reported for the 60/40 PHB/PET at 280°C (1).

2.3 Thermal transitions of the PHB/PET copolyesters

The thermal transitions of PHB/PET copolyesters have been studied in the last decade or so by many investigators ((1-6, 28-35, 37). In order to be able to understand the thermal transitions of PHB/PET copolyesters, it is necessary to have an understanding of their morphology and sequence lengths distribution. The conclusions in the literature are in conflict concerning :

- 1). the thermal transitions
- 2). morphology and texture, and
- 3). the segmental composition uniformity

for these polymers.

It is rather difficult to organize the literature on the basis of the above mentioned topics, since there is an obvious overlap of these topics in many studies. Thus, the literature review about the thermal transitions, morphology, and block sequence lengths of PHB/PET copolyesters has been organized in a chronological order. The earliest study of these polymers was done by Jackson and Kuhfuss (1). Based upon the ^{13}C NMR spectra, they found that the PHB has a random distribution in the copolymer. X-ray diffraction studies on 60 mole % PHB revealed very little PET or HBA crystallinity . The thermal transitions are shown in Table 3. No melting transition was ob-

served for 60 mole % PHB. No glass transition was obtained for compositions containing 55 or more mole % PHB.

Macfarlane, Nicely and Davis (28) reported that PHB/PET copolyesters containing 60 mole % or less PHB were random copolymers. Also, it was reported that compositions containing 40 % or more forms a nematic mesophase on melting. However, the polymers yielding turbid melts did not undergo a liquid crystalline to isotropic transition before decomposition.

Next came a study of thermal transitions of 30 mole % PHB by Krigbaum and Salaris (30). In the DSC thermograms, three peaks were observed. X-ray diffraction patterns revealed that only ethylene-terephthalate units crystallized. The first endotherm was attributed to the melting of PET crystals which were formed during annealing, while peak 2 was attributed to the melting of crystals which recrystallized during the heating scan. A similar multiple melting phenomenon has been reported for PET (31). Endotherm 3 was attributed to the nematic (assumed) to isotropic transition, as indicated by the formation of birefringence at about 230°C and loss of birefringence at 245°C, the latter agreeing with position of peaks in the DSC traces. Also, it was found that 30 mole % is a random copolyester.

Menczel and Wunderlich (6) studied the vitrification behavior of 60/40 PHB/PET. The solid state of flexible, linear macromolecules is commonly not at thermodynamic equilibrium. Thus, in case the heating rate is greater than the prior cooling rate, a hysteresis peak appears at the glass transition, as was observed for the homopolymer of PET. However, the 60/40 HBA/PET copolymer shows two glass transitions around 52-63°C and 152-197°C, and the first glass transition shows hysteresis. Optical studies revealed the presence of two birefringent phases in every temperature region up to 297°C (both are liquid at 297°C). One of the phases solidified (as indicated by the increased resistance to the mechanically induced movement) under the microscope at the higher transition temperature, the other at the lower transition temperature. This would mean that microphase separation occurs. It was speculated that the lower temperature refers to the terephthalate rich copolymer while the higher transition temperature relates to the p-oxybenzoate rich copolymer. A melting endotherm at 247°C was speculated to correspond to the oxybenzoate crystallites. The reasoning for this speculation was that this melting point occurs at a temperature

Table 3. Intrinsic viscosity, glass transition, melting temperature and solubility of PHB/PET copolyesters (ref. 1)

| PHB, mole-% | IV | T_g , °C | Mp, °C | Solubility ^a |
|-------------|-------|----------------|------------------|-------------------------|
| 0 | 0.60 | 69 | 245 | PTCE |
| 5 | 0.41 | 74 | 241 | PTCE |
| 10 | 0.43 | 74 | 235 | CHCl ₃ |
| 15 | 0.46 | 74 | 231 | CHCl ₃ |
| 20 | 0.50 | 77 | 230 | CHCl ₃ |
| 25 | 0.62 | 83 | 235 | CHCl ₃ |
| 30 | 0.51 | 85, 166 | 227 | CHCl ₃ |
| 35 | 0.43 | 79, 158 | 226 | CHCl ₃ |
| 40 | 0.55 | 81, 159 | 226 | CHCl ₃ |
| 50 | 0.69 | 75, 159 | 228 | PTCE |
| 55 | 0.59 | — ^c | — ^c | PTCE |
| 60 | 0.74 | — ^c | — ^c | PTCE |
| 65 | 0.68 | — ^c | — ^c | PTCE |
| 70 | 0.86 | — ^c | 268 ^d | PTCE |
| 80 | Insol | — ^c | 293 ^d | Insol |
| 90 | Insol | — ^c | — ^c | Insol |

^a If insoluble in chloroform (CHCl₃), solubility was tested in 60:40 chloroethane (PTCE).

^c None detected.

^d Very weak endotherm.

beyond the minimum in the phase diagram i.e. 245°C for pure PET (1) (polydimorphism (32) , the endotherm corresponding to PET-like crystallinity should appear at a lower temperature than the melting of PET homopolymer). Also an endotherm around 200°C was reported which has not been clearly assigned.

Meesiri, Menczel, Gaur and Wunderlich (4) conducted an extensive differential calorimetric study on the various PHB/PET copolyesters, including 60/40 and 80/20 HBA/PET compositions. They have made a distinction between their samples. The ones in the early stages of preparation are termed as non-random two phase copolymers and two glass transitions differing by about 100°C have been reported for them (since double glass transitions for 30 to 50 mole % PHB were also reported by Jackson and Kuhfuss (1), they conclude that most likely samples used in (1) were two phase polymers). However, no experimental evidence has been provided for the two phase and single phase random structure assignments in this study. The glass transition from this study (4) and in references 6 and 30, are shown in Fig. 6. The glass transition of the homogenous samples seems to be practically independent of concentration up to at least 63 mole % oxybenzoate. The higher glass transition of the two-phase samples at about 177°C, is also concentration independent, reaching down to 30 mole % PHB. Also, it was found in this study that the hysteresis of the samples cooled slowly through the glass transition remains large. Thus the earlier assumption (6) that the missing hysteresis may be due to the mesophase nature alone is not correct for this copolyester system.

In regard to the crystallization behavior, it is believed by Meesiri et al. (4) that crystallization in the analyzed samples leads to nonequilibrium states. The melting temperature and the enthalpy of fusion of the PHB/PET copolyesters containing less than 65 mole% PHB is lower than the equilibrium melting temperature (280°C) (29) and the heat of fusion (26.9 KJ/mol) (29) of PET. The nonequilibrium data generated in this work (4) and reported in earlier literature (1,6) are plotted in Fig. 7. In contrast to the constant glass transition temperature, there is a 60°C decrease in the PET melting temperature with increasing oxybenzoate content. Also, the overall crystallinity decreases. Thus, it has been suggested by Meesiri et al. (4) that either eutectic phase separation or an isodimorphism phenomenon is taking place. Complete eutectic phase separation (no mixed

crystal formation) is not taking place; a comparison with the copolymer systems of poly(ethylene terephthalate-co-sebacate) and poly(ethylene terephthalate-co-adipate) show that these two have a much larger melting-point depression (about 230°C, to the minimum melting temperature of about 37°C at about 60 mole % copolymer) (ref 29, page-301). For this reason, it has been suggested that mixed crystal formation (isodimorphism) is taking place in the polymer system. It has been suggested that the incorporation of an oxybenzoate unit terminating an ethylene terephthalate unit on the proper side in the PET crystal would lead to a significant increase in crystal size which in turn would contribute to the melting-point lowering of a non-equilibrium-crystallized random copolymer (29). However, all these conclusions have been reached simply on the basis of the observed trend in the melting transitions (Fig. 7).

No experimental support has been provided for either mixed crystal formation or the proposed explanation by which it is supposed to take place. For the 70/30 and 80/20 PHB/PET compositions, because of the much higher melting point, the crystals have been assumed to be of the polyoxybenzoate type. The nematic to isotropic transition was not observed for any composition (contrary to the one observed for 30 mole % by Krigbaum and Salari (30)). Lastly, for a 58 mole % composition, an additional endotherm at a lower temperature was also observed.

The morphology of 80 mole % PHB was investigated by Zacchariadas, Economy and Logan (2). The as received copolyesters, when examined under an optical microscope at room temperature, revealed a relatively uniform phase in which ordered regions of varying size were embedded. The polymer was found to form a nematic mesophase at about 295°C (based upon the birefringence observed under cross polarizers). The rigid aggregates were clearly visible up to about 325°C, and on further heating to 325°C, they broke down to small lamellae. At about 334°C, the lamellae were no longer visible and merged into the surrounding nematic mesophase. On further heating to 535°C, trace amounts of crystalline material still persisted in the melt. The mesophase supercooled without the reformation of the crystal aggregates. The X-ray diffraction patterns of the lamellae was found to similar to those of HBA homopolymer. DSC studies revealed an irreversible endotherm at 303°C. Since the irreversible nature of the transition is consistent with the tendency of the liquid crystal polymer to supercool, it was interpreted as a transition from a semi-crystalline state to a

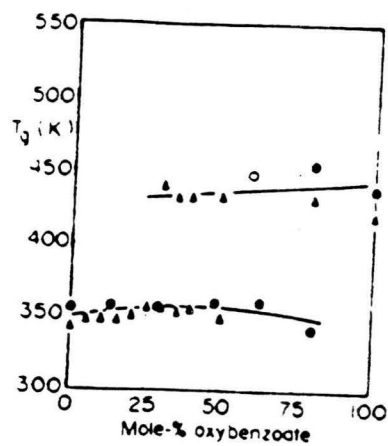


Figure 6. Glass transition temperatures of PHB/PET copolyesters as a function of the composition
 Filled circles - ref.4, open circles - ref.6, filled triangles - ref.1)
 (ref. 4)

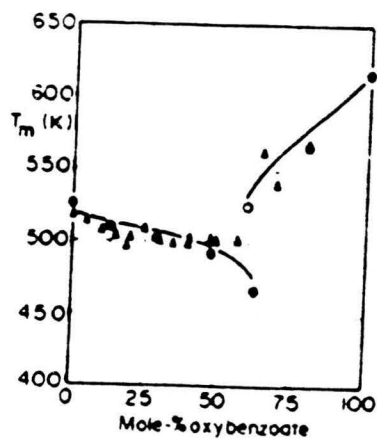


Figure 7. Melting temperatures of PHB/PET copolyesters as a function of the composition composition. Filled circles - ref. 4, open circles - ref. 6, filled triangles - ref. 30. (ref. 4)

liquid crystalline state. It was pointed out that the difference between the DSC melting peak (303°C) and the temperature of lamellar break down at 328°C observed in the optical microscope could be reconciled if the end of the endotherm rather than the peak was considered. Since a reversible endotherm is observed for the HBA homopolymer at 330-350°C and also for the melt blend of 20 % PET and 80 % PHB, it was suggested that HBA crystals present in the copolymers must be less than several percent in light of the absence of any detectable endotherm at 330°C.

Microstructure observations in 60 mole % PHB have been studied in transmitted light by Viney and Windle (3). The microstructure changes as a function of temperature between 190 and 340°C. An interrupted schlieren texture is observed which changes to regular schlieren texture above 340°C. Since the as received pellets were directly examined, the observance of mesophase texture below the melt temperature (which would imply the existence of a mesophase glass) is surprising. At 420°C, the specimen is totally isotropic and begins to degrade. DSC traces show endotherms identifiable with the onset of mobility at 190°C, the transition from smectic to nematic like textures at 340°C and the development of the isotropic phase in the range 350-420°C. Also, a glass transition is observed at 70°C, and an endothermic peak at 250°C (which does not correlate with a change either in microstructure or in mobility). It should be remarked that this is the only study in which the formation of smectic texture has been reported. All the other studies (2, 17, 28, 30) report the formation of nematic mesophase for the 60/40 PHB/PET composition.

An extensive morphological study for 30 to 80 mole % PHB was done by Joseph et al. (33). Here, a two phase morphological model (Fig. 8) has been proposed. A single phase transition has been reported for all compositions (contrary to single phase-single glass transition and two phase-double glass transition results reported by Meeriri et al. (4)). Scanning electron microscopy results on chemically etched, compression molded films showed that selective etching of PET rich regions occur. Further support regarding a heterogeneous morphology was obtained by transmission electron microscopy. Also, a hysteresis endotherm is observed near the glass transition temperature, especially for the lower compositions. The experimentally obtained crystal melting temperatures are higher than the values predicted by theory for random copolymers, in addition the melting endotherms are relatively narrow. For the first time, it was reported that both PET and HBA

crystallites are present in the 60 mole % PHB (corresponding endotherms were seen on the DSC thermograms). The melting endotherms for all compositions have been attributed to the melting of PET crystals (none is observed for 80 mole % PHB). Lastly, the X-ray studies on 60 mole % PHB films moulded at 235°C, revealed that mainly HBA crystallites are present in the sample. Similar WAXS measurements have been made by Acierno et al. (17) on the 60 mole% PHB/PET in fiber form and upon annealing at 240°C for 70 hours, a scattering pattern very similar to homopolymer HBA was obtained (which, in contrast to this study, was interpreted as the HBA crystallinity being the cause of the melting endotherm observed in the DSC scans).

In the above study microphase separation was assumed to result in a two phase morphology. A study of the sequence distributions of HBA segments in PHB/PET copolyesters, based on the proton and carbon NMR spectra of solutions of PHB/PET copolyesters, was done by Nicely, Dougherty and Renfro (34). They showed that the sequence distributions for these copolyesters can be described in terms of a probability model with a single parameter, in which HBA has a slightly greater than random chance of being bonded to another HBA unit which leads to significant deviations from the random structure at higher HBA levels in the copolymer. The measurements are consistent with the results of McFarlane, Nicely and Davis (28), but the improved sensitivity showed that a small but measurable deviation from random chain statistics does occur. The fraction of HBA bonded to another HBA could not be determined for the 80 mole % HBA because no suitable solvent could be found. However, it has been emphasized that if the same model is valid for this composition also, then the 80 mole % PHB would have even more of a tendency to exhibit long runs of HBA units than the 70 mole % HBA, which was found to be the most non-random. Proton wide-line (pulse) NMR spectra on melts showed evidence of both liquid crystalline and isotropic phases for compositions at or above 35 mole % PHB. The compositions of the isotropic and anisotropic phases have been found to contain approximately 35 and 80 mole % PHB, respectively, at 280°C. The phase diagram at 280°C has been constructed (Fig. 9).

Further, it has been argued that a qualitative explanation of the formation of the liquid crystalline phase requires significant amounts of sequences of four or more PHB units to initiate liquid crystalline phase formation. The experimentally determined fraction of HBA in the liquid crystal-

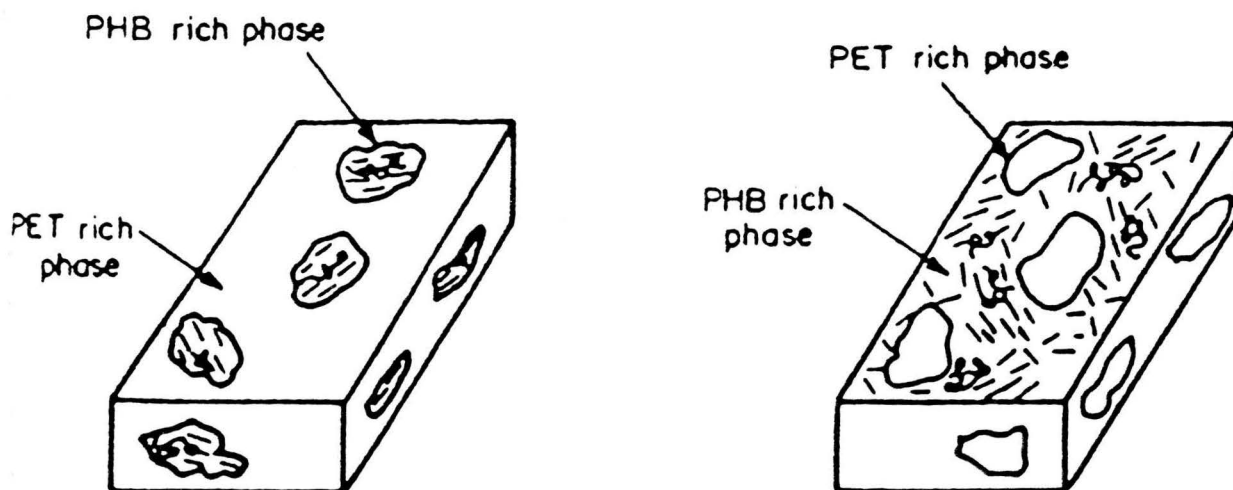


Figure 8. Simplified molecular model at (a) low levels of PHB, (b) high levels of PHB (ref. 33)

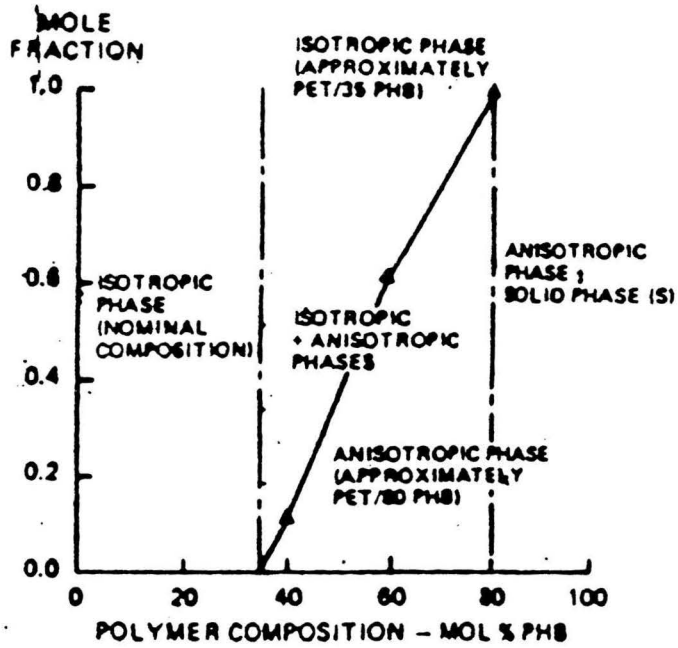


Figure 9. Phase diagram for PHB/PET copolyesters at 280°C (ref. 34)

line phase is right for all sequences with two (for 60 mole % PHB) and three (for 40 mole % PHB) or more HBA units in a row to be included in the liquid crystalline phase. Thus, it has been argued that even though longer (four or more) PHB sequences are required to initiate the liquid crystalline phase, the shorter sequences of HBA (which are experimentally observed in the liquid crystalline phase) probably partition between the isotropic and anisotropic phases.

In a very recent study of 60 mole% PHB/PET, Sun and Porter (35) suggests a dual-domain structure in both the solid and "liquid" states. It has been suggested that a non uniform sequence distribution of HBA units along the copolymer chain leads to microphase separation. The microphase-separated segments aggregate to form domains with distinct chemical compositions (chemidomains). The PET-rich domain is discontinuous and semicrystalline below the melting temperature of PET-like crystallites, while the PHB-rich domain exhibit a semicrystalline to nematic transition. Between the two glass transitions observed, the lower one has been assigned to PET rich segments and the higher one to the motions of HBA rich segments. It should be mentioned that the often observed melting endotherm in the range 230-260°C has been attributed by the authors to the combined effect of a crystalline-mesophase disordering transition in HBA-rich domains and the melting transition of PET-like crystallites.

It is clear from the the literature that the PHB/PET copolymers are two-phase systems for PHB content greater than about 30 mole %. A single glass transition at around 70°C which can be unambiguously assigned to the PET rich phase, has been reported in almost all the studies. However, there is disagreement about how the chain sequence statistics relate to the phase separation. Zachariades, Economy and Logan (2) concluded that 80 mole% PHB/ PET is a blocky copolymer with long sequences of HBA. Joseph et al. (33) concluded that the copolymers are nonrandom copolyesters. Meesiri, Menczel, Gaur, and Wunderlich (4) concluded that the polymers cannot contain long blocks of HBA unless polyesterification below the melt temperature as described by Lenz, Jin, and Feichtinger (26), is allowed to take place. Nicely, Dougherty, and Renfro (34) showed that for the compositions for which the HBA contents are below 60 mole % PHB, the deviation of the sequences from those for a random sequence is so small as to be negligible. They point out that the extended blocks of HBA are unlikely to be the reason for any unusual

properties such as domains found on etching. However, a slight preference of HBA to bond to itself has a much bigger effect at higher HBA levels, leading to a larger portion of longer sequences of HBA than a random model would predict. Thus, for the 70 and 80 mole % PHB, there is substantial non-randomness present and so they are likely to present a different case.

In contrast to the general agreement about the morphology, there is significant conflict among the reported results regarding the thermal transitions of HBA/PET copolyesters. Taking 60/40 PHB/PET as an example, with regard to the glass transition temperature; no T_g (1), a single T_g around 70°C (3, 4, 33), and even two glass transitions around 70°C and $150\text{-}190^\circ\text{C}$ (3, 4, 5, 6) have been reported. There is also disagreement with regard to the 'melting point' of this copolyester. Jackson and Kuhfuss (1) reported the absence of the melting transition. In the studies in which the melting transition was observed (3, 4, 6, 33, 35), it has been mostly assigned to the melting of PET crystallites (diluent effect). However, the X-ray studies revealed the presence of HBA crystallites. This conflict was resolved in a study by Joseph et al. (33), in which they showed that the two endotherms observed in the DSC scans (around 190 and 240°C) were due to the melting of PET and HBA crystallites, respectively. The two melting endotherms have also been observed by Menczel and Wunderlich (6) and Meesiri et al. (4). However, even though the higher endotherm was assigned to the melting of the HBA crystallites (6) and of the PET crystallites (4), no clear assignment for the lower temperature endotherm was given. Viney and Windle (3) also reported the presence of two endotherms (at 190 and 250°C), and the lower endotherm was found to correspond to the onset of mobility, as observed in the optical microscope. Sun and Porter (35) proposed the concept of individual transitions in the different 'chemidomains'. Thus, the transition around $190\text{-}200^\circ\text{C}$ was ascribed to the semicrystalline - mesophase disordering transition in the PHB rich domains and the transition around $230\text{-}260^\circ\text{C}$ was ascribed to the melting of PET crystals in the PET rich domains. From the above discussion, it is clear that our understanding of 60/40 HBA/PET is still far from perfect.

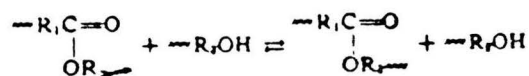
With regard to the 70/30 HBA/PET composition, Jackson and Kuhfuss (1) reported a single melting transition at 268°C . According to Meesiri et al. (4), for all composition of HBA/PET copolyesters containing more than 65 mole% HBA, it can be assumed that crystallization is due

to the oxybenzoate units. For the 80/20 PHB/PET, a single melting transition around 300°C has been reported by Zacchariadas et al. (2) and Meesiri et al. (4). It is generally accepted that this melting transition is due to the HBA crystallinity.

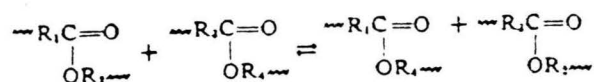
2.4 Interchange reactions (Transesterification) in Polyesters

A molecule of an addition polymer once formed by a chain reaction, is a stable macromolecule which does not normally react further with its neighbors. When a macromolecule such as a polyester has been formed by a condensation reaction, however, the ester links which have been formed in the polycondensation are still reactive, and molecules of different sizes can continue to react together in different ways. Interchange reactions in polyesters may be defined as those reactions which take place between two ester links or end groups and which lead to the formation of two identical groups. In polyesters, where chains are terminated by hydroxyl or carboxyl groups, three different types of interchange are possible.

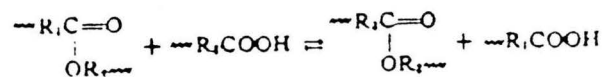
Type 1: There is an interchange between an ester group and a terminal group



Type 2: Here the interchange is between an ester group and a terminal carboxyl group-



Type 3: Involves interchange between two esters groups-



2.4.1 Evidence for occurrence of interchange reactions

First the evidence for each of the three types of interchange reactions will be briefly discussed and then the evidence which is less specific for any one of the reactions will be reviewed. The general evidence will be reviewed by discussing the various parameters i.e. melting point which are used to detect and monitor transesterification.

a. Evidence for Reactions of Type I (Ester/Hydroxyl)

Although linear polyesters other than those derived from hydrocarboxylic acids may be prepared from equivalent quantities of dibasic acid and glycol, an excess of one of the components (usually the glycol) is often used. To this end the hydroxyl ended 'monomer' formed from the acid and two moles of glycol frequently forms the starting material. The subsequent polycondensation to give polyester and free diol is a special and important form of a Type I interchange reaction, of which the first step is:

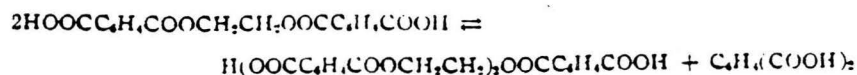


Further steps in which molecules of steadily increasing size are condensed then follow.

The reverse of above reaction is also well known. The reaction with alcohols has been used to degrade high polymers with monohydric alcohols. Flory(38) studied the kinetics of the degradation of poly(decamethylene adipate) by lauryl alcohol, while Korshak and coworkers examined the reaction of poly(hexamethylene sebacate) with cetyl alcohol(1 hexadecanol)(39) and also the reaction of poly(ethylene terephthalate) with cresol and with glycol(40). The reaction has also proved to be of commercial value in the recovery of dimethyl terephthalate from PET by reacting it with methanol(41). It is most difficult to prove that random attack by a terminal hydroxyl group of a polymer molecule on ester links of other macromolecules occurs in a similar way, for it is difficult to isolate this particular reaction. The general evidence below will suggest that this does happen, however.

b. Evidence for Reactions of Type II (Ester/Carboxyl)

The polycondensation of carboxyl-ended units with elimination of dicarboxylic acid has been found to occur (42) when the ethylene ester of *o*-phthalic acid is heated, for free acid is generated in the reaction :



as was reflected by rise of total acidity and the decline of free acid. Similarly, the carboxyl-ended ethylene diadipate undergoes slow elimination of adipic acid at 200c. and 1-2 mm. pressure, with formation of low molecular weight polyester(43). The reverse degradation of PET by adipic acid has also been shown to take place at 200c (40).

c. Evidence for Reactions of Type III (Ester/Ester)

Kursanov, Korshak and Vinogradova(44) have used an isotope exchange method to demonstrate the interchange reaction between carboxyl-ended poly(hexamethylene sebacate) of molecular weight 3400 and deuterated diethyl succinate, $\text{C}_2\text{H}_5\text{OOCCHDCHDCOOC}_2\text{H}_5$. The deuterium content of the polyester, determined by combustion to water and subsequent density determination, was such that about 30% exchange between the two compounds has taken place. A further general method for the demonstration of this type of interchange is to cause esters with no reactive hydroxyl or carboxyl endgroups to polymerize. Bis(2-acetoxyethyl) terephthalate and bis(2-benzyoxyethyl)terephthalate have been shown to polymerize at 305c to give poly(ethylene terephthalate) (60).

d. General Evidence

Further, there is unspecified evidence for the occurrence of interchange reactions. Usually it can be seen that two of the possible types are involved, but no differentiation can be made between them. The general evidence will be discussed along with the various techniques employed to monitor esterification.

1. Melting point

This is the criterion which has been used in most of the studies. It is known that the melting point of a crystallizing component in the blend is lower than the melting point of the corresponding homopolymer (diluent effect). Thus given enough time for the kinetics of crystallization to be completed, an equilibrium exists between the two phases. When a chemical reaction such as transesterification occurs this equilibrium will be disturbed and the melting point is even further lowered. For example, physical blends of poly(ethylene terephthalate) PET and a copolyester of bisphenolA-terephthaloyl-isophthaloyl (PAr) undergo transesterification when held at $T = 280^{\circ}\text{C}$ (45). The DSC melting point of PET in the blend begins to decrease after 15 minutes and, eventually, disappears after 60 min. The temperature of cold crystallization started to increase after 10 min and finally disappeared after 60 min. The glass transition temperature of PET (when miscible blends transesterify the factors determining T_g will change ,e.g., interchain versus intrachain interactions) increases and finally comes to an equilibrium value (after 10 hours), which is intermediate to that of PET and PAr. As transesterification proceeds, blends first convert to block copolymers and finally to random copolymers. Other thermodynamic quantities such as heat of fusion and heat of crystallization also decreased, correspondingly. Degradation studies ruled out significant degradation at these temperatures.

Similarly, melting point depression of poly(butylene terephthalate) PBT in the blend of PBT and PAr was found to increase with the increase in reaction time (46). An induction time of about 60 minutes was reported for this system. Additionally, the single T_g for the transesterified blends was higher than that for the physical blends. In a study done in West Germany to improve the dye uptake of PET (47), melt blends of PET and several other polyesters were held in the molten state for 3 hours. The melting point was observed to decrease with time and the rate of drop was different for each polyesters. It was concluded that during the exchange reactions block polyesters are formed initially, followed by a subsequent formation of copolyesters. The inclusion of the polyester blocks into the PET chains was also verified. After 3 hours the melting point of the reaction product was found to be same as the copolyester prepared from the respective monomers.

Also, in route to the formation of random copolymers, the formation of multiple peaks in the DSC thermogram might be observed. This theoretical possibility has been postulated by Wahrmund, Paul and Barlow (48) in their study of Bisphenol-A Polycarbonate and Polybutylene terephthalate, to explain their failure to develop a more complete phase diagram from their results. They suggest that interchange reactions in their system would, in the extreme case, result in a random copolymer that would show a single T_g (the physical blends show multiple glass transitions). In less extreme cases, such a reaction might not go to completion but would produce multiple phases, and thus either a reduction in 'melting point' or 'multiple melting points' would be observed. Transesterification in this system was later followed by Devaux, Godard and Mercier(51) and they did find that transesterification does occur. However, since they followed transesterification by NMR, the above mentioned prediction could not be verified.

In the case of liquid crystalline polymers, instead of a semicrystalline - isotropic transition, a semicrystalline - mesophase transition takes place. Since transesterification directly affects the polymer chains, it should also affect the mesophase order in the case of a liquid crystalline polymer. Paci, Barone and Pier (61) reported a progressive reduction in the enthalpy of isotropization (smectic to isotropic transition) in the blend of poly(butylene terephthalate) (PBT) and liquid crystalline poly(biphenyl - 4,4' - ylene sebacate) (PB8). This was observed when the blend was heated at 290°C for different time intervals. It was proposed that the smectic structure of the PB8 is altered because transesterification leads easily to a disruption of the chain periodicity and, therefore, of the lamellar organization of the macromolecules.

2. Molecular Weight

When two samples of poly(decamethylene adipate) were mixed (49), a drop in viscosity occurred which corresponded to a drop in weight average molecular weight, though there was no change in the number average molecular weight. It is known that a small change in the number of longer chains will cause a much larger change in the weight average molecular weight than in the number average molecular weight (63). The drop was doubtlessly caused by molecular weight equilibration brought about by the interchange reaction. Rafikov, Korshak and Chelnokova (50)

took a narrow molecular weight fraction of poly(ethylene adipate) of molecular weight 1100 which could not be fractionated further. After heating this material for 42 hr. at 170c. in a sealed tube, they obtained a product which could again be fractionated and which had a molecular weight distribution very similar to the original polyester. Thus transesterification leads to molecular weight equilibration and enables the molecular weight distribution to be re-established after a disturbance.

3. Solubility

If only one of the components of the blend is soluble in a particular solvent, then chemical association between the components can be monitored by monitoring the change in solubility with reaction time. This was done in the study of the blends of poly(butylene terephthalate)(PBT) and a copolyester of bisphenol A - terephthalaloyl - isophthaloyl (PAr) (46). In chloroform only PAr is soluble. As the reaction conditions were held constant the amount of an insoluble component of the 50/50 PAr/PBT blend increased, and finally the blend became completely insoluble. The transesterification was further confirmed by the DSC analysis.

Similarly, in a transesterification study of Bisphenol-A Polycarbonate(PC) and Polybutylene Terephthalate(PBT)(51), it was observed that at short reaction times, a sharp decrease of the solubility in methylene chloride (a good PC solvent) takes place while at longer times, a completely soluble product is obtained. This decrease and increase corresponds to the formation of block copolymer and random copolymer respectively, as was subsequently confirmed by the NMR analysis.

4. N.M.R. analysis

Since transesterification leads to a distribution of block sequence lengths and the number of blocks per chain, NMR studies can be done to determine the sequence distributions and the degree of randomness. Transesterification in PC and PBT system (51) was established by ^1H and ^{13}C NMR studies. Yamadura and Murano (62) studied the change in average sequence length and the degree of randomness, due to transesterification, for several condensation polyesters by NMR. However transesterification in a system of PBT and PAr could not be confirmed as attempted by an NMR sequence distribution study (46).

5. Drop in viscosity and Dynamic mechanical measurements

As pointed out before transesterification leads to a drop in weight average molecular weight and thus will also lead to a drop in the viscosity or intrinsic viscosity(46, 47, 49, 52). Kimura and Porter (46) attempted to find changes in the temperature dependence of E' and $\tan\delta$ for the transesterified and physical blends of PBT and PAr. No differences were observed. However, since the DSC analysis clearly showed the differences between the transesterified and physical blends, dynamic mechanical analysis might be less sensitive to the changes brought about by transesterification, than the thermal analysis.

Thus, transesterification affects the glass transition temperature, crystallization temperature, melting temperature, enthalpy of semicrystalline - mesophase transition, weight average molecular weight and its distribution, viscosity, solubility in a particular solvent and block sequence lengths of a polymer. Transesterification in any given polymer system can therefore be followed by the judicious choice of one or more of these parameters.

These parameters are, however, not the only means of monitoring transesterification. For example, Drosher and Schmidt (59) devised a novel scheme to study transesterification in PET (polyethylene terephthalate). PET films containing 30 weight% of an oligoester of the structure Bz - T - E - T - DE - T - E - T - Bz were annealed at temperatures between 200 and 300°C. Here Bz, T, E, and DE denote the benzyloxy, the terephthaloyl, the oxyethyleneoxy, and the di(oxyethylene)oxy group, respectively. The film was heated to the desired temperature and maintained there for varying amounts of time. Thereafter, the sample was quenched and stirred in chloroform to dissolve the low molecular weight material. The polymer was filtered off and its DE content was determined by ^1H NMR. Tables 4 & 5 list the annealing and reaction times, respectively, and the amount of DE units transferred. Only 12% of the DE units were transferred after annealing for 3780 minutes at 200°C, in contrast to the reaction rate at 300°C, where in only 5 minutes, 49% of the DE units were transferred from the oligoester to the polymer chain.

Table 4. Ester-interchange reaction in a PET film containing 30 wt% of Bz-T-E-T-DE-T-E-T-Bz

(ref. 59)

| temperature °C | reaction time min | yield % |
|-------------------|----------------------|------------|
| 200 | 10 | <3 |
| | 120 | <3 |
| | 3780 | 12 |
| 225 | 33 | <3 |
| | 180 | 3 |
| | 850 | 25 |

Table 5. Ester-interchange reaction in the melt

| temperature °C | reaction time min | yield % |
|-------------------|----------------------|------------|
| 250 | 7 | 4 |
| | 19 | 52 |
| | 36 | 65 |
| | 66 | 78 |
| | 122 | 88 |
| | 180 | 90 |
| | 360 | 92 |
| | 982 | 97 |
| 275 | 5 | 29 |
| | 13 | 53 |
| | 16 | 59 |
| | 33 | 87 |
| | 82 | 92 |
| | 175 | 94 |
| 300 | 5 | 49 |
| | 12 | 68 |
| | 30 | 91 |
| | 70 | 95 |

2.4.2 Kinetics of Interchange

Like any other chemical reaction, one would like to know the kinetics of transesterification reaction. However, because of the unique nature of the transesterification reaction, it is rather difficult to measure its kinetics. Kinetic studies have been predominantly concerned with the preparative polycondensation reactions. If diol and diacid are reacted at a given temperature, the rate of the increase of molecular weight can be followed by measuring the ratio of the rate of increase of viscosity or the rate of change of endgroup concentration. However, the results are very difficult to interpret because both esterification and polycondensation reactions are proceeding simultaneously. This difficulty is overcome by starting with a monomer such as bis(2-hydroxyethyl) terephthalate in which hydroxyl/ester (type I) reaction alone can increase the molecular weight. The extent of the reaction can be followed by measurements of endgroup concentrations, molecular weight, or mass of diol evolved. This reaction has been studied by many researchers (52, 53, 54, 55, 56).

Flory (38) investigated the kinetics of alcoholysis of poly(decamethylene adipate) by 1,10-decanediol and by lauryl alcohol, by measuring changes in the melt viscosity during reaction. To exclude the possibility of direct polycondensation, polymers were prepared by allowing an excess of decamethylene glycol to react with adipic acid until the viscosity became constant. By assuming that the rate of removal of the degrading alcohol was proportional to the concentration of ester links, alcohol, and catalyst, and that all ester links were equally available for attack by alcohol, Flory developed an expression for the expected change of melt viscosity with time with which the experimental results were in excellent agreement. A basic assumption in this method is that even though the hydroxyl groups at the end of polymer chains can also react with ester groups, such interpolymer interchange will not have any effect on the overall viscosity. Flory (64) also made a comparison of direct polycondensation and ester-interchange reactions, employing the same method.

In systems where all three types (also direct polycondensation) can take place, the kinetics are modelled by studying the model reactions representing the different individual reactions and then comparing the rate constants and the activation energies to determine the rate controlling reaction (51, 57). The success of this method lies in the right choice of the model reactions which are assumed to correspond to the different types of transesterification reactions in the polymer. Also, it has been found that transesterification reactions are catalysed by heavy metals, and there is a significant difference between the activation energies for the catalysed and uncatalysed reactions (58). The additives present in the polymers have been found to catalyze the transesterification reaction during the melt blending (51). Since modelling the transesterification kinetics in even a simple system is so involved, most of the transesterification studies which are carried out with the intent of determining the equilibrium nature of the polymer system, limit themselves to monitoring the extent of transesterification reactions.

2.5 Crystallization near melt temperature

In addition to the transesterification reaction, another phenomenon of crystallization near the melt temperature can place in the polyesters. Since one of the research objectives is to determine if the melt blend obtained after a single pass through the extruder would represent an equilibrium composition, any change which can possibly occur in the blend in the melt state is relevant to this work. Some studies which have reported the occurrence of crystallization near the melt temperature in PHB/PET as well as other polyester systems have been discussed in this section.

Transesterification or reorganization reactions (presumably between hydroxyl end groups and ester units of the copolymer), below the melt temperature of the copolymer, were investigated by Lenz and Schular (25) for poly(ethylene terephthalate- co - succinate). These crystallization - induced reactions were shown to result in an increase in the melting point, degree of crystallinity and blockiness. These are exactly opposite to the effects observed when the transesterification occurs in the melt state. According to the authors, these reorganization reactions were based on the

principle of crystallization induced reactions of copolymers, according to which a partially crystalline copolymer will develop an increasingly blocky structure if its repeating units can undergo interchange reactions below the melting point in such a manner that the newly placed units of the crystallizable component are taken into the crystalline regions and become inaccessible to further reaction. Thus, it would follow that these reorganization reactions will result in increase in melting point and blocky character of the copolymer only before the crystallites melt; after that the repeating units in the molten phase will be subject to randomization as they are released from the lattice and become accessible for ester-interchange.

Investigation of the crystalline-induced reactions in the melt state for liquid crystalline polymers was carried out by Lenz, Jin and Feichtinger (26). It was found that initial liquid crystalline polymers (PHB/PET and poly(3-chloro-4-oxybenzoate-co-ethylene terephthalate) formed a mixture of soluble and insoluble mixtures. The soluble fraction was found to be more randomized and the insoluble fraction was believed to be multiblock, crystalline oxybenzoate copolymers. The formation of the insoluble fraction was very slow. For 46 molar% PHB/PET, only 10% by weight of the product was present in the insoluble fraction after two weeks of reaction time. These results were interpreted as meaning that crystallization reaction is occurring, though at a very slow rate. Nothing has been said about the melting point of the soluble fraction.

The formation of high melting crystal during melt annealing has been reported for a thermotropic polymer, Vectra 900, by Lin and Winter (65, 66). It has been shown that annealing in the melt state causes a slow recrystallization of the nematic melt, as reflected in the gradual increase in the complex modulus by 3 orders of magnitude in 200 minutes. An additional higher temperature endotherm is observed in the DSC thermograms of the annealed samples, whose enthalpy change is proportional to the growth of complex modulus. It has been suggested that the crystalline solid acts as physical cross-links, tying the polymer chains together in a three-dimensional network, consequently, the moduli increase rapidly along with enthalpy change of the endotherm. If the polymer is heated to 320°C, then no significant crystallization occurs on annealing above the melting point of 280°C. However, in this case, crystallization occurs in the supercooled state which can be observed by the increase in the complex modulus by several orders of magnitude.

From these studies it is clear that annealing below the crystal-melting temperature leads to an increase in the melting point, degree of crystallinity and blockiness for many polyester systems. These effects are believed to be due to the crystallization induced reaction. Thus, above the melt temperature, this crystallization phenomenon can take place only if some residual crystallinity is present in the melt. It has been reported by Lenz and coworkers (26) that such a crystallization phenomenon does take place above the melting point for some compositions of PHB/PET copolyesters, though at an extremely slow rate. Lin and Winter (66) showed that no significant crystallization occurs on annealing above melt temperature for the samples in which all the crystallinity has been removed. Thus, it can be concluded that the phenomenon of crystallization above the melt temperature is very slow and it can occur above the melt temperature only if some residual crystallinity is present in the sample.

2.6 Summary

As discussed in the chapter 1, even though the copolyesters of PHB/PET (60/40 and 80/20 PHB/PET) have higher strength and modulus than the PET homopolymer, both the 60/40 and 80/20 PHB/PET compositions have some advantages and limitations. For example, even though the 60/40 PHB/PET copolyester have much higher mechanical properties as compared to the 80/20 PHB/PET copolyester, its heat distortion temperature is only 64°C in contrast to the 80/20 PHB/PET which has a heat distortion temperature of 154°C. An interesting question then arises as to what will happen if 60/40 and 80/20 PHB/PET copolyesters are melt blended. In fact, it was found from a study done in our laboratory that blending the matrix polymer PPS with the blend of 60/40 and 80/20 PHB/PET results in an insitu formation of reinforced thermoplastic composite. Then the interest in the blend of 60/40 and 80/20 PHB/PET grew. It was found that the heat distortion temperature of the blend of 60/40 and 80/20 PHB/PET is better than that of 60/40 PHB/PET copolyester. However, it is known that the mechanical properties of the 70/30 PHB/PET are significantly lower than those of 60/40 PHB/PET composition. Thus, it was of in-

terest to determine to compare the mechanical properties of the blend with that of 70/30 PHB/PET composition. This constituted the first objective of this work. At this point it should be mentioned that to the author's knowledge, no similar work on the blending of any two liquid crystalline polymers has been reported.

Both the liquid crystalline polymer in the blend (i.e. 60/40 PHB/PET and 80/20 PHB/PET) are copolyesters. Thus, due to the presence of ester bonds in the blend, the transesterification reaction can occur in the extruder during the melt blending. Thus, the next question which arises is whether the properties of the blend are dependent on its residence time in the extruder. The residence time in the extruder is quite short. Literature review revealed that the minimum induction time for the transesterification reaction has been reported to be about 10 minutes. However, in the extruder, in addition to the high temperatures, the blend is subjected to both shear and mixing. These additional effects might increase the transesterification rate in the extruder. Even though, studies have been done to monitor the transesterification reaction during the melt blending in a processing machine like an extruder, there exists no information about the difference in the transesterification reaction inside and outside the extrusion environment. Thus, there is a good possibility that the transesterification reaction can occur in the extruder when the blend is passed a number of times through it. Even a limited amount of reaction might significantly affect the properties. Also it is clear from the literature review that it will be quite difficult to model the kinetics of the transesterification reaction in the blend because the constitutive components of the blend are copolyesters of similar chemical structure (it will be difficult to model the individual reactions). However, we are lucky that through a large number of studies the effect of transesterification reaction on a number of polymer/blend properties is known. For example, it has been well established that the 'melting point' of the polymer system always decrease as a result of transesterification reaction. Thus, we have at our disposal the ways of identifying and monitoring the transesterification in the blend.

In addition to the transesterification reaction, another phenomenon of crystallization above the melt temperature can also result in the non-equilibrium state of the extruded blend. Thus, sufficient reasons exist to suspect that we might be dealing with a non-equilibrium system.

3. Experimental

The objective of this research was presented in the first chapter. In this chapter, an outline of the general plan to achieve these objectives is presented in section 3.1. In section 3.2, a very brief description of the materials used in this study along with the nature of the as received samples is given. A description of the sample preparation for different purposes is given in section 3.3. The processing equipment used in this study were the single screw extruder and the injection-molder. In section 3.4, a description of the equipment along with the processing conditions is given. Finally, in section 3.5, some of the characterization techniques which are used in this study are discussed.

3.1 Plan of investigation

To determine the anisotropic mechanical properties, the virgin mixture of 60/40 PHB/PET and 80/20 PHB/PET in 50:50 weight% ratio (zero extrusion pass material) was injection-molded at different temperatures. The tensile properties of the injection-molded plaques were determined in the machine and transverse directions. The flexural properties were also determined for the plaques which were obtained at the injection-molding temperature of 330°C. Unfortunately, 70/30 PHB/PET was not available in sufficient quantities for the generation of injection-molded plaques.

Thus, pure 60/40 PHB/PET and 80/20 PHB/PET compositions were injection-molded and their mechanical properties were compared with those reported in the literature. This enabled us to look at the mechanical properties of 70/30 PHB/PET which have been reported in the literature.

To determine if the blend approaches the equilibrium composition of 70/30 PHB/PET, the blend obtained after a single extrusion pass was passed through the extruder several number of times. Since transesterification reaction was expected to occur in the extruder, it was expected that the blends with different residence times in the extruder will differ from each other with regard to their thermal transitions, morphology and rheology. Thus, the multiple extruder pass samples were analyzed along with the 70/30 PHB/PET by means of the DSC, DMA, TMA, SEM and RMS, and the mechanical properties of injection-molded plaques were also determined. Since the residence time in the extruder is quite short, transesterification studies were carried out outside the extruder, on a larger time scale, in a no-shear (simple annealing) and steady-shear environment in the RMS. The samples withdrawn at different time intervals were subsequently analyzed by means of the DSC.

3.2 Materials

The 60/40 PHB/PET, 70/30 PHB/PET and 80/20 PHB/PET (p-hydroxybenzoic acid / polyethylene terephthalate) copolyesters used in this study were obtained from Tennessee Eastman company. The preparation of these polymers has been given by Jackson and Kuhfuss (1). In most of the experiments, the copolyesters were used in either the original pellet form or the films cast from the pellets (MSO No. T88 3721). The only exception was the pure 60/40 PHB/PET and pure 80/20 PHB/PET used in the injection-molding, where the copolyesters were in 'flake' form (a new batch of material, MSO No. T82 1681).

3.3 Sample preparation

3.3.1 Injection molded plaques

To determine the anisotropic mechanical properties, injection-molded plaques were obtained. For the injection-molding, a virgin mixture of 60/40 PHB/PET and 80/20 PHB/PET (zero extrusion pass material) in 50:50 weight% ratio was tumbled into the Arburg injection-molder. To minimize hydrolysis by moisture absorption, this mixture had been dried at 120°C for about 72 hours. End gated injection-molded plaques of thickness 1/12 inches were obtained. To obtain the melt blend, the virgin mixture of 60/40 PHB/PET and 80/20 PHB/PET in 50:50 wt.%, was extruded in a single screw extruder. The extrudate emerging from the circular die was immediately quenched in water and then pelletized through a pelletizer. Let us call these pellets as the 'one extrusion pass' material. These pellets were again dried at 120°C for about 72 hours and then extruded, giving a 'two extrusion pass' material. This cycle of drying and extruding was repeated to give 'three extrusion pass' and 'four extrusion pass' material. These multiple extrusion pass materials were then injection-molded to give plaques. Also, zero extrusion pass flakes and one extrusion pass pellets of pure 60/40 PHB/PET and pure 80/20 PHB/PET copolyesters were injection molded.

3.3.2 Compression molded films

Even though 'multiple extrusion pass' and 70/30 PHB/PET pellets were directly used for the DSC, SEM and RMS studies, films for these materials had to be obtained (though, thereby introducing an undesirable additional thermal and mechanical history effects) for TMA and DMA analysis. After being dried at 120°C for about three days, the pellets were compression molded into thin films using a DAKE model 44225 hydraulic press (at 310°C and 4500 kg force pressure for

seven minutes). The pellets are more desirable than the compression molded films for the characterization of multiple extruder pass blends. This is because of two reasons. First, in the case of the films, the blend spends more time in the melt state than the residence time of even the four extrusion pass material. However, the rate of transesterification reaction in the extruder versus the press might not be same. Secondly, even though all the 'multiple extrusion pass' samples are being subjected to a similar thermal and mechanical treatment during the film preparation, due to the random nature of transesterification reaction, the changes taking place in the press might be different for each film.

3.3.3 Samples for SEM and optical microscope

The dried extrudate of the multiple extrusion pass blends (which had not been chopped into small pellets) was examined through a scanning electron microscope (JEOL JSM - 35C). The samples were fractured under liquid nitrogen prior to mounting on aluminum stubs and sputtered with gold for enhanced conductivity. Electron micrographs of fracture surface normal to flow direction were taken. Hot stage optical microscopy was performed on Zeiss optical microscope that was equipped with a polarizer and analyzer. A single pellet was sandwiched between glass slides and hand pressed into a thin layer at the melt temperature. After annealing, the film was examined from room temperature to 305°C.

3.4 Processing Equipment

3.4.1 Extruder

A single screw Killion (serial number 8743F) was used for melt blending the 60/40 and 80/20 PHB/PET and also to extrude pure 60/40 PHB/PET and 80/20 PHB/PET compositions. The screw characteristics are: $L/D = 24$ (12 flights seed, 6 compression flights and 6 metering flights) and the overall compression ratio was 3:1. The surface of the screw is nickle plated and was thoroughly cleaned before each extrusion operation. For the blend, the extrusion temperature of the various heating zones, starting from the feed zone (zone 1) were: zone 1 - 200°C, zone 2 - 265°C and zone 3 - 275°C. Even though it was realized that these temperatures are too low to completely melt the HBA crystallinity, it was not possible to exceed these temperatures since the melt strength of the extrudate was already just enough for it to be fed into the pelletizer. A clamp (235°C) and a circular die (200°C) arrangement was used. The extrudate emerging from the circular die was immediately quenched in water and then pelletized through a pelletizer. A slack was maintained between the emerging extrudate and the pelletizer, so that the drawdown could be kept to a minimum. During the extrusion, the temperature of the water rose from 30°C to 38°C. The melt temperature of the blend at the end of the screw was about 290°C. The temperature setting for the extrusion of 60/40 PHB/PET were : entry zone 1 - 200°C, zone 2 - 265°C, zone 3 - 245°C, clamp - 235°C, die - 200°C. The temperature setting for the extrusion of 80/20 PHB/PET were : entry zone 1 - 230°C, zone 2 - 300°C, zone 3 - 320°C, clamp - 245°C, die - 200°C. The screw speed in all cases was between 40-50 (arbitrary units). The average residence time of the material as a function of the screw speed is given in the next chapter.

3.4.2 Injection molder

An Arburg injection-molder (serial no. 117976) was used for the injection-molding of the blend and also of the pure 60/40 and 80/20 PHB/PET compositions. A clamping force of 25 tons is available in this machine. The injection-molding was done in a semi-automatic mode. The description of the injection-molding cycle are given elsewhere (73, 74). The injection-molding conditions for the multiple extrusion pass blends and for the zero extrusion pass material were : Injection pressure = 700 psi, Holding pressure = 650 psi, Injection speed = 3.6 (arbitrary units), Screw speed = 340 rpm, Clamp closing speed = 3.6 (arbitrary units), Clamp opening speed = 3.6 (arbitrary units) and the shot size varied from 4 cm to 4.5 cm for the different injection-molding temperatures.

There are three heating zones for the extruder and one for the nozzle. The temperature of the feeding zone (zone 1) was maintained at 220°C for the multiple extrusion pass and zero extrusion pass blends. The temperature of the other two zones and the nozzle was same. This temperature was varied from 310 to 350°C to give injection-molding plaques at different 'injection-molding temperature'. The injection-molding conditions for the pure 60/40 and 80/20 PHB/PET compositions (zero and one extrusion pass) were the same except for the temperature profiles. For the 60/40 PHB/PET, the temperature profiles starting from the feed zone were : 150°C, 260°C, 260°C and 260°C. For the 80/20 PHB/PET, the temperature profiles were : 250°C, 340°C, 340°C and 340°C.

3.5 Characterization Techniques

3.5.1 Mechanical testing

Samples to be mechanically tested were obtained in both the machine and transverse directions. It is known that the mechanical properties of 60/40 and 80/20 PHB/PET copolyesters

are highly anisotropic (1). Thus it was expected that the mechanical properties of the blend would also be anisotropic and would depend on the angle at which the samples are cut relative to the flow direction. Therefore care was taken to cut the injection-molded plaques strictly in the machine and transverse direction. The cutting die which was used for generating the dog bone samples for the tensile tests corresponds to a type specified in the ASTM D 638M in the actual gauge length (1 cm) but has a much smaller total length. For the flexural tests, rectangular strips were cut from the plaques which could be loaded on the three point bend apparatus (Fig. 10).

These samples were used to generate the stress-strain curves in the Instron 1122 universal testing machine in equilibrium with the laboratory conditions. Crosshead speeds of 1 mm/min. and 2 mm/min. were used for tensile and flexural tests, respectively. These speeds were calculated by the procedure specified in ASTM D 638M and ASTM D 790 M-86, respectively. An average of five readings were taken. A computer program was written to carry out the calculations for the tensile properties (Appendix B).

3.5.2 Differential Scanning Calorimetry (DSC)

Differential scanning calorimetry is a very useful tool in the thermal analysis of the polymers. A detailed discussion about the DSC and its limitations can be found in references 68, 69 and 70. Since DSC was utilized to a significant extent in this study, few basic aspects about it are reviewed. A Perkin-Elmer DSC 4 was used in the analysis. In the DSC technique the samples and the reference materials are maintained isothermal to each other by proper application of electrical energy, as they are being heated or cooled at a linear rate. The curve obtained is a recording of heat flow, dH/dT , in mwatts or mcal/sec., as a function of temperature. A typical DSC thermogram of a semicrystalline polymer appears in Fig. 11, and some of the parameters that can be monitored, the glass transition (T_g), cold crystallization temperature (T_c), and melting temperature (T_m) are shown. Glass transition can be defined either as the inflection point at the discontinuity in specific heat at the glass transition, the intersection point of the projection of the baseline with the tangent

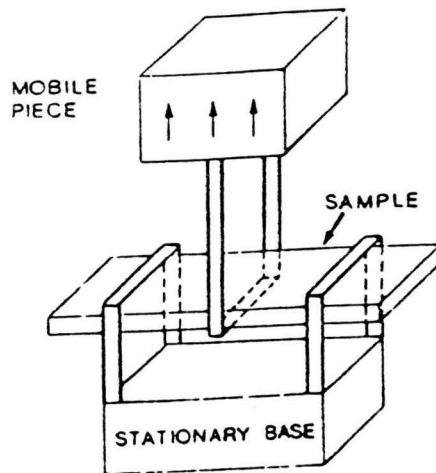


Figure 10. Schematic of the three point bend apparatus used for the flexural tests in conjunction with the Instron mechanical tester

to the discontinuity (intersection method), or the temperature corresponding to the midpoint of the discontinuity. Perkin-Elmer DSC - 4 computer determines the T_g by the last method. In the true thermodynamic sense, an endothermic curve peak is indicated by a peak in the upward direction (increase in enthalpy), while an exothermic peak is recorded in the opposite direction. The area enclosed by the DSC curve peak is directly proportional to the enthalpy change. Thus, the area under the crystallization and melting peaks represent enthalpies of crystallization and melting respectively. For a main chain liquid crystalline polymer, the melting transition shows surprisingly small heat of melting (67). In contrast to the isotropic-mesophase transition, complete supercooling to the glassy mesophase state is possible; also, the crystallization from the mesophase glass may be irreversible (67).

For the DSC analysis, the sample pellets instead of films, were used. Using the individual pellets have the disadvantage that the amount and to a lesser extent the degree of perfectness of the crystals will vary within the pellets from the same sample pool. The reason for this choice is that the differences in the residence time in the extruder for the multiple extruder pass materials is quite short. Thus, it is highly desirable that they should not spend time in the melt state. The pellets (multiple extrusion pass materials and 70/30 PHB/PET) were annealed, and transferred directly from the heating oven to the DSC pans, which were then hermetically sealed. This was done to minimize moisture absorption, which can significantly effect the results. The pans were then transferred to the DSC and were allowed to equilibrate with the room temperature for 15 minutes (the temperature of the pans drops to the room temperature in about 5 minutes). The samples were then heated from room temperature to a temperature past the melting point at a heating rate of 10 deg./minute.

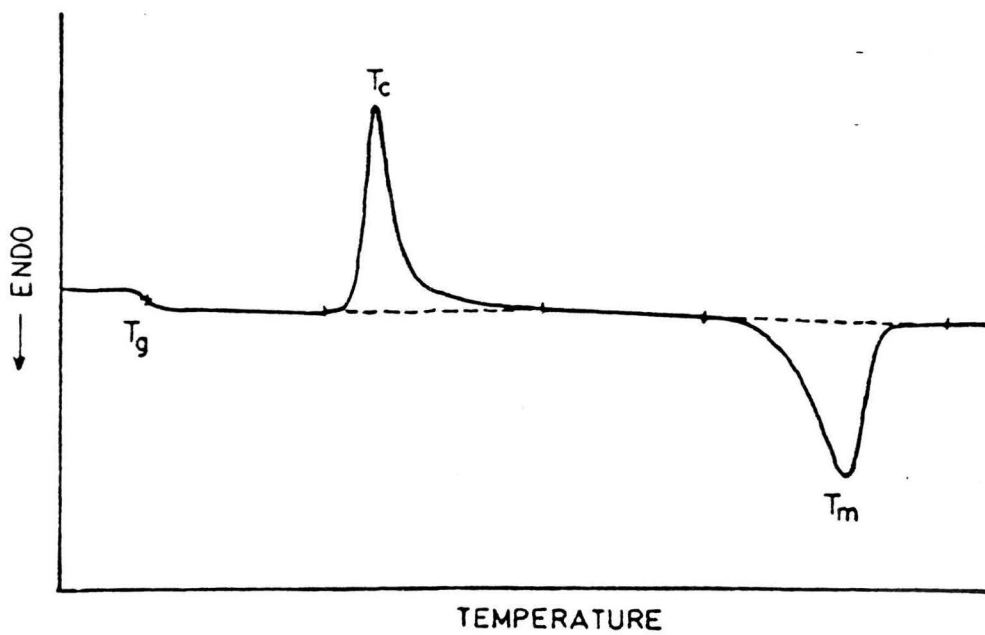


Figure 11. Schematic of a typical DSC scan of a semicrystalline polymer: (a) T_g - Glass transition temperature, (b) T_c - Crystallization temperature, (c) T_m - Melting temperature

5.5.3 Dynamic mechanical analysis (DMA) and Thermal mechanical analysis (TMA)

Dynamic mechanical analysis is a technique in which the dynamic storage modulus (E'), dynamic loss modulus (E'') and dynamic loss tangent (damping) ($\tan \delta$) of a substance is measured under oscillatory load as a function of temperature, as the substance is subjected to a controlled temperature program. The sample is oscillated at a fixed frequency (1 Hz) and an amount of energy, equal to that lost by the sample, is added on each cycle to keep the sample in oscillation at constant amplitude.

Thermal mechanical analysis is a technique in which the deformation of a substance is measured under nonoscillatory load as a function of temperature as the substance is subjected to a controlled temperature program. In this study, probe penetration mode with a loading of 10 grams was used.

5.5.4 Rheometrics Mechanical Spectrometer (RMS)

The rheological properties of the multiple extrusion extrusion pass and 70/30 PHB/PET pellets in shear flow were measured using a Rheometric Mechanical Spectrometer (RMS 605) (71, 72). The RMS can be used as a rotary rheometer with a pair of cone & plate and parallel plate geometries, which can be operated in either dynamic or steady mode. The bottom plate is driven by a motor and the top plate is connected to a transducer which measures the torque. From the deformation history and stress, the RMS computer directly outputs the rheological properties using a second order fluid constitutive equation. The rheological properties of the dried samples in a nitrogen atmosphere were measured at 290 and 300°C. A cone and plate arrangement (which has the advantage of having the constant shear rate throughout the gap) with a plate radius of 12.5 mm and a cone angle of 0.1 radian was used in the dynamic mode at a strain of 10%.

For the annealing (no-shear) studies, one extrusion pass pellets were heated in RMS to the desired temperature (300 and 310°C). Samples were withdrawn at different time intervals and quenched in water (to freeze in the changes which might have been brought about by the transesterification reaction). These on subsequent drying and annealing were examined through DSC. To study the effect of shear on the transesterification reaction, the one extrusion pass pellets were sheared in a cone & plate geometry in steady mode (at 300 and 310°C, shear rate = 10 1/sec). After quenching and drying, the sheared products were analyzed by means of the DSC.

4. Results and Discussion

The general plan of investigation to achieve the research objectives mentioned in Chapter 1 was outlined in the previous chapter. The experimental results in conjunction with the results of the other investigators are been discussed in this chapter. The results of mechanical properties which pertain to the first research objectives are discussed in section 4.1. In this section, the mechanical properties of the 'zero extrusion pass, as well as 'multiple extrusion pass' blends along with those of pure 60/40 and 80/20 PHB/PET compositions are discussed. Following this the results which pertain to the equilibrium nature of the blend are discussed. In section 4.2, the DSC results are discussed. In this section, the results are presented in the order : low temperature annealing results, pure 60/40 and 80/20 PHB/PET results, multiple extrusion pass blends and 70/30 PHB/PET results, melt annealing results, and the results of the blend sheared in the RMS. In section 4.3, the DMA and TMA results of the multiple extrusion pass blends and 70/30 PHB/PET are discussed. This is followed by a discussion of the SEM results in section 4.5 and of the RMS results in section 4.5. Finally, the results of the optical microscopy which pertains to the mesophase character of the blends are discussed in section 4.6.

4.1 Mechanical properties

To determine the anisotropic mechanical properties of the 'zero extrusion pass' and multiple extrusion pass' blend, plaques gated along one edge were injection-molded and then cut along and across the flow direction. Since it is known that the angle at which the samples are cut relative to the flow direction can significantly affect the mechanical properties (16), care was taken to cut the samples strictly in the machine and transverse direction.

4.1.1 Zero extrusion pass material

Since the temperature at which injection-molding is carried out significantly affects the mechanical properties, the virgin mixture of 60/40 PHB/PET and 80/20 PHB/PET in a 50:50 weight ratio (zero extrusion pass) was injection-molded at temperatures ranging from 300 to 350°C. The tensile modulus, strength and elongation at break are listed in Table 6. The standard deviations of the properties are given in the parenthesis. A plot of property versus temperature shows an interesting maximum (in the machine direction) and a minimum (in the transverse direction), for most of the properties. Tensile strength in the machine direction shows a maxima of 120 MPa at 320°C (Fig. 12). In the transverse direction, a minima is observed at 330°C (Fig. 13), but all the values are within ± 5 MPa. Also the strength in the transverse direction is only 1/3 to 1/4 of that in the machine direction. A maximum in the tensile modulus (m.d) is observed at 320°C of 2765 MPa (Fig. 14). Again the values of tensile modulus in the transverse direction are very close to each other (Fig. 15). Elongation at break (m.d) shows a maxima at 320°C of about 8 % (Fig. 16). Samples which were cut in the transverse direction did not break at the maximum stress point. Also, it was clear from visual inspection that the samples were not 'yielding'. Thus, the elongation at the midpoint of the break point and maximum stress point was calculated (Fig. 17).

Table 6. Anisotropic tensile properties of the injection-molded plaques of the 'zero extrusion pass' blend as a function of the cylinder temperature of the injection-molder

| Material | | Zero extruder pass | | | | | |
|---------------------------|--|--------------------|------------|------------|------------|------------|------------|
| | | 300 | 310 | 320 | 330 | 340 | 350 |
| Cylinder Temperature °C | | | | | | | |
| Property | | | | | | | |
| 1. Tensile strength | | | | | | | |
| Machine Direction | | | | | | | |
| MPa | | 81.6(9.0) | 110.2(6.4) | 120.5(6.5) | 111.1(5.2) | 101.9(6.1) | 82.9(12.0) |
| 10 ³ psi | | 11.8(1.3) | 16.0(0.9) | 17.5(0.9) | 16.1(0.8) | 14.8(0.9) | 12.0(1.2) |
| Transverse Direction | | | | | | | |
| MPa | | 25.6(2.5) | 23.3(0.9) | 22.1(1.4) | 21.3(0.5) | 23.9(2.1) | 23.8(1.1) |
| 10 ³ psi | | 3.7(0.3) | 3.4(0.1) | 3.2(0.2) | 3.1(0.1) | 3.5(0.2) | 3.5(0.2) |
| 2. Tensile modulus | | | | | | | |
| Machine Direction | | | | | | | |
| MPa | | 2191(400) | 2653(146) | 2766(155) | 2643(248) | 2465(79) | 2436(282) |
| 10 ⁵ psi | | 3.2(0.6) | 3.8(0.2) | 4.0(0.2) | 3.8(0.4) | 3.6(0.1) | 3.5(0.4) |
| Transverse Direction | | | | | | | |
| MPa | | 1048(128) | 911(87) | 932(52) | 852(120) | 882(224) | 802(43) |
| 10 ⁵ psi | | 1.5(0.2) | 1.3(0.1) | 1.4(0.8) | 1.2(0.2) | 1.3(0.3) | 1.2(0.1) |
| 3. Elongation(percentage) | | | | | | | |
| Machine Direction | | | | | | | |
| | | 5.7(0.6) | 6.2(0.4) | 7.7(1.4) | 7.1(0.6) | 6.2(0.2) | 5.1(0.4) |
| Transverse Direction | | | | | | | |
| | | 6.3(1.4) | 13.9(2.6) | 14.0(2.3) | 10.4(1.6) | 7.5(1.7) | 6.1(1.0) |

TENSILE STRENGTH (ALONG THE FLOW DIR)

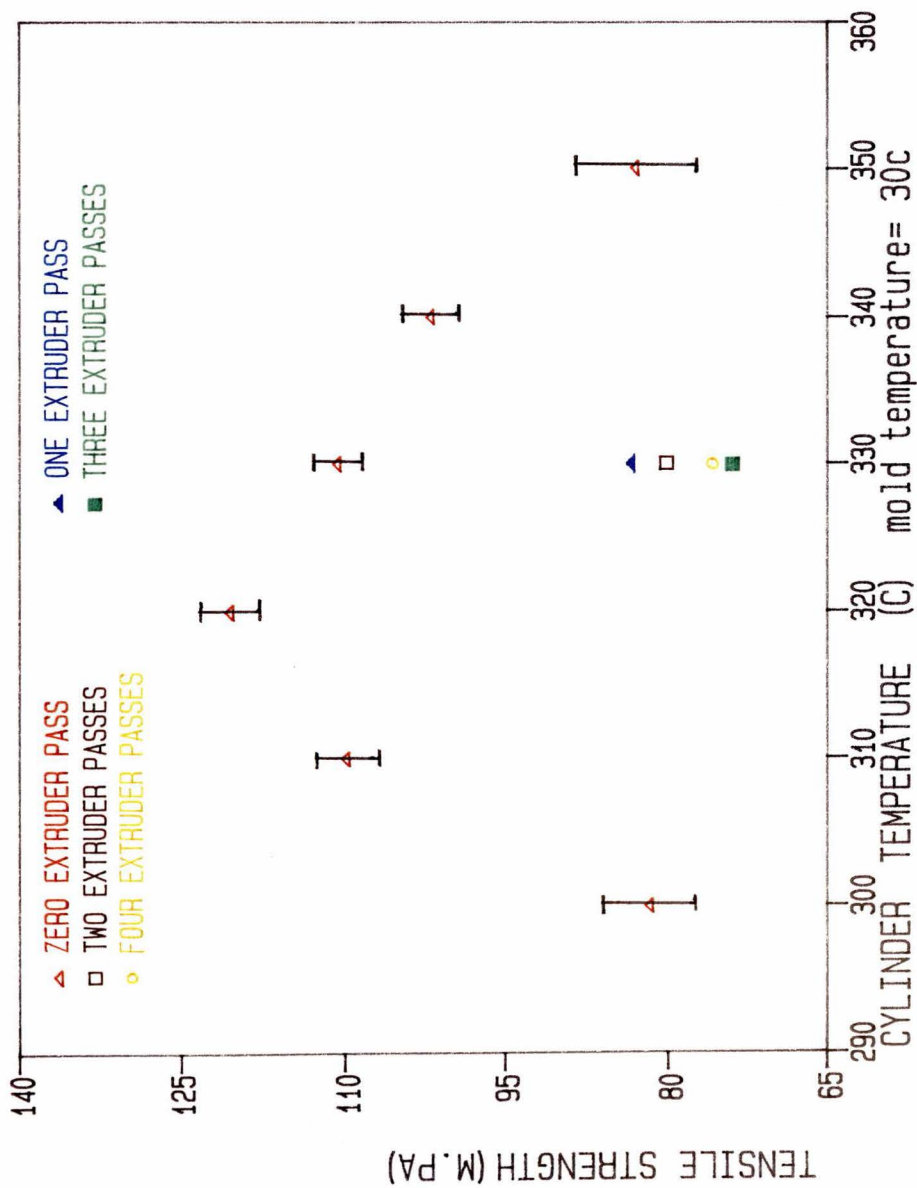


Figure 12. Plot of tensile strength in the machine direction versus the injection-molding temperature for the multiple extrusion pass blends

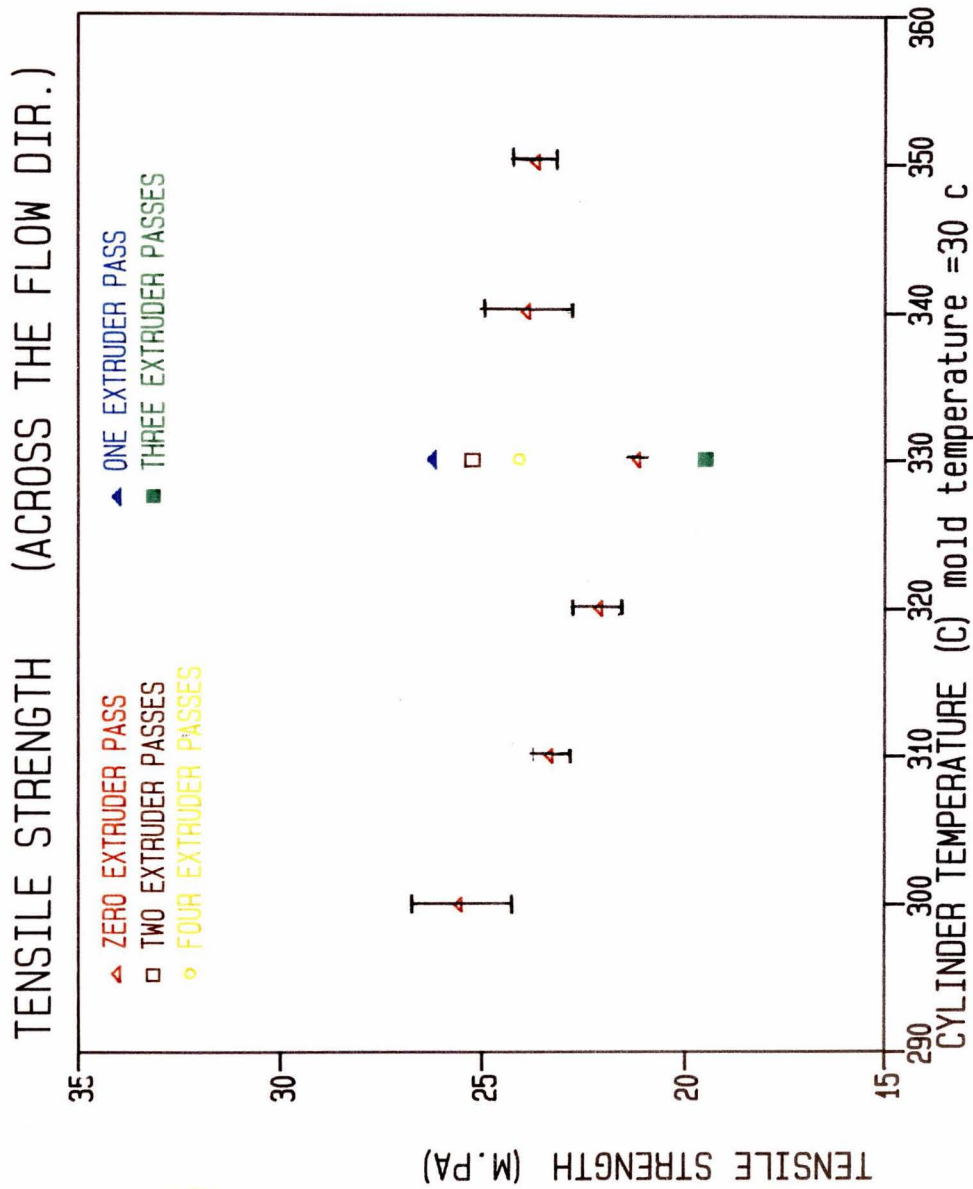


Figure 13. Plot of tensile strength in the transverse direction versus the injection-molding temperature for the multiple extrusion pass blends

TENSILE MODULUS (ALONG THE FLOW DIR)

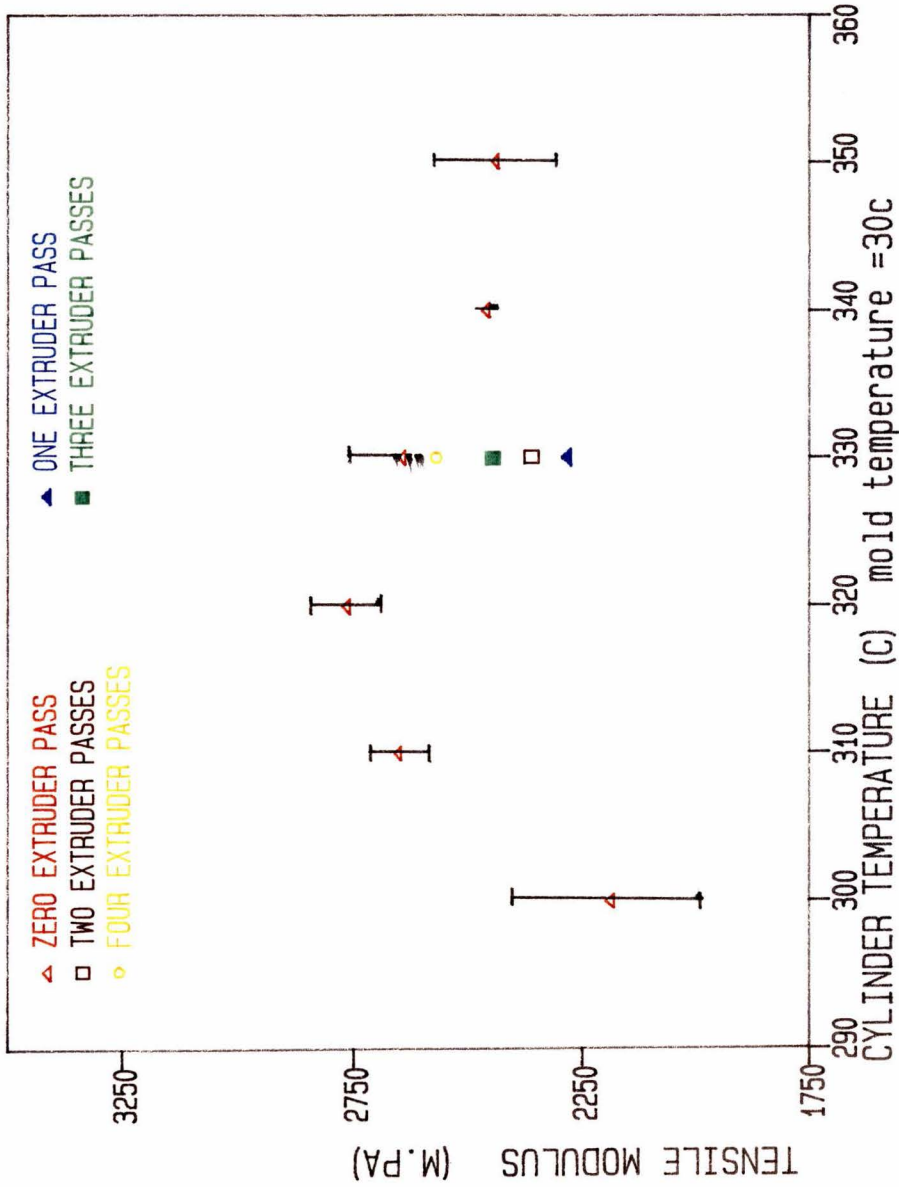


Figure 14. Plot of tensile modulus in the machine direction versus the injection-molding temperature for the multiple extrusion pass blends

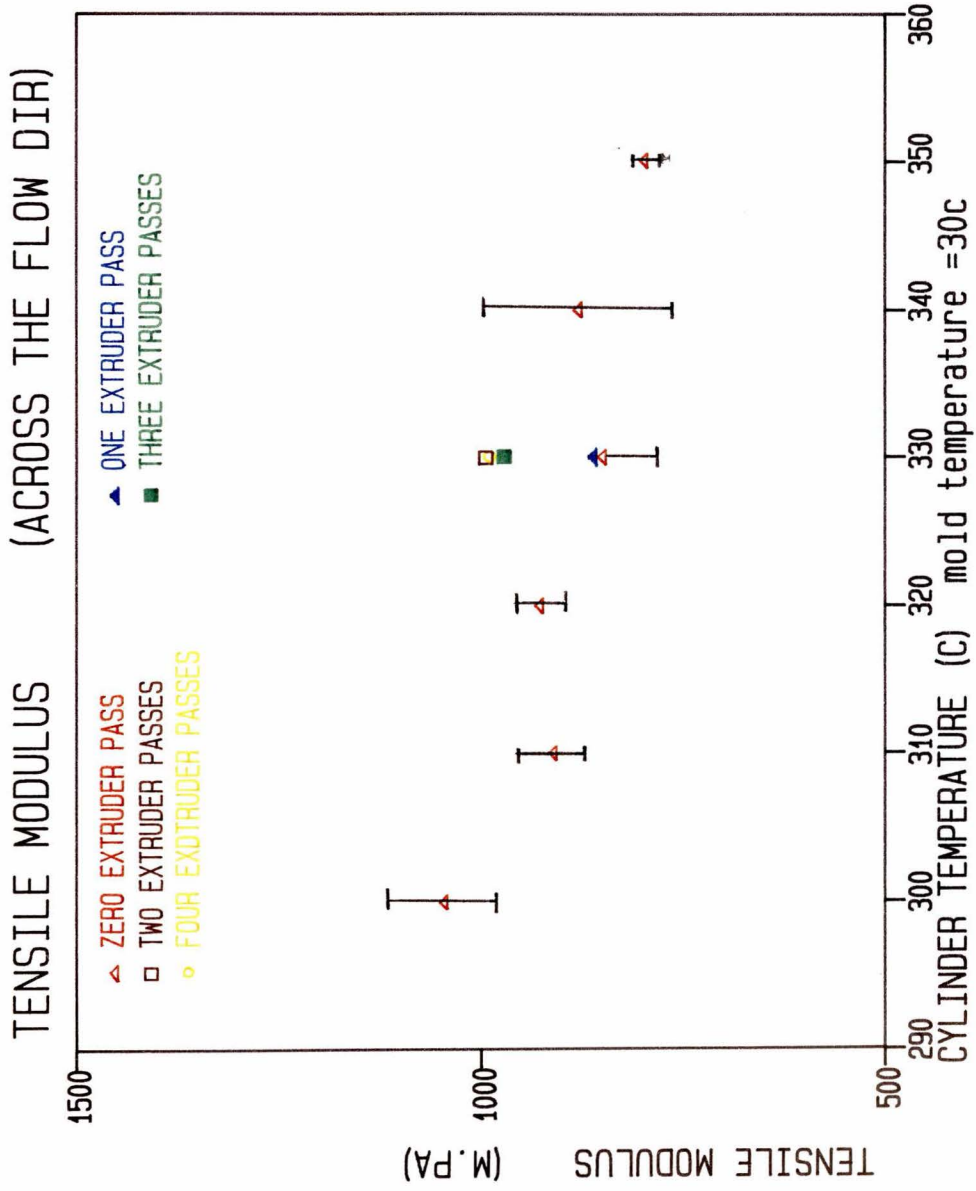


Figure 15. Plot of tensile modulus in the transverse direction versus the injection-molding temperature for the multiple extrusion pass blends

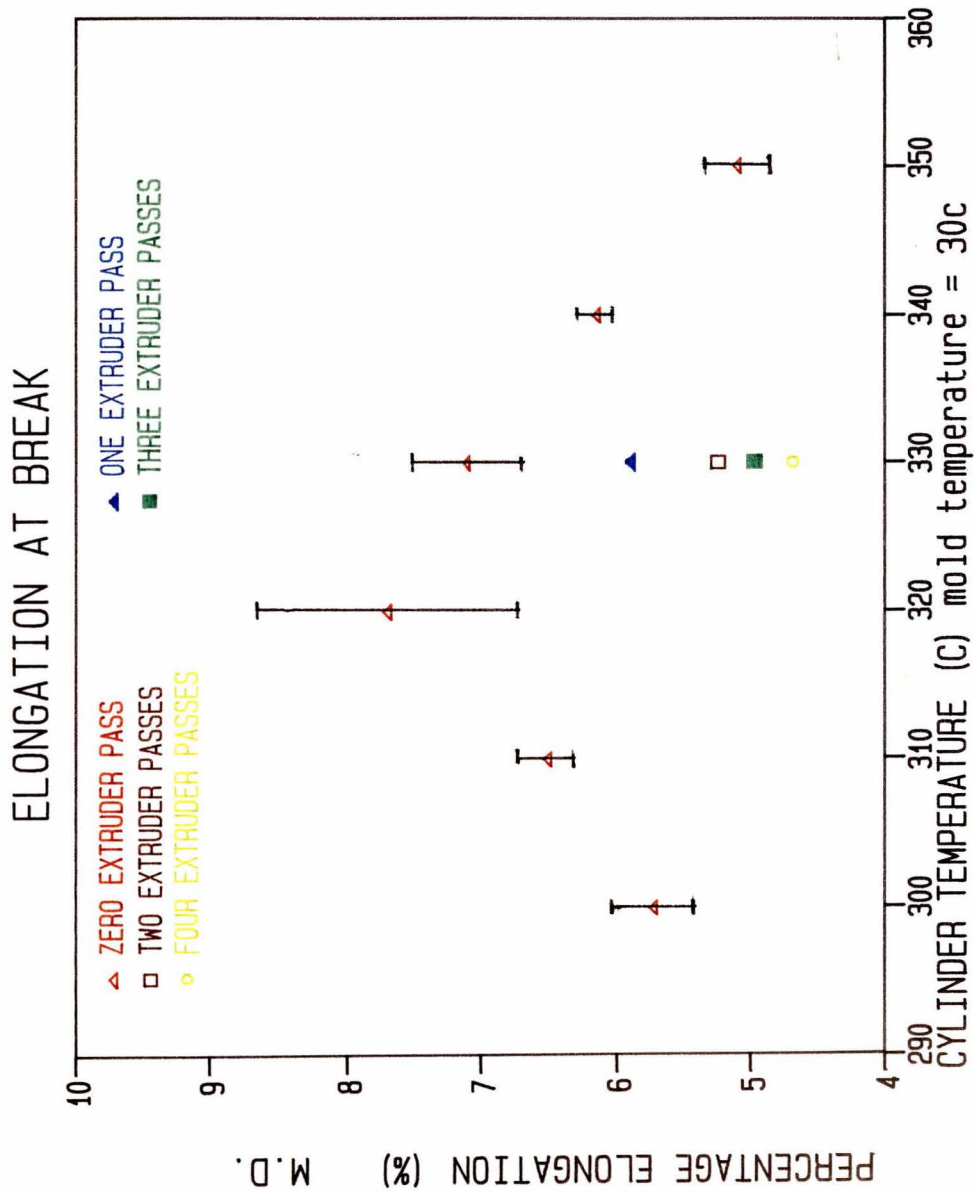


Figure 16. Plot of elongation at break in the machine direction versus the injection-molding temperature for the multiple extrusion pass blends

Elongation at midpoint of break pt & max stress pt

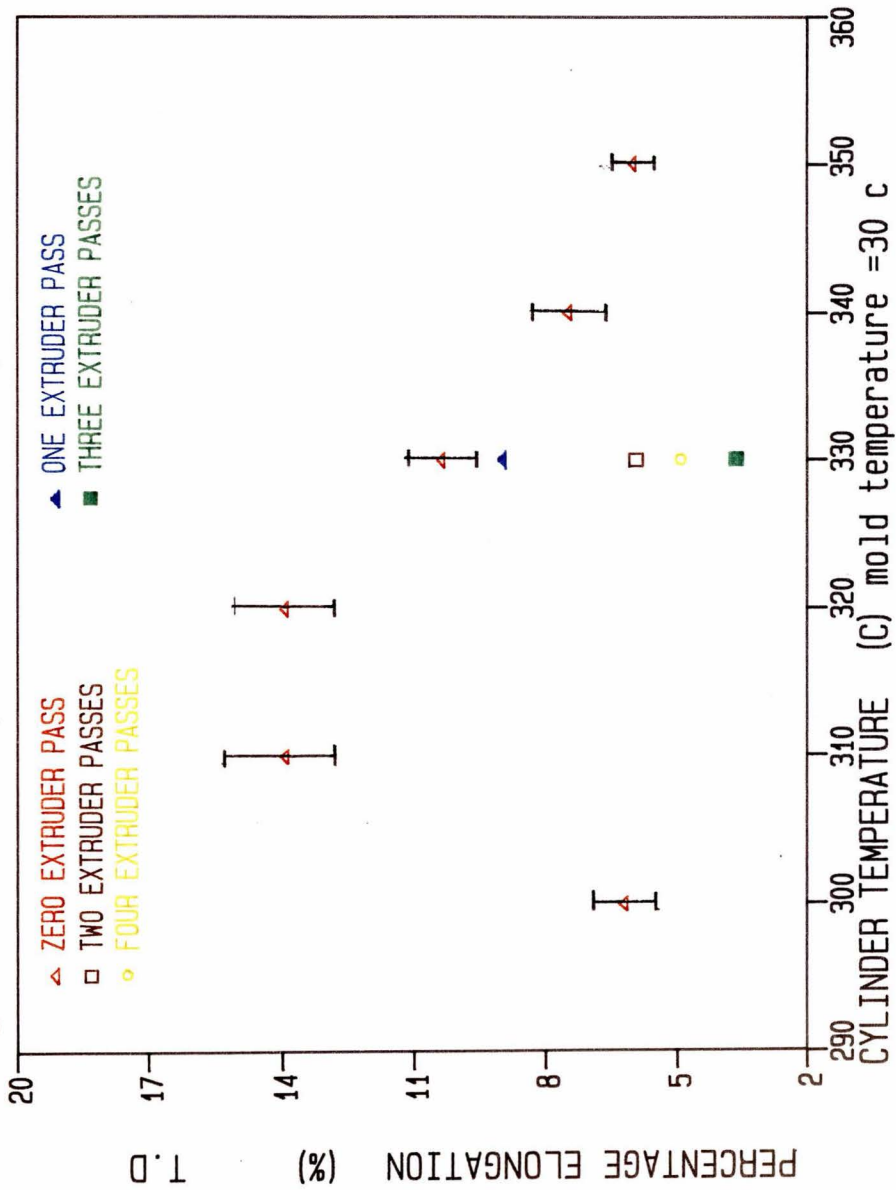


Figure 17. Plot of elongation at the midpoint of the maximum stress point and the break point in the transverse direction versus the injection-molding temperature for the multiple extrusion pass blends

Flexural strength and modulus were determined for the plaques which were obtained at the injection-molding temperature of 330°C. The zero extrusion pass blend shows a very high modulus (2.2 million psi) and strength (19600 psi) in the machine direction. These are shown in Table 7 along with the results for multiple extrusion pass samples for comparison, which will be discussed later. The flexural modulus in the transverse direction is only about 1/4 of that in the machine direction and the flexural strength in the transverse direction is only about 1/10 of that in the machine direction. Thus the flexural properties are also highly anisotropic. Similar anisotropy in the mechanical properties was reported by Jackson and Kuhfuss (1) for 60/40 and 80/20 PHB/PET compositions. The flexural modulus in the transverse direction for 60/40 and 80/20 PHB/PET compositions was only about 1/7 and 1/4, respectively, of that in the machine direction. The flexural strength in the transverse direction for both 60/40 and 80/20 PHB/PET was about 1/3 of that in the machine direction. However, there is a significant difference between the tensile and the flexural properties. This difference might be due to the possible presence of a highly oriented skin layer which would effect the flexural properties to a greater extent as compared to the tensile properties, which are a measure of the average properties of the cross-section of the sample. The existence of a skin layer in the injection-molded parts of 60/40 and 80/20 PHB/PET copolyesters has been reported by reported by Joseph et al. (14).

Unfortunately, enough of 70/30 PHB/PET was not available for injection-molding. No data has been reported in the literature concerning the mechanical properties of the injection-molded 'plaques' of 70/30 PHB/PET composition. However, Jackson and Kuhfuss (1) have reported the mechanical properties of the injection-molded tensile and flexural bars of 70/30 PHB/PET (Table 1, Chapter 2)) (values obtained from directly in injection-molded specimens would be higher than those for the plaques of the same thickness as can be seen by comparing the properties of 'plaques' versus 'directly injection-molded bars' of 60/40 and 80/20 PHB/PET compositions (Table 2 versus Table 1, Chapter 2)).

Additionally, the type of injection-molding machine, the thickness of the injection-molded parts and the injection-molding temperature also affects the results. The thickness of the plaques of 70/30 PHB/PET used by Jackson and Kuhfuss (1) was about 1/8 inches. The thickness of the

Table 7. Anisotropic flexural properties of the blend as a function of the number of extrusion passes (injection-molding temperature = 330 °c)

| Material | Zero Extrusion Pass | One Extrusion Pass | Two Extrusion Pass | Three Extrusion Pass | Four Extrusion Pass |
|----------------------|---------------------|--------------------|--------------------|----------------------|---------------------|
| Property | | | | | |
| 1. Flexural Modulus | | | | | |
| Machine Direction | 15781(1364) | 14646(1301) | 10750(946) | 10318(987) | 8847(56) |
| MPa | 22.8(2.0) | 21.2(1.9) | 15.6(1.4) | 14.9(1.4) | 12.8(1.8) |
| 10 ⁵ psi | | | | | |
| Transverse Direction | 3923(262) | | | | |
| MPa | 5.7(0.4) | | | | |
| 10 ⁵ psi | | | | | |
| 2. Flexural Strength | | | | | |
| Machine Direction | 135.4(12.2) | 110.6(7.2) | 106.7(8.7) | 98.3(12.0) | 92.6(5.1) |
| MPa | 19.6(1.8) | 16.0(1.0) | 15.4(1.3) | 14.3(1.7) | 13.4(0.7) |
| 10 ³ psi | | | | | |
| Transverse Direction | 14.9(2.9) | | | | |
| MPa | 2.1(0.4) | | | | |
| 10 ³ psi | | | | | |

injection-molded plaques generated in this work is about 1/12 inches. This difference is significant because Jackson and Kuhfuss also showed that decreasing the thickness of the samples leads to a marked increase in the properties (in the flow direction). Additionally, they also showed that the type of injection-molding machine used also affects the results. The injection-molding machine used by Jackson and Kuhfuss is different from the injection-molding machine used in this work.

Since Jackson and Kuhfuss (1) have reported the results of the 60/40 and 80/20 PHB/PET compositions at 260 and 340°C, respectively, it was necessary to injection-mold the compositions of 60/40 and 80/20 PHB/PET injection-molded at 260°C and 340°C, respectively. The injection-molding of the 60/40 and 80/20 PHB/PET was done for two reasons. First, because of the difference in plaque thickness and the type of injection-molding machine, we could not use the results of pure 60/40 PHB/PET and pure 80/20 PHB/PET compositions (quantitatively) reported in reference 1 to compare them with those of the blend. Second, if the flexural properties of pure 60/40 and 80/20 PHB/PET plaques matched with those reported by Jackson and Kuhfuss (Table 2, Chapter 2), we would be able to look qualitatively at the reported properties (i.e. the relative magnitude) of the directly injection-molded bars of 70/30 PHB/PET versus pure 60/40 and 80/20 PHB/PET compositions.

The flexural properties of the zero extrusion pass (pure) 60/40 PHB/PET and pure 80/20 PHB/PET (Table 8) agree well with those reported by Jackson and Kuhfuss (Table 2) at the same corresponding injection-molding temperatures. From Table 8 it can be seen that the mechanical properties of the 60/40 PHB/PET composition are significantly better than those of 80/20 PHB/PET composition. The reported values of directly injection-molded tensile and flexural bars of 70/30 PHB/PET (at 280°C, melting temperature is around 268°C) and 80/20 PHB/PET (at 340°C, melting temperature is around 300°C) are lower than 60/40 PHB/PET (at 260°C, melting temperature is around 230-260 °C) (Table 1). The highest tensile strength for the blend is slightly higher (about 4%, which is within the experimental error) than that for the 60/40 PHB/PET (from Table 2) and the flexural modulus for the blend is substantially higher (about 40%) than that for the 60/40 PHB/PET. Thus, the blend of 60/40 PHB/PET and 80/20 PHB/PET represents an advantage over the 70/30 PHB/PET composition as well as 60/40 and 80/20 PHB/PET compositions.

Table 8. Anisotropic flexural properties of the 'zero extrusion pass' and 'one extrusion pass' pure 60/40 PHB/PET (at 260°C) and pure 80/20 PHB/PET (at 340°C)

| Material | 60 HBA/PET Zero Extrusion Pass | 60 HBA/PET One Extrusion Pass | 80 HBA/PET Zero Extrusion Pass | 80 HBA/PET One Extrusion Pass |
|----------------------|---|--|---|--|
| Property | | | | |
| 1. Flexural Modulus | | | | |
| Machine Direction | | | | |
| MPa | 11187(2119) | 10784(1757) | 7594(865) | 6837(1228) |
| 10 ⁵ psi | 16.2(3.1) | 15.6(2.5) | 11.0(1.4) | 9.9(1.8) |
| Transverse Direction | | | | |
| MPa | 1174(101) | 1048(84) | 1191(79) | 1236(76) |
| 10 ⁵ psi | 1.7(0.1) | 1.5(0.1) | 1.7(0.1) | 1.8(0.1) |
| 2. Flexural Strength | | | | |
| Machine Direction | | | | |
| MPa | 119(21) | 119(17) | 103(5.6) | 90(11.3) |
| 10 ³ psi | 17.2(3.0) | 17.2(2.5) | 14.9(0.8) | 13.0(1.6) |
| Transverse Direction | | | | |
| MPa | 22(4.2) | 24(4.6) | 31(5.9) | 31(1.4) |
| 10 ³ psi | 3.2(0.6) | 3.5(0.7) | 4.5(0.9) | 4.5(0.2) |

4.1.2 Tensile properties of the 'multiple extrusion pass' blend

The tensile properties of the injection-molded plaques obtained by the injection-molding of 'one, two, three and four extrusion pass' materials at 330°C are shown in Table 9. These are lower than the corresponding values (tensile modulus and strength) for the zero extrusion pass plaques in the machine direction and higher than those in the transverse direction. These have been additionally plotted along with those of zero extrusion pass results in Figs. 12 to 17. The tensile properties for nearly all the multiple extrusion pass materials are within the experimental error. However, it can be concluded that the tensile strength in the machine direction decreases as one increases the number of extruder passes through the extruder from none to one.

4.1.3 Flexural properties of the 'multiple extrusion pass' blend

The flexural properties of the multiple extrusion pass material are tabulated in Table 7. The properties were determined only in the machine direction due to the paucity of the material. Unlike the tensile properties, there is a marked decrease in strength and modulus with increase in the number of extrusion passes. For example, the flexural modulus decreases from 15781 MPa for the zero extrusion pass blend to only 8847 MPa for the four extrusion pass material. This difference in the drop in the tensile and flexural properties of the multiple extrusion pass blends would tend to indicate the possible loss of some orientation in the assumed skin layer with the increase in the residence time in the extruder. It is possible that the chemical association amongst the polymer chains in the blend (as shown later, transesterification reaction does occur in the extruder) may affect the formation of two-dimensional mesophase order in the melt. This is consistent with the observation made by Paci et al. (61) that transesterification leads to a disruption of the chain periodicity and, therefore, of the lamellar organization of the liquid crystalline polymers. Thus, transesterification reaction might affect the ability of chains to orient and to retain the orientation

Table 9. Anisotropic tensile properties of the blend as a function of the number of extrusion passes (injection-molding temperature = 330°C)

| Material | One Extruder Pass | Two Extruder Pass | Three Extruder Pass | Four Extruder Pass |
|----------------------------------|-------------------|-------------------|---------------------|--------------------|
| Property | | | | |
| 1. Tensile strength | | | | |
| Machine Direction | | | | |
| MPa | 83.7(1.9) | 79.9(5.2) | 73.7(9.8) | 75.4(3.1) |
| 10 ³ psi | 12.1(0.3) | 11.6(1.4) | 10.7(1.4) | 10.9(0.4) |
| Transverse Direction | | | | |
| MPa | 26.3(2.4) | 25.2(1.3) | 19.5(6.0) | 24.1(2.6) |
| 10 ³ psi | 3.8(0.4) | 3.7(0.2) | 2.8(0.9) | 3.5(0.4) |
| 2. Tensile modulus | | | | |
| Machine Direction | | | | |
| MPa | 2282(324) | 2353(158) | 2436(164) | 2560(109) |
| 10 ⁵ psi | 3.3(0.5) | 3.4(0.2) | 3.5(0.2) | 3.7(0.1) |
| Transverse Direction | | | | |
| MPa | 863(77) | 998(180) | 970(76) | 988(68) |
| 10 ⁵ psi | 1.3(0.1) | 1.4(0.3) | 1.4(0.1) | 1.4(0.1) |
| 3. Elongation(percentage) | | | | |
| Machine Direction | | | | |
| | 5.9(0.3) | 5.2(0.5) | 4.9(0.34) | 4.7(0.1) |
| Transverse Direction | | | | |
| | 9.1(2.2) | 6.0(3.5) | 3.5(1.4) | 4.8(1.1) |

before solidification in the mold. Thus, the greater drop in the flexural properties compared to the tensile properties can be explained if the following are true :

1. An oriented skin layer is formed in the mold.
2. This skin layer affects the flexural properties to a greater extent as compared to the tensile properties, which are a measure of the average properties of the cross-section of the sample.
3. The chemical reaction in the blend affects the formation of the skin layer.

Flexural properties of the 'zero extrusion pass' and 'one extrusion pass' samples of pure 60/40 and pure 80/20 PHB/PET (Table 8) show no significant difference. If the explanation about the transesterification reaction in the blend being the cause of the decrease in the flexural properties with the increase in the number of extruder passes is accepted, then it would follow that compared to the blend, the transesterification reaction in the extruder for pure 60/40 and 80/20 PHB/PET systems is not significant. This is not unreasonable in light of the fact that unlike the blend (where the 60/40 and 80/20 PHB/PET compositions are brought together for the first time), the as received pure 60/40 and 80/20 PHB/PET pellets might have already been equilibrated with respect to the transesterification reaction. Also, in the case of the pure 60/40 PHB/PET, the deviation of the sequences of HBA from those for random sequences is so small as to be negligible (34). Thus, transesterification in the pure 60/40 PHB/PET system should not cause any change in its properties (thermal and mechanical) except to possibly bring about the molecular weight equilibration (if the polymer is already not equilibrated with respect to its molecular weight distribution).

4.2 DSC results

It was expected that due to the presence of ester bonds, the transesterification reaction will take place during the extrusion, which would lead the blend towards the 70/30 PHB/PET composition. Since transesterification leads to a decrease in the 'melting point', the multiple extrusion pass

blend and 70/30 PHB/PET pellets were analyzed by means of the DSC at a heating rate of 10 deg./minute.

4.2.1 Low temperature annealing results

As was mentioned in the Experimental Chapter, all the multiple extrusion pass samples after having been dried for three days at 120°C were stored in a low pressure dehumidified environment for a few months. When the one extrusion pass samples were analyzed by means of DSC, a peak at 113°C was observed (Fig. 18 and Table 10). Also shown in the same figure are the DSC thermograms of the one extrusion pass samples annealed at 150°C for 30 and 150 minutes.

The peak at 113°C, which disappears for the samples which had been annealed for 30 and 150 minutes, should be due to the water present in the sample. The other two higher temperature peaks are discussed later. There is some difference in these higher temperatures peaks for the three cases shown in Fig. 18. This difference can not be due to the incomplete crystallization kinetics (since the half time of crystallization of PET is only 100 seconds at 150°C (75), it is probably safe to assume that the crystallization kinetics of the crystallizing components should be complete in three days for which all the samples had been originally annealed at 120°C). The difference in the peak temperatures is either due to the fact that individual pellets (and not films) were used for DSC characterization (individual pellets even from the same sample pool can not be expected to exhibit exactly same thermal behavior) or because of the evaporation of water (liquid-vapor phase transition for pure water occurs at 100 °c at 1 atm. pressure). Even though the endotherm attributed to water in the unannealed sample disappears after annealing for 30 minutes, it does not preclude the existence of traces of water. This water content will vary in the 30 minutes and 150 minutes annealed samples and thus might be responsible for the small variation in the peak temperatures (the moisture might cause the hydrolysis of the blend). Thus, for the subsequent DSC analysis,

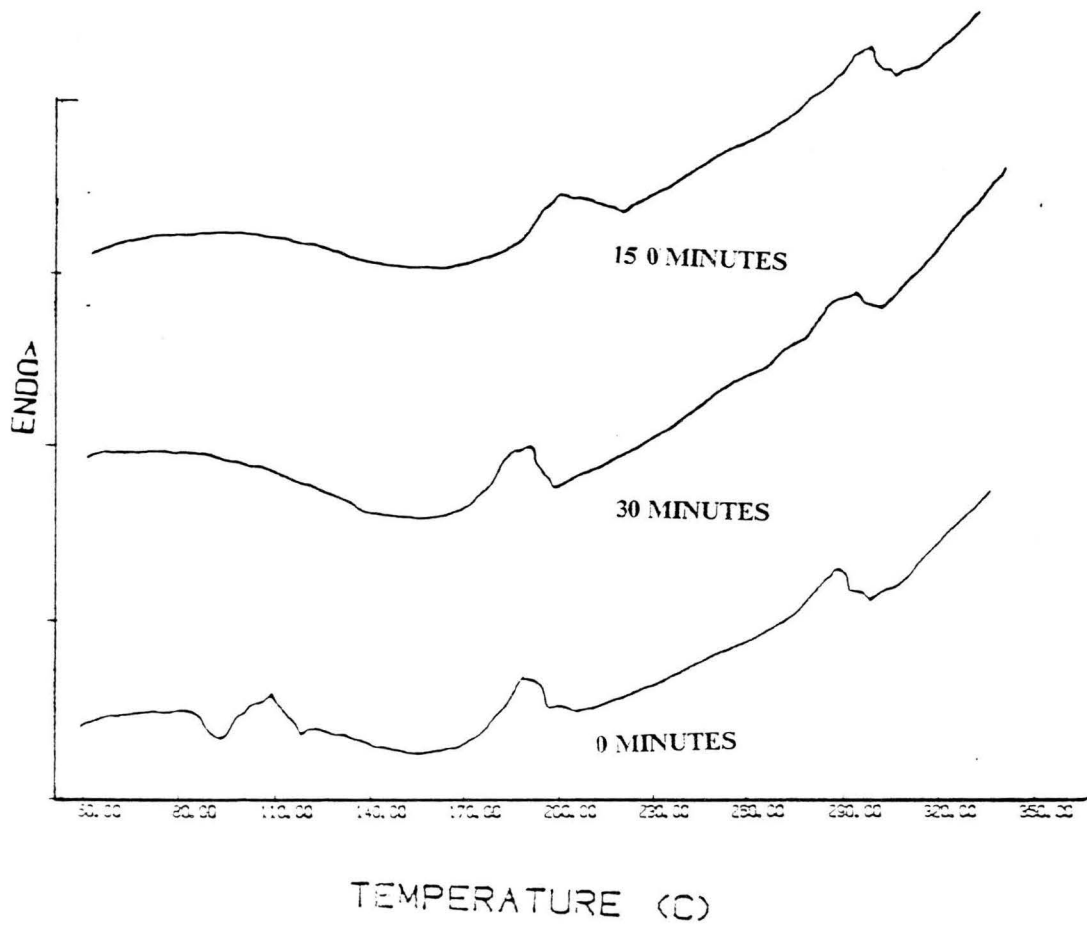


Figure 18. Differential scanning calorimetric results for the one extrusion pass samples annealed at 150°C for different lengths of time

Table 10. Differential scanning calorimetric results for the one extrusion pass samples annealed at 150°C for different lengths of time

| Annealing Time (Minutes) | Low Temperature Peak °C | ΔH J/gm | High Temperature Peak(s) °C | ΔH J/gm |
|-----------------------------|----------------------------|--------------------|--------------------------------|--------------------|
| 0 | 113 194 | 2.12 2.64 | 293 | 1.03 |
| 30 | 193 | 2.62 | 287 | 1.42 |
| 150 | 200 | 2.10 | 292 | 1.56 |

all the samples (multiple extrusion pass blend) were dried for three additional days. This period of three days was enough for complete drying, as is indicated in the following section.

4.2.2 Pure 60/40 PHB/PET and 80/20 PHB/PET

Since the thermal transitions reported in the literature for PHB/PET copolyesters, especially 60/40 PHB/PET, are not consistent, DSC analysis of pure 60/40 and 80/20 PHB/PET was carried out. The intent was to locate the melting transitions in the pure 60/40 and 80/20 PHB/PET compositions. This was necessary for the understanding of the melting endotherms which were observed for the blends.

Two sets of samples were analyzed. The samples in the first set were annealed for 3 (for 60/40 PHB/PET), 4 (for 70/30 PHB/PET) and 5 (for 80/20 PHB/PET) days and the samples in the second set were all annealed for 3 days. The DSC results are shown in Fig. 19 and Table 11. The results for the 70/30 PHB/PET have been shown along with those of the multiple extrusion pass blends in Figs. 20 & 21 and Tables 12 & 13. Since excellent agreement is obtained for the peak temperatures of the corresponding endotherms in the two sets, it can be concluded that annealing time, beyond the minimum of three days at 120°C, has no effect on the results. Two endotherms are observed for both 60/40 and 80/20 PHB/PET compositions which are discussed below.

4.2.2.1 80/20 PHB/PET results

The higher temperature endotherm has a peak temperature of about 302 °C. Zachariades et al. (2) reported that the 80/20 PHB/PET DSC thermograms shows a peak maxima at 303°C. This peak was explained as the crystallization to nematic transition and being related to the melting of the HBA rich lamella. Meesir et al. (4) also reported the 'melting point' of the 80/20 PHB/PET at $T = 286-293$ °C corresponding to different thermal history of the sample. Again, they assigned this as the transition from crystallization to nematic state. Thus, the peak obtained at about 302°C

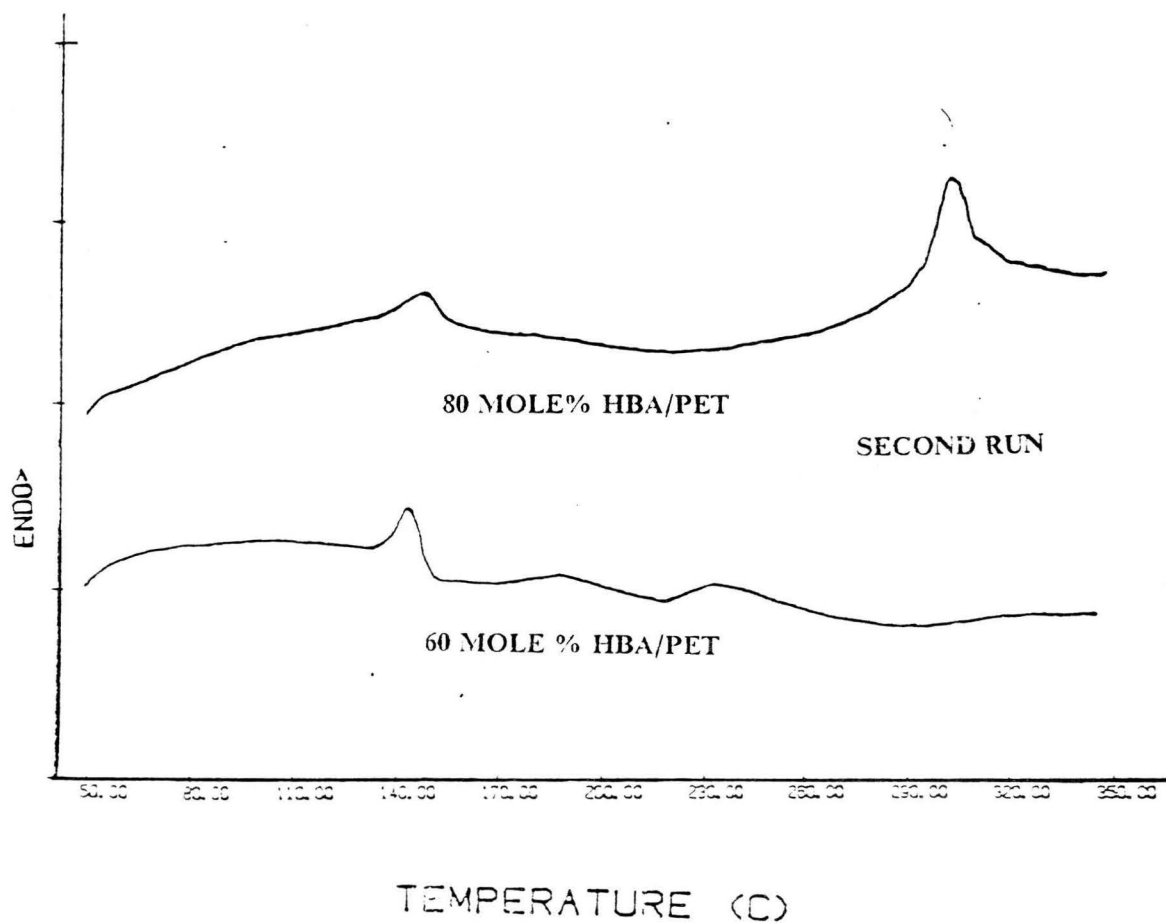


Figure 19. Differential Scanning Calorimetric Results For Unextruded 60 HBA/PET And Unextruded 80 HBA/PET Annealed AT T = 120 °C

Table 11. Differential Scanning Calorimetric Results For Unextruded 60 HBA/PET And Unextruded 80 HBA/PET Annealed AT T = 120 °C

| Material | Low Temperature Peak(s) °C | ΔH J/gm | High Temperature Peak °C | ΔH J/gm | Glass Transition Temperature °C |
|-----------------|-----------------------------------|----------------|---------------------------------|----------------|--|
| 60 HBA/PET | 143 | 2.22 | None | -- | None |
| | 143 | 1.78 | 235 | 2.43 | 210 |
| 80 PHB/PET | 151 | 0.46 | 301 | 2.71 | None |
| | 148 | 1.38 | 302 | 2.47 | None |

is consistent with the reported results and it is very likely due to the melting of the oxybenzoate units.

The lower temperature peak has never been reported in the literature for the 80/20 PHB/PET copolyester. This peak occurs in the temperature range of 140-150°C which is 20-30°C above the annealing temperature. The phenomenon of a melting endotherm near the annealing temperature has been observed for a number of polymers (31, 76). The theoretical treatment for this phenomenon has been given by Hoffman et al. (77). Thus, this peak is likely due to the melting of the PET crystallites annealed at the annealing temperature.

4.2.2.2 60/40 PHB/PET results

There is some disparity in the results of the two sets (Fig. 19). This is probably due to the fact that the baseline of the instrument in the second set was much better than in the first set of experiments. The following discussion pertains to the results of the second set. The two endotherms have been reported in the literature (4, 6, 33) for the 60/40 PHB/PET compositions. Joseph et al. (33) attributed the lower temperature endotherm (around 190°C) to the melting of the PET crystallinity (partial diluent effect) and the higher temperature endotherm (around 240°C) to the melting of HBA crystallites. Thus, by analogy we may assign the higher temperature peak at 235°C to the melting of HBA crystallites and the lower one to the that of PET crystallites. The lower temperature peak (140°C) is significantly lower than the corresponding temperature of 190°C in reference 33. However, as pointed before, the lower temperature peak occurs about 20°C above the annealing temperature and is likely due to the PET crystallites. In addition to the two endotherms, a glass transition at about 210°C is observed. This temperature is somewhat higher than the glass transition temperature reported at around 140-190°C by several researchers (3, 6, 35).

4.2.3 'Multiple extrusion pass' blends and 70/30 PHB/PET

For all the 'multiple extrusion pass' blends and 70/30 PHB/PET copolyester, two endotherms are observed in the DSC thermograms. The low temperature annealing results stressed the need for

an additional annealing/drying of the blends. The two sets of samples were annealed at 120°C for three days and an additional set was annealed at 150°C for three days. The results for the samples annealed at 120°C are shown in Figs. 20 & 21 (and in Tables 12 & 13) and for those annealed at 150°C are shown in Fig. 22 and Table 14. The higher temperature endotherm is likely to be due to the HBA crystallinity and the lower endotherm probably corresponds to the PET crystallites.

The lower peak temperature in Fig. 20 varies between 140-150°C which is 20-30°C above the annealing temperature. Similar phenomenon of a melting endotherm near the annealing temperature was also observed for pure 60/40 and 80/20 PHB/PET polyesters. However, for the two extrusion pass sample (Fig. 20), this peak shifts to 180°C. It is possible that the two extrusion pass sample was accidentally annealed at 150°C instead of 120°C. The 70/30 PHB/PET samples in all cases (Figs. 20, 21 and 22) were annealed at 150°C. The second set of 'multiple extrusion pass' samples were annealed initially at 150°C (i.e the quenched extrudate dried at 150°C). These dried samples were again annealed at 120°C for three days before DSC characterization. The lower temperature peak occurs between 183-193°C (Fig. 22) which is near the annealing temperature of 150°C. The 'multiple extrusion pass' samples annealed at 150°C (Fig. 23) also show melting endotherms between 192-194°C.

The higher temperature endotherm shows some interesting behavior with the increase in the number of extruder passes. Even though no significant lowering of the 'high temperature peak' occurs with the increase in the number of extruder passes (for the samples annealed at 120°C), the splitting of this peak is seen in the thermograms of the four extrusion pass samples. The occurrence of multiple peaks in a system undergoing transesterification has been theoretically postulated by Wahrmund et al. (48). The splitting of the peaks would correspond to the formation of multiple phases in the extruder due to the incomplete transesterification reaction. It is significant that the temperature of the multiple peaks in the four extrusion pass samples (Figs. 21 & 22) are different. This is discussed below along with the results for the samples annealed at 150°C.

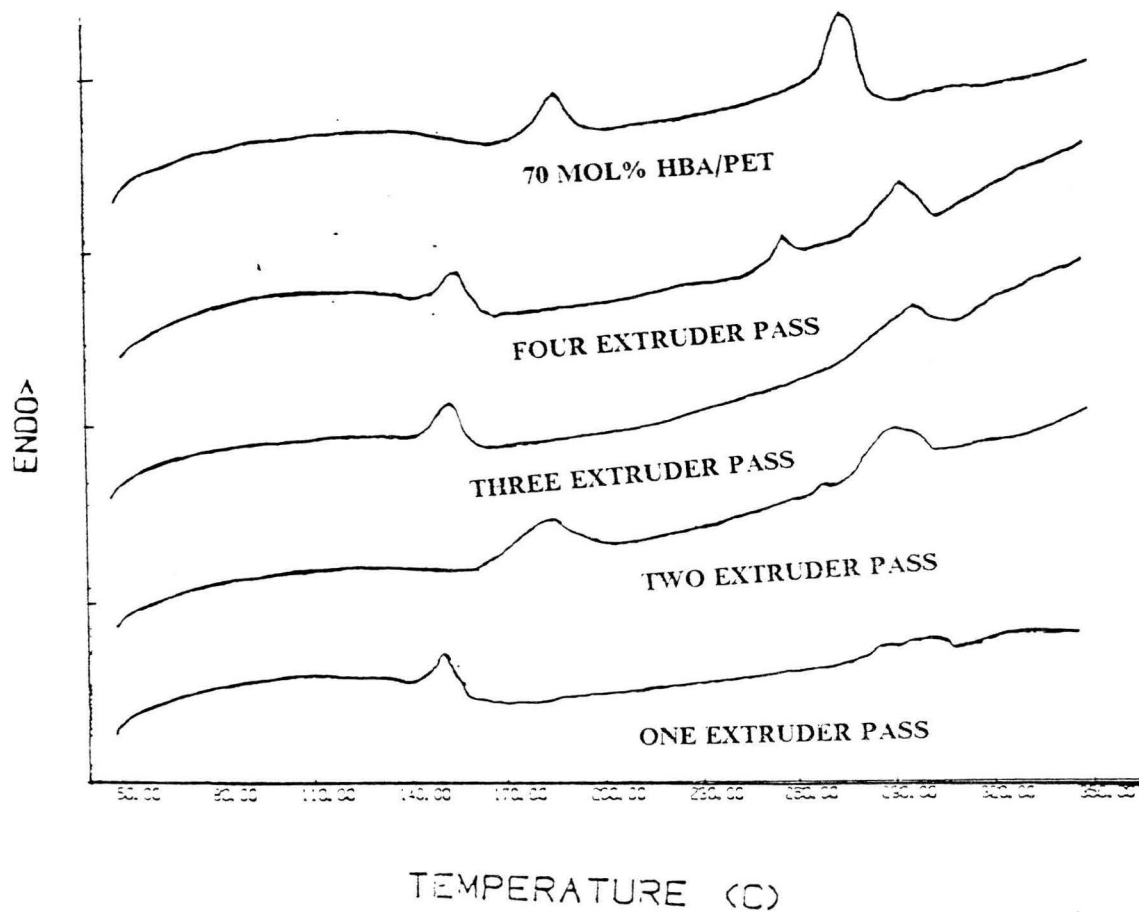


Figure 20. Differential Scanning Calorimetric Results For Multiple Extrusion Passes Of The Blend Of 60% & 80% PHB/PET And For The Unextruded 70% HBA/PET Annealed At $T = 120^{\circ}\text{C}$

Table 12. Differential Scanning Calorimetric Results For Multiple Extrusion Passes Of The Blend Of 60% & 80% PHB/PET And For The Unextruded 70% HBA/PET Annealed At T = 120°C

| Number of Extruder Passes | Heating | | | | Cooling | |
|---------------------------|-------------------------|-----------------------------|-----------------------------|-----------------------------|---------------------------------------|-----------------------------|
| | Low Temperature Peak °C | ΔH J/ μm | High Temperature Peak(s) °C | ΔH J/ μm | Recrystallization Temperature Peak °C | ΔH J/ μm |
| One | 145 | 1.00 | 296 | 1.23 | 236 | 2.56 |
| Two | 180 | 2.58 | 286 | 2.20 | 246 | 1.71 |
| Three | 149 | 1.36 | 292 | 2.04 | 242 | 1.49 |
| Four | 149 | 1.35 | 288 252 | 2.07 0.67 | 241 | 1.32 |
| Unextruded 70 HBA/PET | 183 | 1.90 | 270 | 2.98 | | |

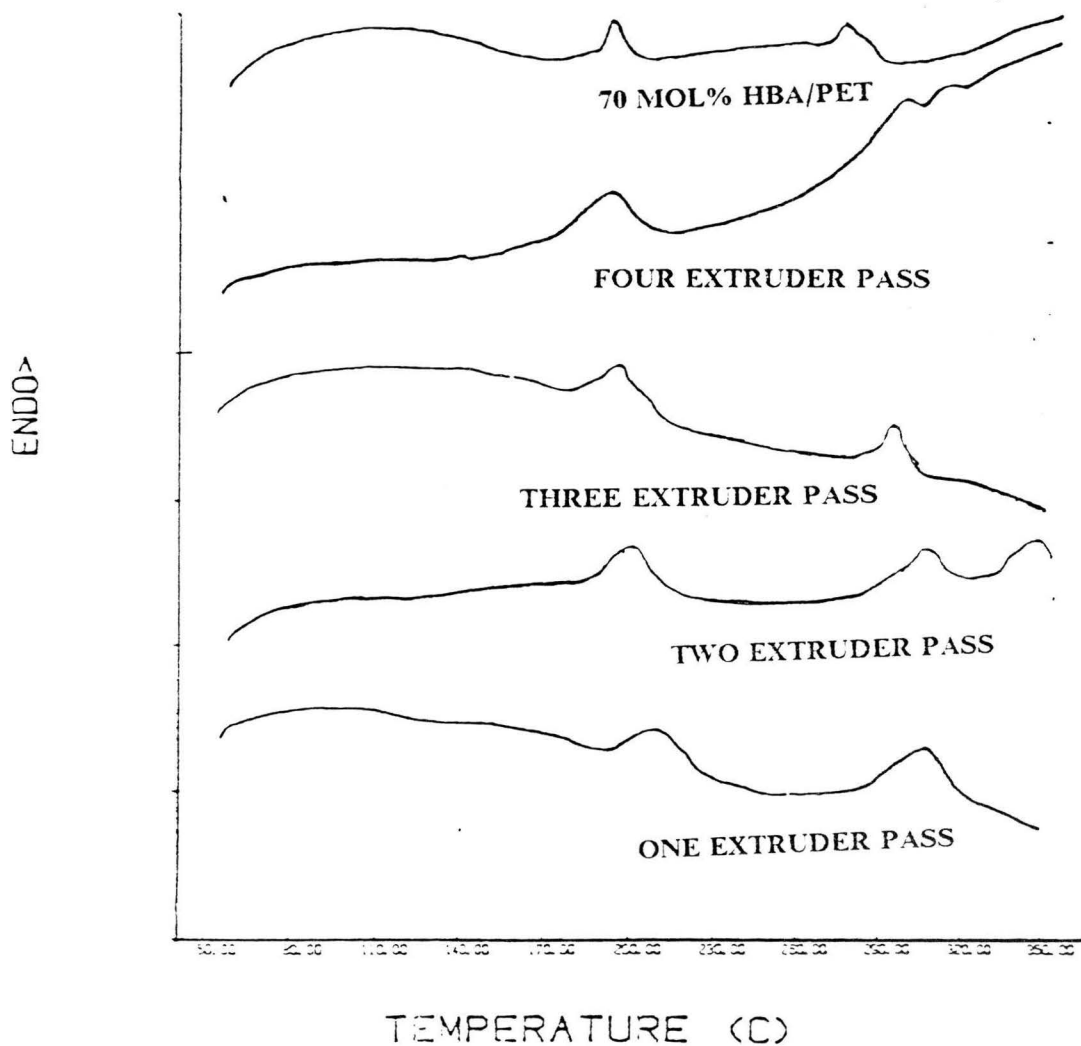


Figure 21. Differential Scanning Calorimetric Results For The Multiple Extrusion Pass Blend Of 60% & 80% PHB/PET And For The Unextruded 70% HBA/PET Annealed At $T = 120^{\circ}\text{C}$

Table 13. Differential Scanning Calorimetric Results For The Multiple Extrusion Pass Blend Of 60% & 80% PHB/PET And For The Unextruded 70% HBA/PET Annealed At T = 120°C

| Number of Extruder Passes | Heating | | | | | Cooling | |
|---------------------------|-------------------------|-----------------|-----------------------------|----------------------|---------------------------------------|-----------------|--|
| | Low Temperature Peak °C | ΔH J/gm | High Temperature Peak(s) °C | ΔH J/gm | Recrystallization Temperature Peak °C | ΔH J/gm | |
| One | 193 | 3.40 | 288 | 3.64 | 227 | 1.53 | |
| Two | 186 | 3.90 | 286 328 | 2.43 ---- | 225 | 1.97 | |
| Three | 187 | 3.49 | 285 | 2.33 | 240 | 1.34 | |
| Four | 185 | 4.24 | 283 300 274 | 0.38 0.24 0.38 | 228 | 3.81 | |
| Unextruded 70 HBA/PET | 180 | 2.49 | 269 | 1.16 | | | |

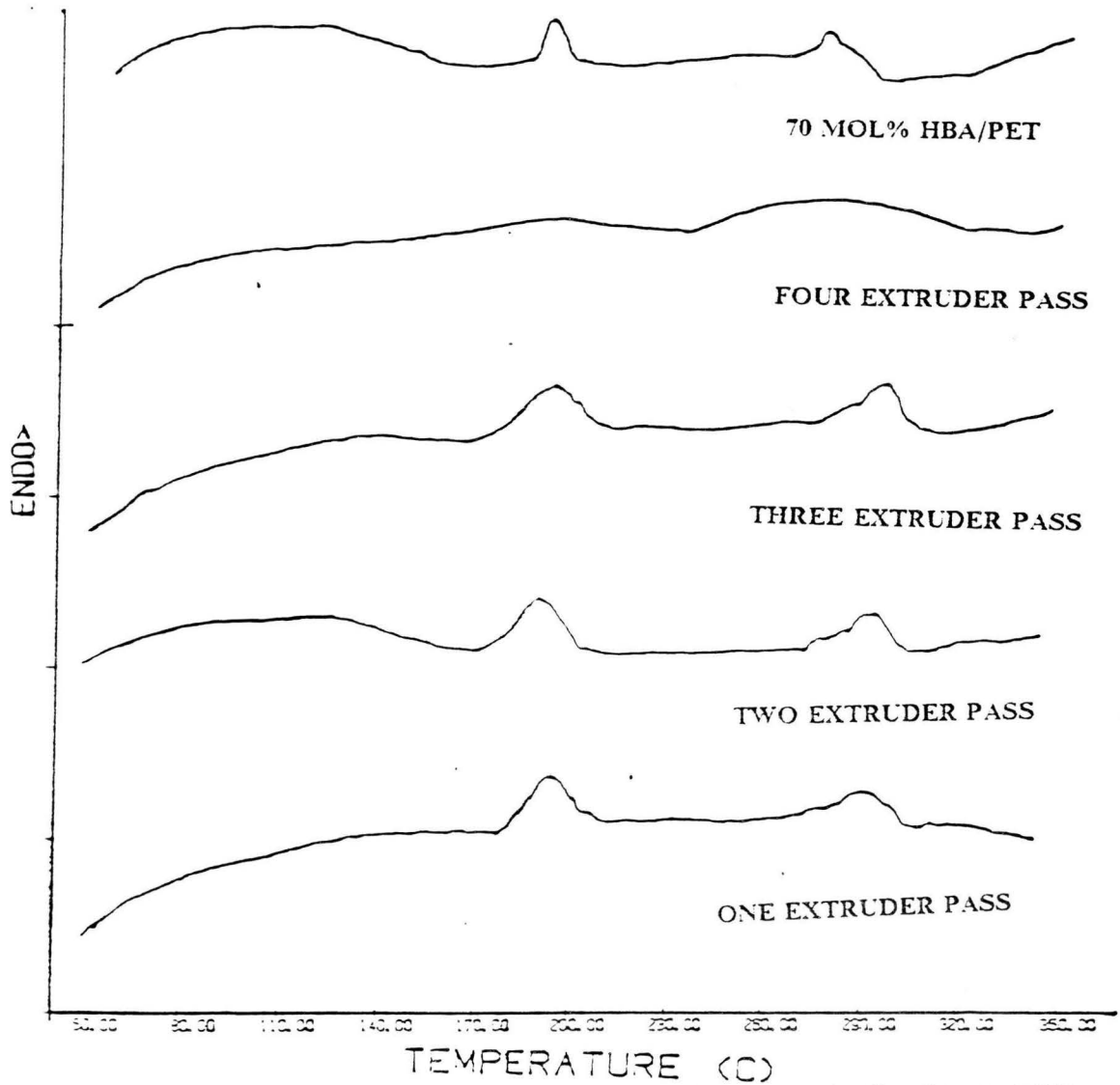


Figure 22. Differential Scanning Calorimetric Results For The Multiple Extrusion Pass Blend Of 60% And 30% PHB/PET And For Unextruded 70% HBA/PET Annealed At $T = 150^{\circ}\text{C}$

Table 14. Differential Scanning Calorimetric Results For The Multiple Extrusion Pass Blend Of 60% And 80% PHB/PET And For Unextruded 70% HBA/PET Annealed At T = 150°C.

| Number of Extruder Passes | Low Temperature Peak °C | ΔH J/gm | High Temperature Peak °C | ΔH J/gm |
|---------------------------|-------------------------|-----------------|--------------------------|-----------------|
| One | 194 | 2.82 | 291 | 2.09 |
| Two | 189 | 3.40 | 294 | 2.10 |
| Three | 192 | 4.20 | 294 | 2.80 |
| Four | 192 (150-234) | 2.20 | 278 (234-314) | 5.97 |
| Unextruded 70 HBA/PET | 185 | 1.76 | 271 | 1.55 |

The DSC thermograms of the multiple extrusion pass samples annealed at 150°C (Fig. 22) shows no difference in the higher temperature peak for the one, two and three extrusion pass samples, but for the four extrusion pass sample, extreme broadening of the two peaks (lower temperature endotherm extends from 150 to 234°C and the higher temperature endotherm from 234 to 314°C) occurs. The broadening of a peak can be associated with the increase in the randomness of the polymer structure (33). The higher temperature peak is most probably associated with the HBA crystallinity and in the 80/20 HBA/PET (and therefore in the blend) the HBA block sequence distribution is non-random. The results of the higher temperature peak would therefore also suggest that with the increase in the residence time in the extruder, the system is becoming more random. This is consistent with the fact that the transesterification reaction leads to a system with a more random structure (45, 51, 62).

In most of the systems of the type: A homopolymer + B homopolymer transesterification leads to an initial increase and then decrease in the block sequence lengths. In the blend of 60/40 and 80/20 PHB/PET, only the 80/20 PHB/PET component exhibits significant deviations from the random structure. Also, the 60/40 and 80/20 PHB/PET polyesters are chemically similar. Thus, transesterification in the blend would lead to a continuous decrease in the block sequence lengths. If sufficient time is available, then transesterification would finally result in a totally random 70/30 PHB/PET composition. After this stage, even though transesterification would still take place amongst the polymer chains, it will not produce any statistical change in the system. The DSC thermogram of the 'equilibrium composition' (non-random as received 70/30 PHB/PET) shows the lower temperature peak at around 180°C and the higher temperature peak at 270°C. Even though it can be concluded from Figs. 20, 21 and 22 (and Tables 12, 13 and 14) that transesterification does take place in the extruder, nothing can be said from these results about whether transesterification also leads the blend towards the equilibrium composition of 70/30 PHB/PET

Since the splitting of the peak occurs for the four extrusion pass samples, it would appear that there is an induction period before which significant transesterification reaction can occur. Similar induction times of 10 minutes (45) and 60 minutes (46) in the blend of different copolyesters have been reported. The fact that an induction time exists at all would seem to indicate that the

transesterification is at least initially diffusion controlled. The average residence time for the single extrusion pass blend corresponding to an average screw speed of 45 (arbitrary units) is about 1.5 minutes (Table 15). Thus, based on the DSC results, it would appear that there is an induction time between 4.5-6 minutes for transesterification reaction in the extruder. Finally, the splitting of the 'higher temperature peak' for the four extrusion pass material occurs in a different way for the two four extrusion pass samples annealed at 120°C (Figs. 20 & 21) and also for the four extrusion pass sample annealed at 150°C (Fig. 22). This random splitting of the 'higher temperature peak' is consistent with the accepted fact that transesterification by its very nature is essentially a random process (38).

4.2.4 DSC results of the samples annealed in RMS

The residence time in the extruder is quite short (about 6 minutes for the four extrusion pass samples). Also, the extrusion temperature is very close to the peak temperature of the melting endotherm of the blend (the melt temperature at the exit was around 290°C). Thus, the transesterification studies were carried out outside the extruder at higher temperatures and on a larger time scale in the RMS. The one extrusion pass pellets were heated in the RMS at two temperatures (310 and 300°C). The samples were withdrawn at different time intervals and quenched in water (to freeze in the changes which might have been brought about by the transesterification reaction). These quenched samples on subsequent drying and annealing (for three days at 120°C) were examined by means of DSC. The DSC results for the samples annealed at 310°C are shown in Fig. 23 and Table 16 and for those annealed at 300°C are shown in Fig. 24 and Table 17. The splitting of the higher temperature endotherm is strikingly clear from these results. This splitting occurs for the samples which had been annealed for 3-5 minutes (at 310°C) and 10-15 minutes (at 300°C) or more. Thus it can be concluded that transesterification reaction occurs at a faster rate in the extruder, where the melt temperature at the exit was around 290°C and splitting

Table 15. Average residence time of the blend in the extruder as a function of the extruder speed

| Extruder Speed (Arbitrary Units) | Average Residence Time (Seconds) |
|-------------------------------------|-------------------------------------|
| 30 | 120 |
| 40 | 100 |
| 50 | 80 |
| 60 | 60 |

of the higher temperature peak was observed for the four extrusion pass samples, which had a residence time of about 6 minutes.

On comparing the results of Figs. 23 & 24, it becomes quite clear that the splitting of the higher temperature peak not only starts earlier but also is much more pronounced for the samples annealed at 310°C. A shoulder can be observed on the left side of the second peak for the sample which was annealed at 310°C for only one minute. Thus, it can be concluded that an increase in temperature leads to an increase in the rate of the transesterification reaction.

Similar to the random splitting of the high temperature peak for the four extrusion pass samples, there is no pattern in which the peaks split (Fig. 23 & 24). Consistent with the random nature of the transesterification reaction, for the sample annealed at 310°C (Fig. 23) for 5 minutes, a large peak appears suddenly at 233°C (which corresponds to the higher temperature peak observed for the pure 60/40 PHB/PET) and it disappears altogether for the sample annealed for 10 minutes. We can try to conjecture an image of what might have caused the sudden appearance and disappearance of this peak. The appearance of this peak would correspond to the formation of a local phase (which would be rich in the component responsible for the endotherm at 233°C). When this phase is quenched and subsequently annealed at 120°C, we observe the endotherm at 233°C in the DSC thermogram. However, the random transesterification reaction is meanwhile going on in the blend (in the RMS). Thus, this local phase, due to the interchange reactions with the adjacent chains, totally disappears after some time and therefore no endotherm is observed at 233°C for the samples annealed for 10 minutes at 310°C.

Finally, for the samples annealed at 310°C (Fig. 23), we observe that the split peaks formed from a single sharp peak finally merge to form one giant peak. The giant peak would then correspond to the melting of a distribution (in terms of their perfectness) of the crystallites. Also, unlike the four extrusion pass samples, the split peaks in some cases occur at temperatures higher than 296°C (Figs. 23 and 24). There can be two explanations for the occurrence of higher temperature peaks. First, since transesterification is a random process, it might give rise to some crystals which would melt at higher temperature. Second, it is possible that crystallization of HBA units occurs

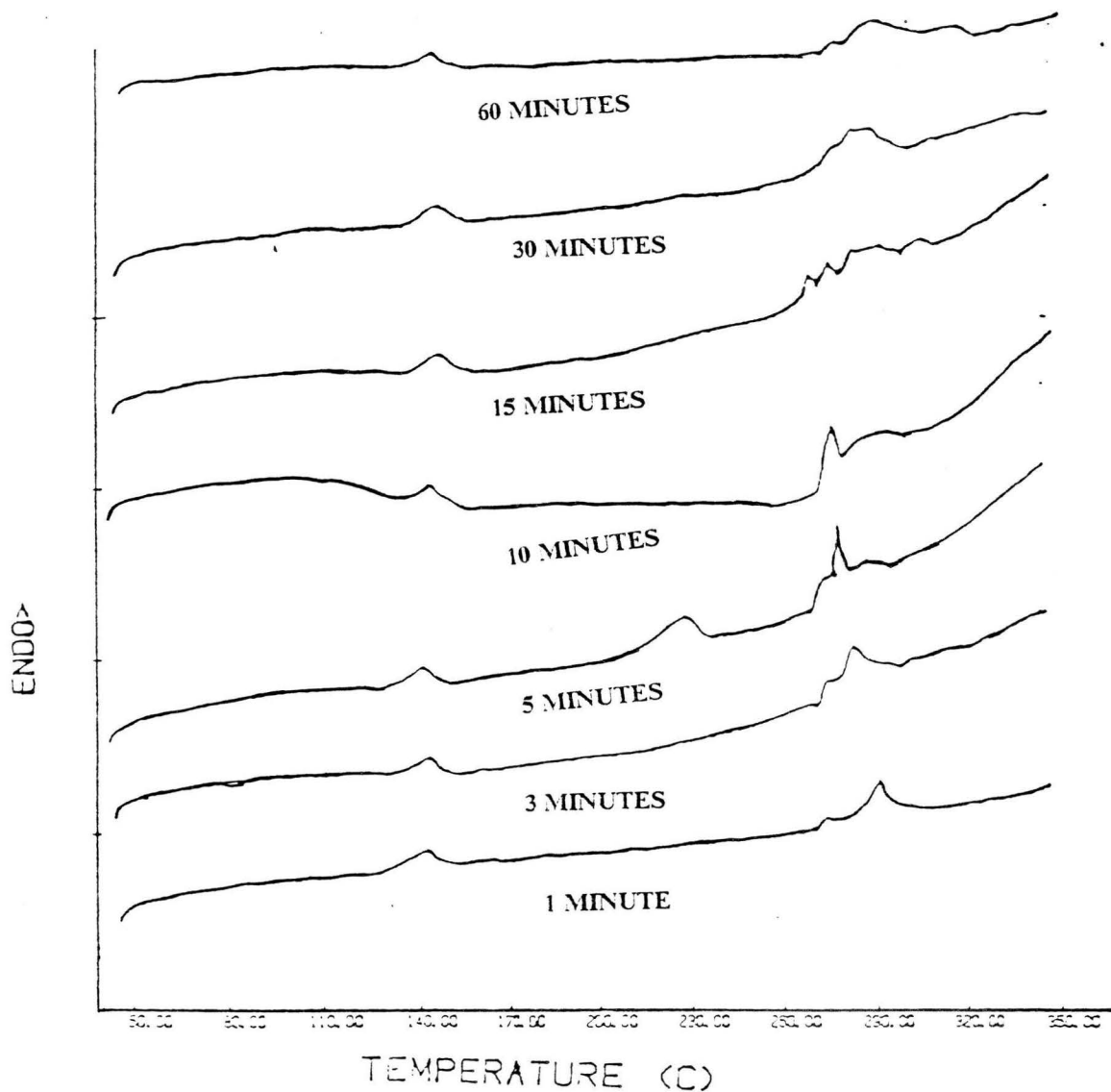


Figure 23. Differential Scanning Calorimetric Results For The One Extrusion Pass Samples Annealed In RMS At $T = 310^{\circ}\text{C}$ For Different Lengths Of Time

Table 16. Differential Scanning Calorimetric Results For The One Extrusion Pass Samples Annealed In RMS At T = 310 °C For Different Lengths Of Time

| Annealing Time In RMS (Minutes) | Low Temperature Peak °C | ΔH J/gm | High Temperature Peak(s) °C | ΔH J/gm |
|---------------------------------|-------------------------|-----------------|-----------------------------|----------------------|
| 0 | 145 | 1.00 | 296 | 1.23 |
| 1 | 144 | 1.38 | 294 | 1.88 |
| 3 | 144 | 0.86 | 285 | 1.90 |
| 5 | 145 | 1.00 | 282 233 | 0.84 3.03 |
| 10 | 145 | 0.77 | 290 278 | {2.05 |
| 15 | 148 | 0.92 | 304 285 277 272 | {2.44 |
| 30 | 146 | 1.34 | 338 283 225 | 0.21 4.63 0.21 |
| 60 | 145 | 0.92 | 290 | {5.07 |

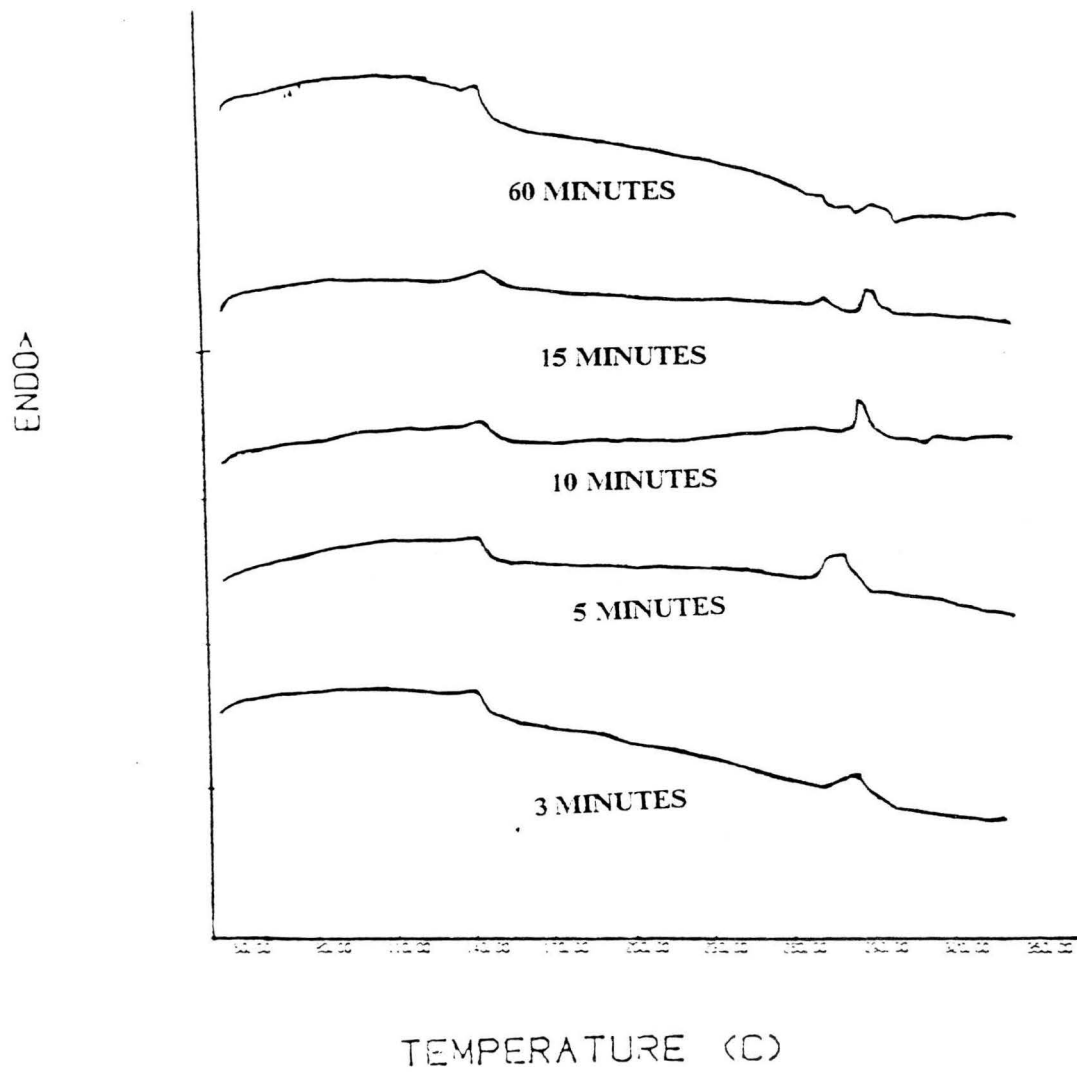


Figure 24. Differential Scanning Calorimetric Results For The One Extrusion Pass Samples Annealed In RMS AT T = 300c °C For Different Lengths Of Time

Table 17. Differential Scanning Calorimetric Results For The One Extrusion Pass Samples Annealed In RMS AT T = 300c °C For Different Lengths Of Time

| Annealing Time In RMS (Minutes) | Low Temperature Peak °C | ΔH J/gm | High Temperature Peak(s) °C | ΔH J/gm |
|---------------------------------|-------------------------|-----------------|-----------------------------|----------------------|
| 0 | 145 | 1.00 | 296 | 1.23 |
| 1 | 144 | 1.38 | 294 | 1.88 |
| 3 | 144 | 0.86 | 285 | 1.90 |
| 5 | 145 | 1.00 | 282 233 | 0.84 3.03 |
| 10 | 145 | 0.77 | 290 278 | {2.05 |
| 15 | 148 | 0.92 | 304 285 277 272 | {2.44 |
| 30 | 146 | 1.34 | 338 283 225 | 0.21 4.63 0.21 |
| 60 | 143 | 0.40 | 297 316 339 | 1.09 0.79 0.56 |

in the blend in the melt state. This is possible since some residual crystallinity is present in the extruded blend. Thus, crystallization-induced-reaction (25, 26) can take place and result in HBA crystals of higher melting temperatures. However, there is still no evidence which would indicate that the transesterification in the blend is leading it towards an equilibrium composition.

4.2.5 DSC results of the samples sheared in RMS

To investigate the effect of shearing on the transesterification reaction, the one extrusion pass samples were sheared in a cone & plate geometry in steady mode (at 310 and 300°C, shear rate = 10 1/sec). Unlike the annealing studies, the samples were sheared for only 18 minutes to minimize the degradation. After quenching and drying, the sheared samples were analyzed by means of DSC. The results are shown in Figs. 25 & 26 (and Tables 18 & 19). Unlike the simply annealed samples (at 300 and 310°C), there is no splitting of the higher temperature peak and two cases of splitting of the lower temperature peak. This can either mean that transesterification rate is decreased by shearing or that the mixing due to shearing results in a single melting peak.

The latter conclusion is supported by the two observations. First, for the samples sheared at 310°C for three minutes (Fig. 25) the heat of fusion is 8.9 J/gm which is nearly four times the corresponding energy values observed in the simple annealing studies. Additionally, the heat of fusion drops for the samples which were sheared for 10 and 15 minutes. It has been reported in the literature (45, 61) that transesterification leads to a decrease in the enthalpy of fusion. The reason this decrease in the enthalpy was not observed earlier might be due to the fact that individual pellets have been used for DSC characterization. It can be expected that the amount of crystallinity will vary in the same sample pool from one pellet to another. This variation in the amount of crystallinity coupled with the fact that the observed enthalpy changes are very small (about 2 J/gm) may be sufficient to overshadow the expected decrease in enthalpy. Thus, it appears likely that the

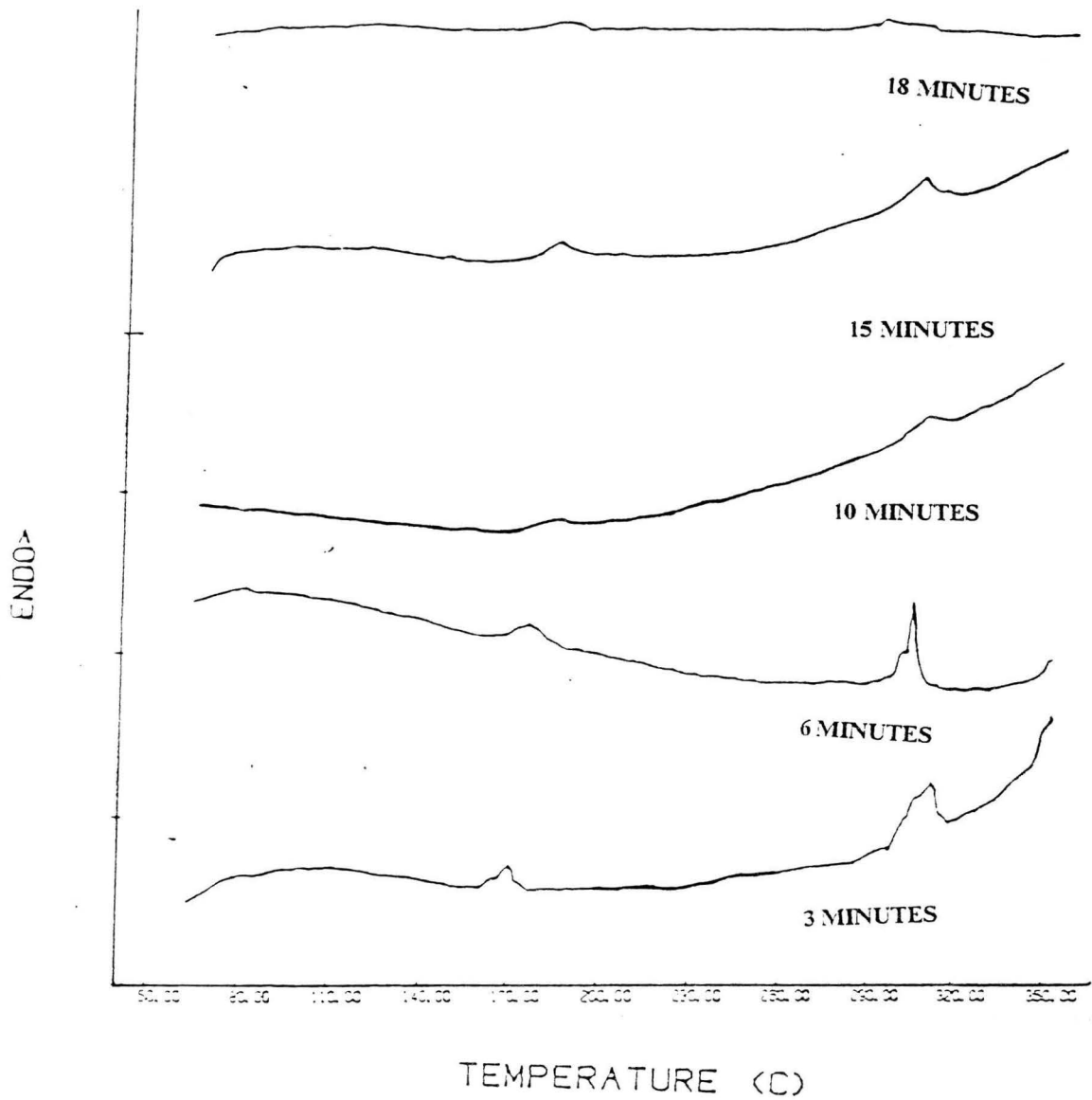


Figure 25. Differential Scanning Calorimetric Results For The One Extrusion Pass Samples Sheared In RMS (Parallel Plate, Steady Mode, 10 1/Sec) At T = 310 °C For Different Time

Table 18. Differential Scanning Calorimetric Results For The One Extrusion Pass Samples Sheared In RMS (Parallel Plate, Steady Mode, 10 1/Sec) At T = 310 °C For Different Time

| Shearing Time (Minutes) | Low Temperature Peak °C | ΔH J/gm | High Temperature Peak °C | ΔH J/gm |
|-------------------------|-------------------------|-----------------|--------------------------|-----------------|
| 0 | 145 | 1.00 | 296 | 1.23 |
| 3 | 159 | 2.67 | 298 | 8.90 |
| 6 | 163 | 3.15 | 289 | 7.99 |
| 10 | 173 | 1.25 | 292 | 2.37 |
| 15 | 170 | 1.75 | 288 | 2.42 |
| 18 | 168 | 1.49 | 273 | 4.86 |

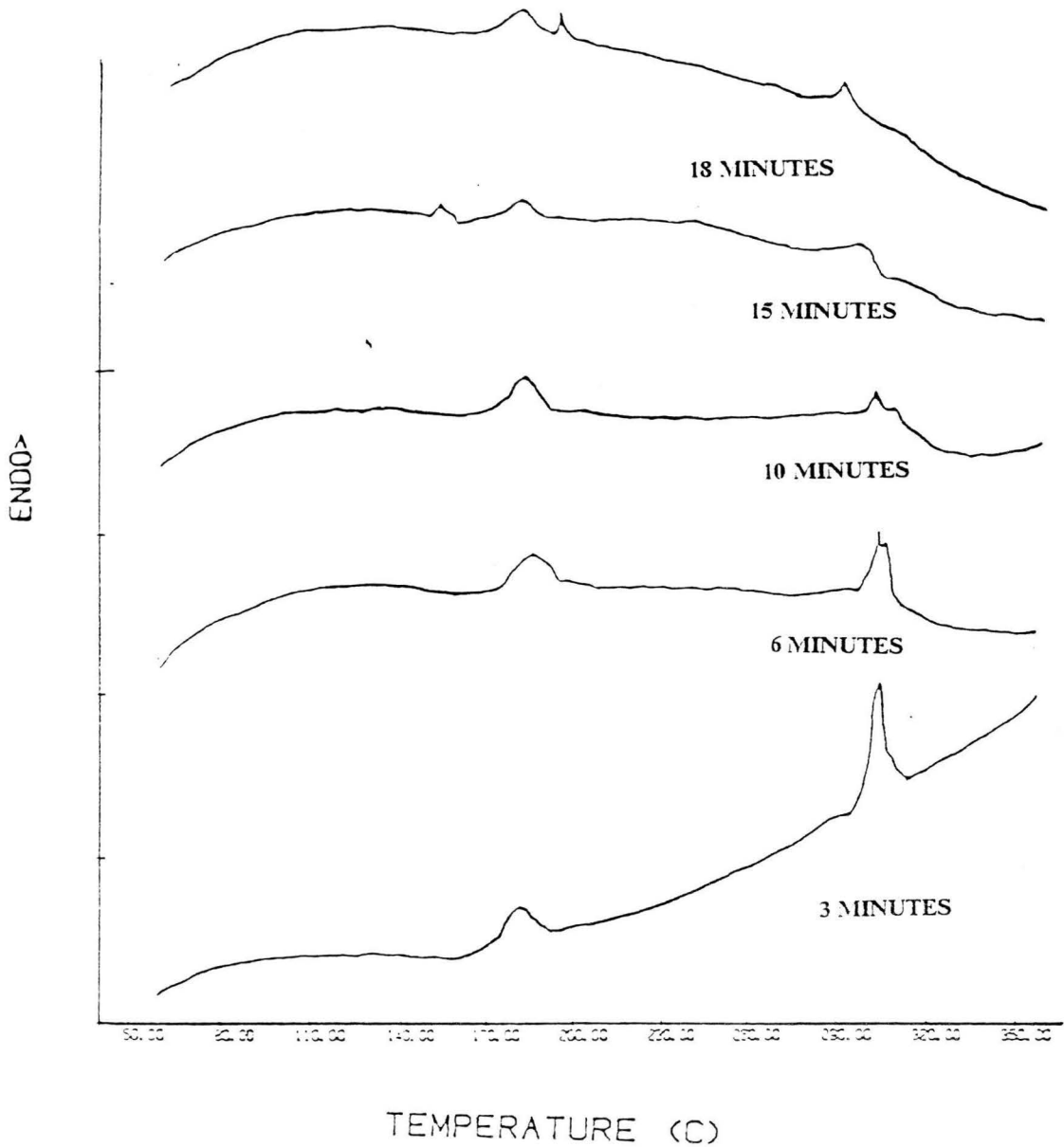


Figure 26. Differential Scanning Calorimetric Results For The One Extrusion Pass Samples Sheared In RMS (Parallel Plate, Steady Mode, 10 l/Sec) At T = 300 °C For Different Time

Table 19. Differential Scanning Calorimetric Results For The One Extrusion Pass Samples Sheared In RMS (Parallel Plate, Steady Mode, 10 1/Sec) At T= 300 °C For Different Time

| Shearing Time (Minutes) | Low Temperature Peak(s) °C | ΔH J/gm | High Temperature Peak °C | ΔH J/gm |
|-------------------------|----------------------------|--------------|--------------------------|---------|
| 0 | 145 | 1.00 | 296 | 1.23 |
| 3 | 171 | 1.45 | 292 | 3.37 |
| 6 | 174 | 1.98 | 291 | 1.66 |
| 10 | 170 | 1.95 | 289 | 2.01 |
| 15 | 166 140 | 0.54 0.61 | 284 | 2.01 |
| 18 | 179 166 | 0.48 2.13 | 275 | 1.68 |

mixing due to shearing results in a single melting peak with a very high enthalpy value and that the decrease in the enthalpy is indicative of the transesterification reaction.

The second observation which would suggest that the absence of the multiple peaks is not indicative of a reduction in the transesterification rate in the shearing environment is that the peak temperature of the higher endotherm decrease (it decreases steadily for the samples sheared at 300°C, Fig. 26). This decrease is consistent with the known fact that transesterification leads to a decrease in the melting point (45, 46, 47, 48). The temperature of the higher temperature peak for the samples sheared for 18 minutes is approximately equal to the temperature of the high temperature peak of the unextruded and unsheared 70/30 PHB/PET (269-271°C). Thus, the structure of the blend indeed approaches the equilibrium composition of 70/30 PHB/PET.

Thus, the rate of transesterification is most probably increased by shearing. However, nothing can be said about the effect of temperature on transesterification rate in the shearing environment from Figs. 25 & 26. Also, in contrast to the simple annealing case, no comparison can be made about the transesterification reaction rate in the extruder and in the shearing environment. During the extrusion, the blend is subjected not only to high temperatures but also to shear and mixing due to the velocity component of the fluid which is normal to the flow direction. The annealing studies in the RMS showed that transesterification proceeds at a faster rate in the extruder compared to a no-shear (annealing) environment. This might be due to the shearing environment and the mixing in the extruder. The shearing in the blend might serve the same purpose as a 'stirrer in a batch reactor' and thus might accelerate the chemical reaction. Thus, from the DSC study, we can conclude that transesterification does occur in the extruder. Additionally, at longer reaction times, transesterification results in the blend approaching the equilibrium composition of 70/30 PHB/PET. From the comparison of the results of the extruded samples, annealed samples and the sheared samples, it can be concluded that transesterification proceeds at a faster rate in the extruder, and that shearing also, most likely, tends to increase its rate. In addition, the transesterification rate increases with an increase in temperature.

In Chapter 2, it was pointed out that the phenomenon of crystallization can also occur in the extruder. This phenomenon has been reported for PHB/PET (26) as well as other systems (25, 65,

66) above as well as below the melt temperature. Even though these crystallization - induced reactions are significant below the melt temperature, their rate is extremely slow above the melt temperatures (26). No crystallization above the melt temperature was observed by Winter et al. (66) for the sample which had been preheated to a temperature higher than the melt temperature. From the results of Winter (66) and also from the very definition of crystallization - induced reaction (25, 26), it follows that crystallization can occur above the melt temperature only if some residual crystallinity is present in the sample. It is expected that since the extrusion temperature for melt blending was quite low, some residual crystallinity will be present in the extruder. Thus, crystallization - induced reaction can occur in the blend. However, such a crystallization - induced reaction during the extrusion should be insignificant due to the extremely short residence time in the extruder (6 minutes for the four extrusion pass blend). For example, for the 46/54 PHB/PET, it was shown (26) that even after two weeks of reaction time, the crystallization - induced reaction had occurred to a small extent. Additionally, a decrease in the melting point, degree of crystallinity and blockiness is observed for the blend which is the exact opposite to what would have been observed if crystallization - induced reaction was the dominant reaction. Thus, it can be concluded that the crystallization - induced reaction does not take place to a significant extent in the blend and the transesterification reaction is the dominant reaction occurring in the blend in the melt state.

In addition to the DSC, the change in the thermal behavior of the blend due to the transesterification reaction can also be studied by means of other characterization techniques. Thus, dynamic mechanical analysis (DMA) and thermal mechanical analysis (TMA) of the blends transesterified to varying degrees (i.e. the multiple extrusion pass blends) and the equilibrium composition (70/30 PHB/PET) was done to find the changes in the thermal behavior.

4.3 DMA and TMA results

In the DSC study, it was indicated that transesterification occurs in the blend and is leading the blend towards an equilibrium composition. In order to further confirm this, the compression

molded films of multiple extrusion pass blends and 70/30 PHB/PET were examined by means of DMA and TMA. The DMA results are shown in the Table 20. Even though the melting temperature increases by 6°C for the two extrusion pass blend, it drops by more than 10°C for the three extrusion pass material and by about 20°C more for the four extrusion pass material. Also, the melting temperature of the four extrusion pass blend is quite close to that of 70/30 PHB/PET. These results confirm the conclusion reached in the DSC study that transesterification does occur in the extruder and the system is approaching an equilibrium composition of 70/30 PHB/PET. However, in contrast to the DSC results which showed that significant transesterification occurs during the fourth extrusion pass, DMA results point to an absence of any induction time (or less than 1.5 minutes) for the transesterification reaction in the blend. Also, the approximate temperature of the melting temperatures and the great reduction in the melting temperatures with the increase in the number of extrusion passes differs from those based on the DSC results. The DMA and DSC results are not expected to be directly related because of the different sample history and the different modes of measurement i.e. dynamic mechanical versus thermal. A glass transition is also present in all samples in the range of 111-128°C for the extruded samples and around 108°C for the 70/30 PHB/PET. This would mean that a glass transition at a lower temperature than the above temperatures (time temperature superposition) should be observed in the DSC thermograms of the amorphous blend.

Figure 27 shows the TMA penetration curves as a function of temperature for the multiple extrusion pass blends and 70/30 PHB/PET. The TMA results revealed no difference in the softening profiles of one, two and three extrusion pass blends. The four extrusion pass material has a rather similar softening profile as 70/30 PHB/PET material. Also, the softening profile of the four extrusion pass sample would indicate the presence of crystallites of varying degrees of development, which corresponds to the splitting peak phenomenon observed in the corresponding DSC thermograms. Also, the agreement of the TMA results with the DSC results would point to the presence of an induction time between 4.5 - 6 minutes.

Table 20. Dynamic Mechanical Analysis Results For the Multiple Extrusion Pass Blend And The 70/30 PHB/PET Films Annealed At 120°C

| Number of Extruder Passes | Glass Temperature °C | Melting Temperature °C |
|---------------------------|----------------------|------------------------|
| One | 111 | 265 |
| Two | 117 | 272 |
| Three | 129 | 260 |
| Four | 120 | 241 |
| Unextruded 70 HBA/PET | 108 | 243 |

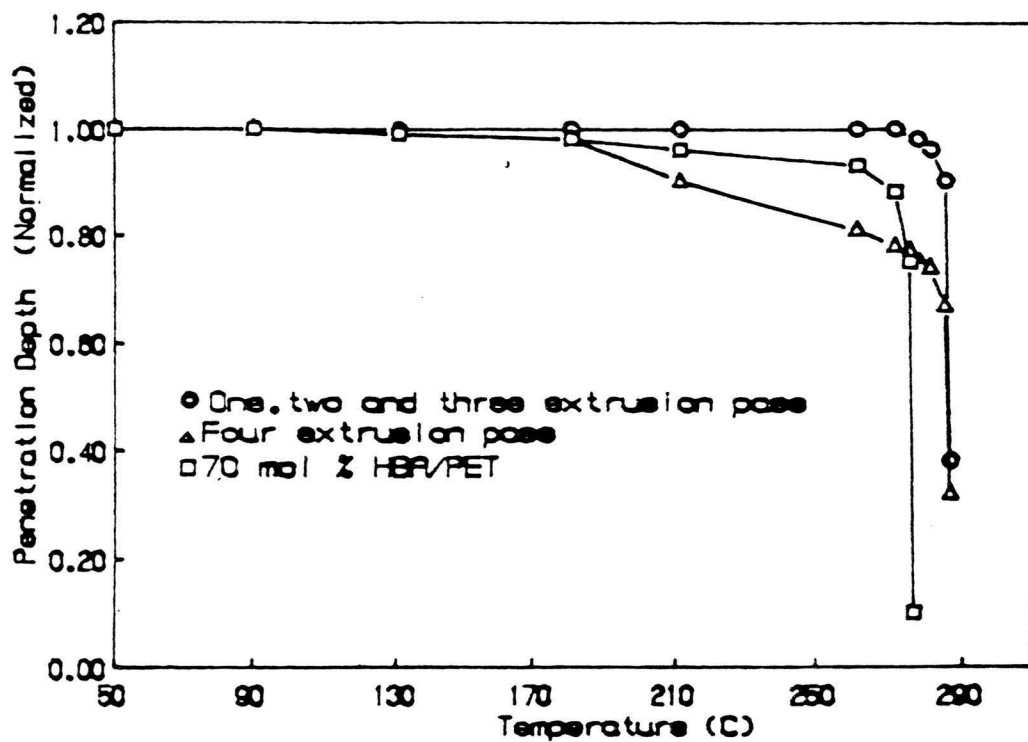


Figure 27. Thermal Mechanical Analysis Results For The Multiple Extrusion Pass Blend And 70/30 PHB/PET Films Annealed At 120°C

4.4 SEM results

The micrographs of the multiple extrusion pass blends and 70/30 PHB/PET are shown in Figs. 28-32. All the samples show fibrillar structure. There is a second phase present in the micrograph of one extrusion pass samples. It is possible that this dispersed phase is rich in PHB. The reason for this speculation is that the extrusion temperature was not high enough to melt the PHB crystals which disappears around 328°C (2).

The second phase is present only in the one extrusion pass sample. The disappearance of the second phase in two, three and four extrusion pass samples can be explained by the occurrence of transesterification reaction between the dispersed and the continuous phase. Thus, the SEM results would indicate an induction time of 1.5 to 3.0 minutes for the transesterification reaction.

From the DSC, TMA, DMA and SEM studies, it is evident that transesterification affects the thermal behavior and the morphology of the blend. It is known that the transesterification affects the rheology of the polyester. It leads to a reduction in the average chain length, and thus a decrease in weight average molecular weight (49) and viscosity (38, 46, 47, 49, 52). Thus, it was expected that the multiple extrusion pass blends would exhibit different rheological behavior.

4.5 RMS results

The multiple extrusion pass blends and 70/30 PHB/PET copolyester were studied in the RMS to identify the differences in their rheology. Correct measurements of dynamic properties should be done in the regions of strains in which the material exhibits linear viscoelastic behavior. Thus, strain sweep was performed on the one extrusion pass blend to locate the strain values over which the dynamic properties remain constant. This is shown in Fig. 33. It is evident that the rheological functions are not constant over any region. It is possible that the non-linearity exhibited in the strain sweep might be due to the initial polydomain texture present in the polymer. To verify

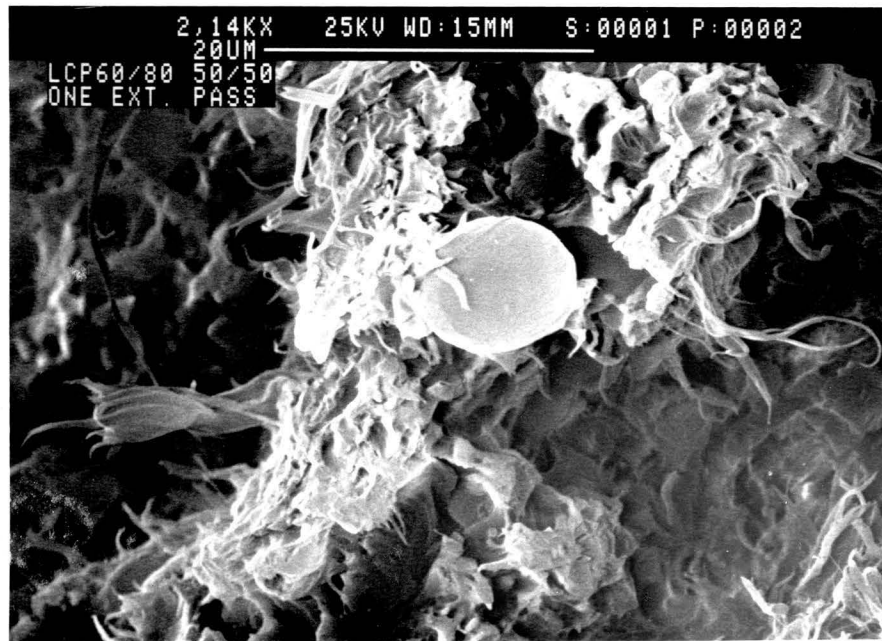
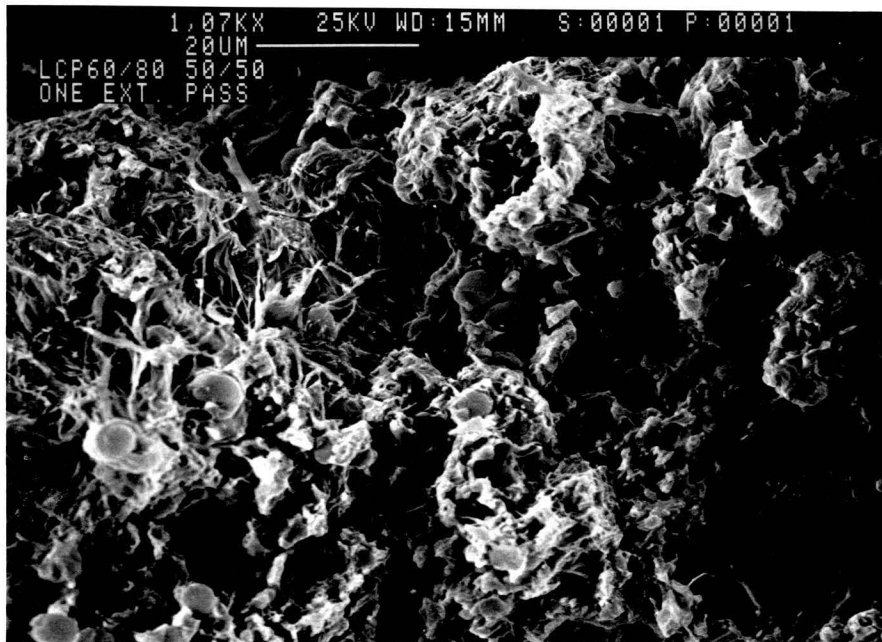


Figure 28. SEM of the 'one extruder pass' blend

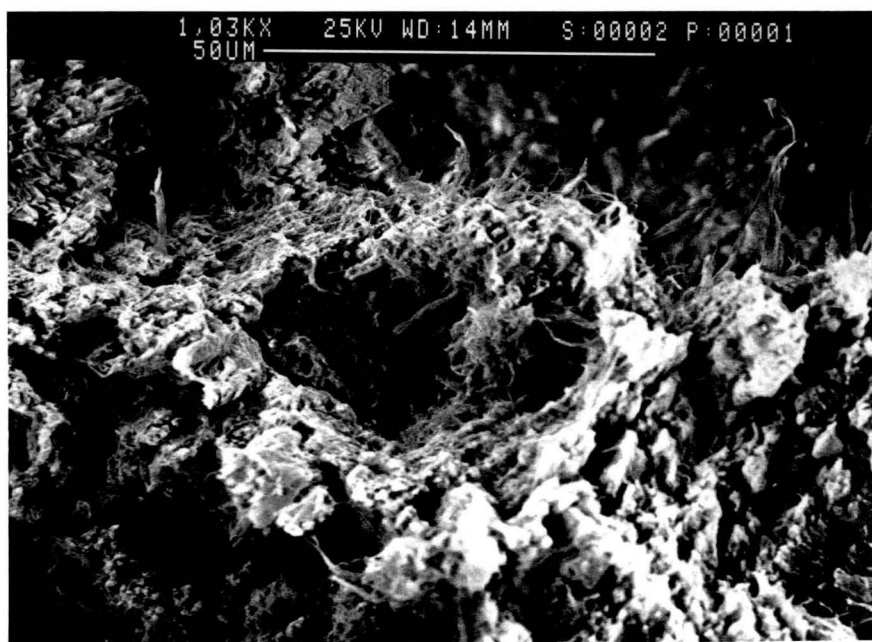


Figure 29. SEM of the 'two extruder pass' blend

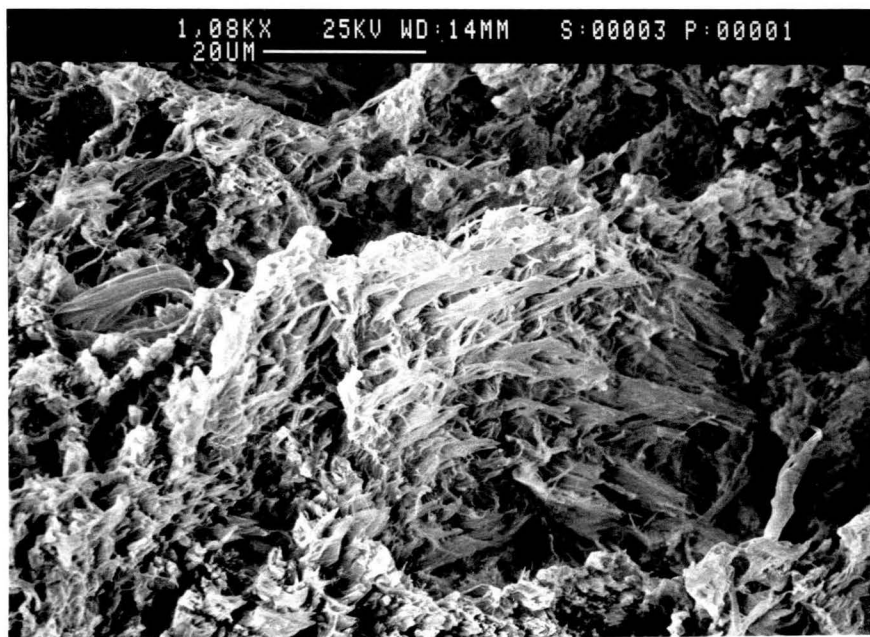


Figure 30. SEM of the 'three extruder pass' blend

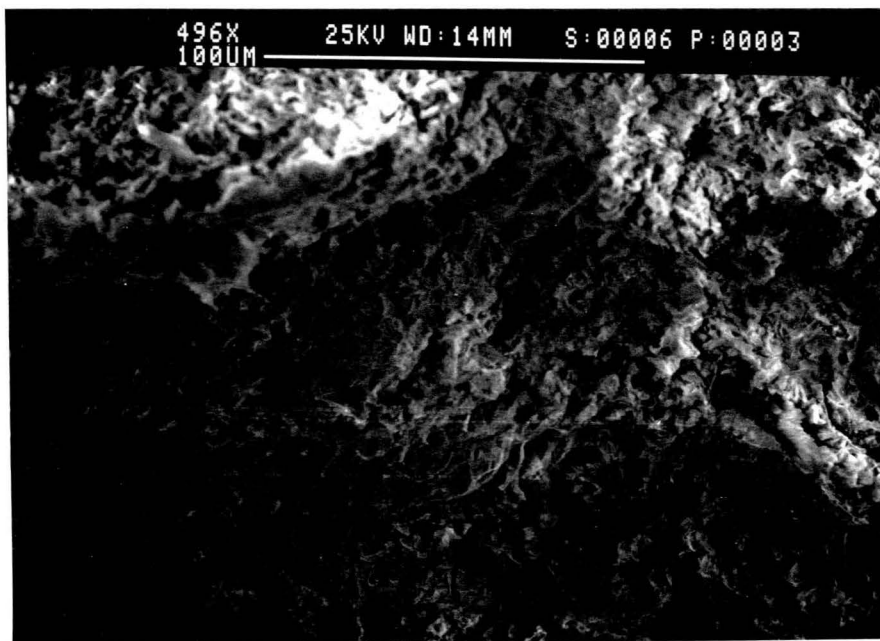


Figure 31. SEM of the 'four extruder pass' blend

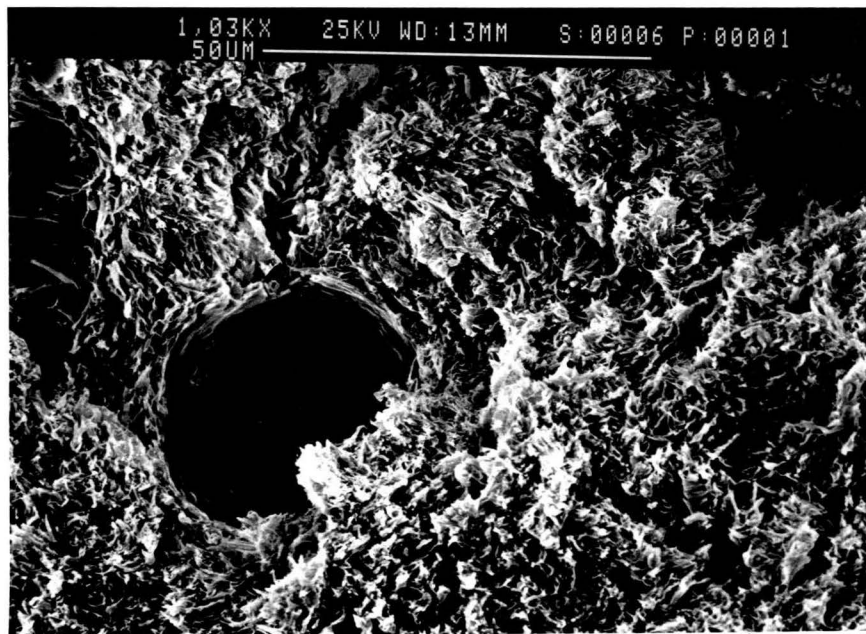


Figure 32. SEM of the 70/30 PHB/PET composition

this, the material was subjected to a strain of 2% at 10 rad/sec frequency (290°C) for 60 seconds. Then the strain sweep was performed on the material. This is shown in Fig. 34. It is clear that the rheological functions are much more linear as can be seen by comparing their values at 40 % strain, though an initial decrease still occurs. Thus, the non-linearity in the Fig. 33 was in fact due to the initial polydomain structure as can be seen from Fig. 34. The sharp decrease in the rheological properties at the start of the flow even for the material which had been subjected to a time sweep (Fig.34) also supports this conclusion. During the dynamic experiments, the initial polydomain structure will be broken in the initial stages of the experiment. Thus, Fig. 34 is a better representation of the linear behavior of these materials. A strain value of 10% was chosen for the subsequent experiments.

To compare the rheological properties of the multiple extrusion pass and 70/30 PHB/PET samples, dynamic frequency sweeps were performed in the RMS at 290 and 300°C. At 310°C and above, the torque was too low to be accurately measured. The plots of complex viscosity, storage modulus and loss modulus versus frequency are shown in Figs. 35-44. For comparison, each of these rheological functions for all the samples have been plotted separately. These curves which have been drawn without the error bands are shown in Figs. 45-50. In the following paragraph, the reproducibility of these results and the presence of thermal and shear history in the multiple extrusion pass samples are discussed. Following this, the differences in the rheology of multiple extrusion pass blends are discussed.

The reproducibility of the results is quite good at higher frequencies. But at lower frequencies there is some scattering of the data. This may be due to two reasons. At low shear rates the shear and thermal history of the samples plays an important role. It has been shown by a number of researchers (22, 23, 24) that prior overheating the samples and then cooling it down to the temperature of the experiment could drastically decrease the rheological behavior. Thus, care was taken to avoid the overshoot of the set temperature and the sample was discarded whenever this happened. Nevertheless, some of the scattering at lower frequencies may be due to overheating. The shear history of the samples was even more difficult to control. Since the extrusion conditions of the multiple extrusion pass blends were identical, the processing history of the samples can be re-

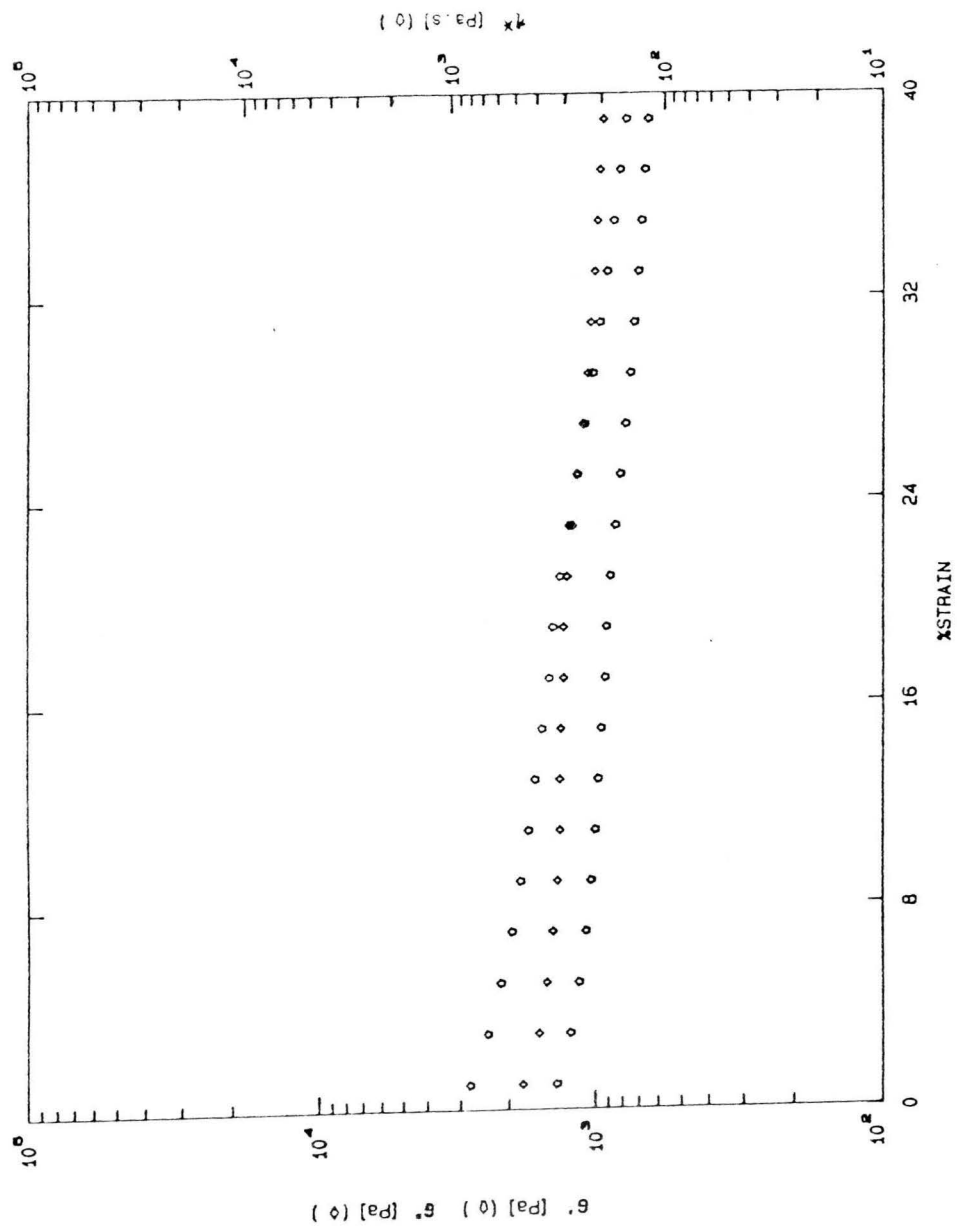


Figure 33. Strain sweep of the one extrusion pass blend at 290°C (cone & plate geometry, frequency = 10 rad/sec)

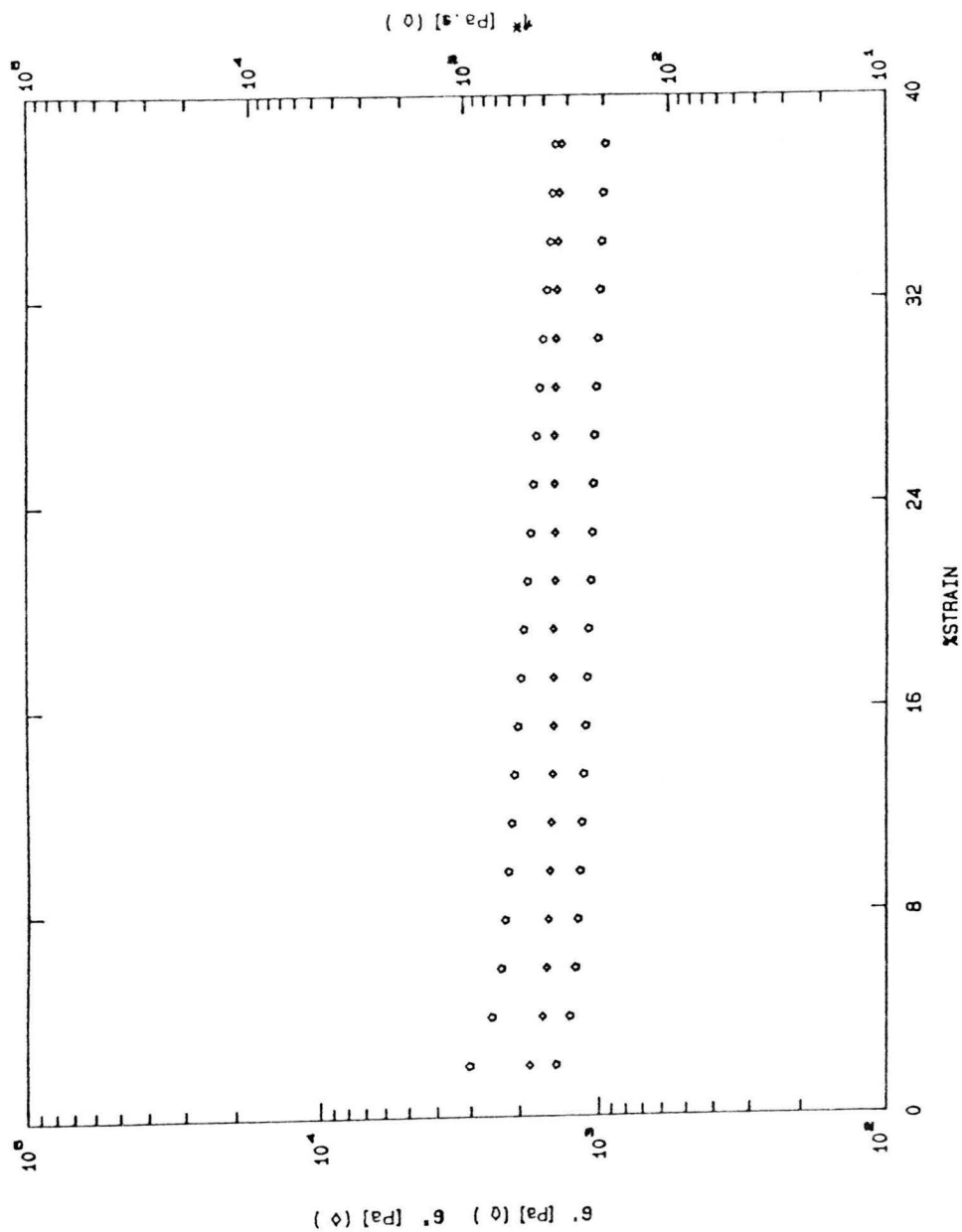
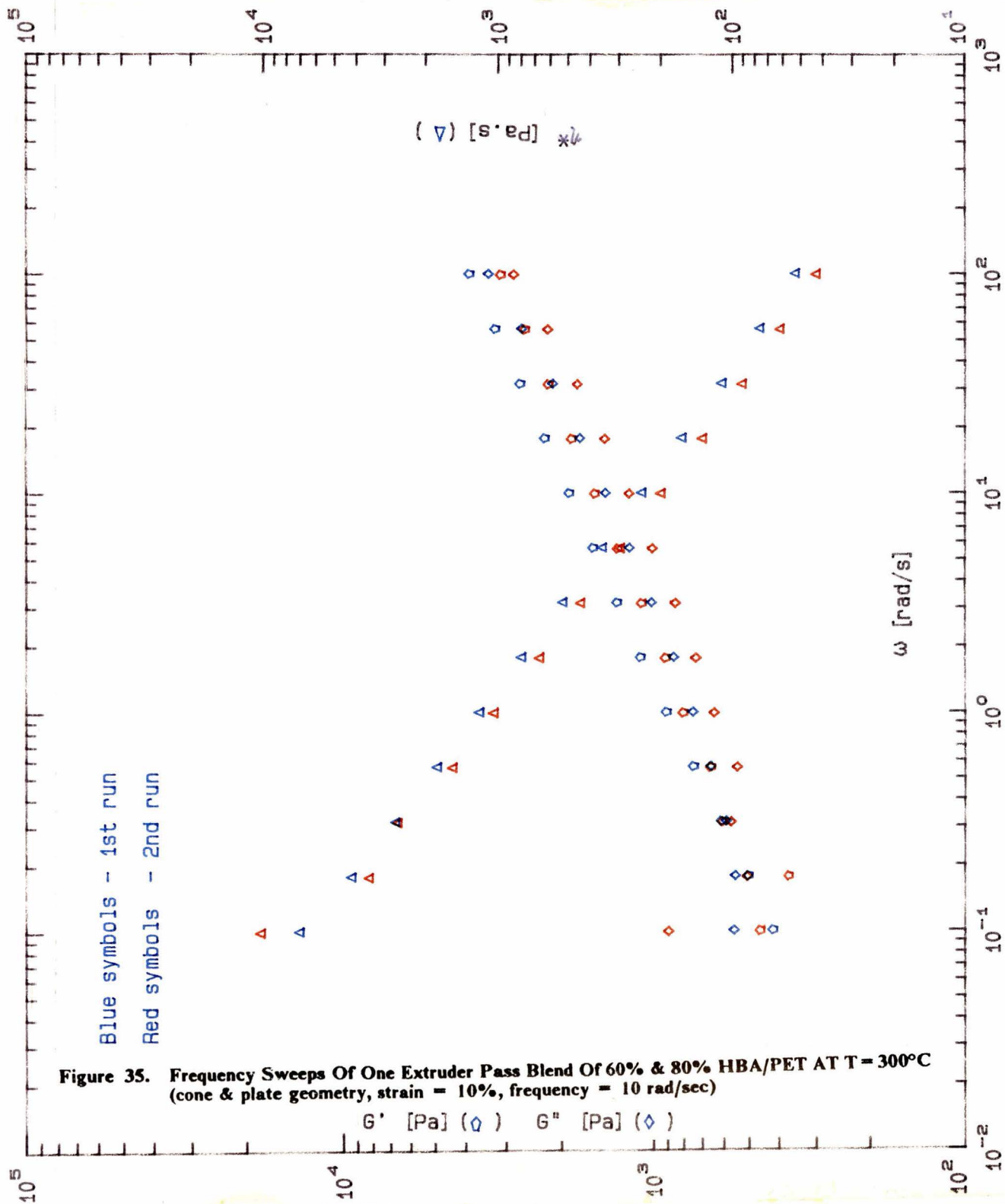
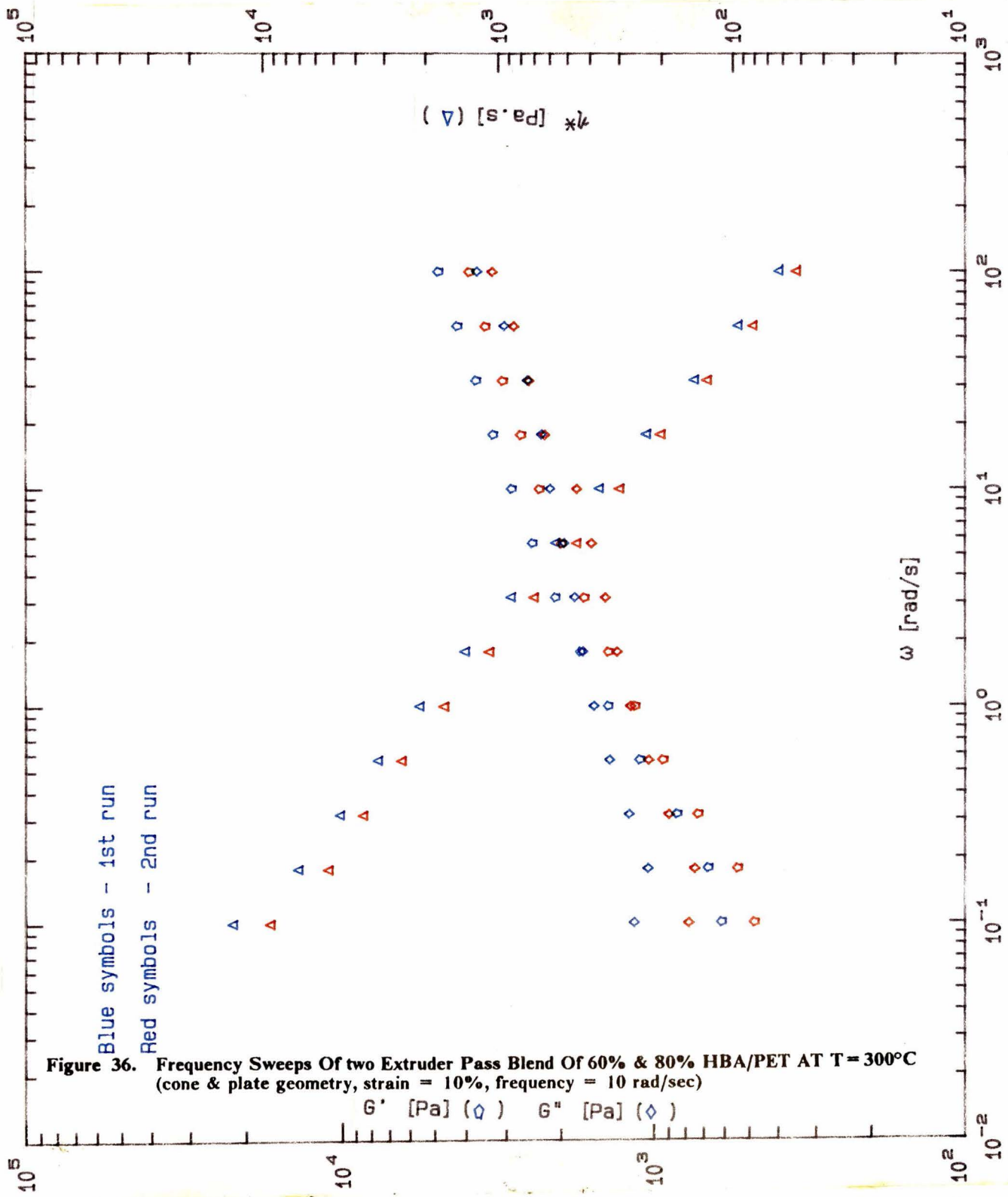
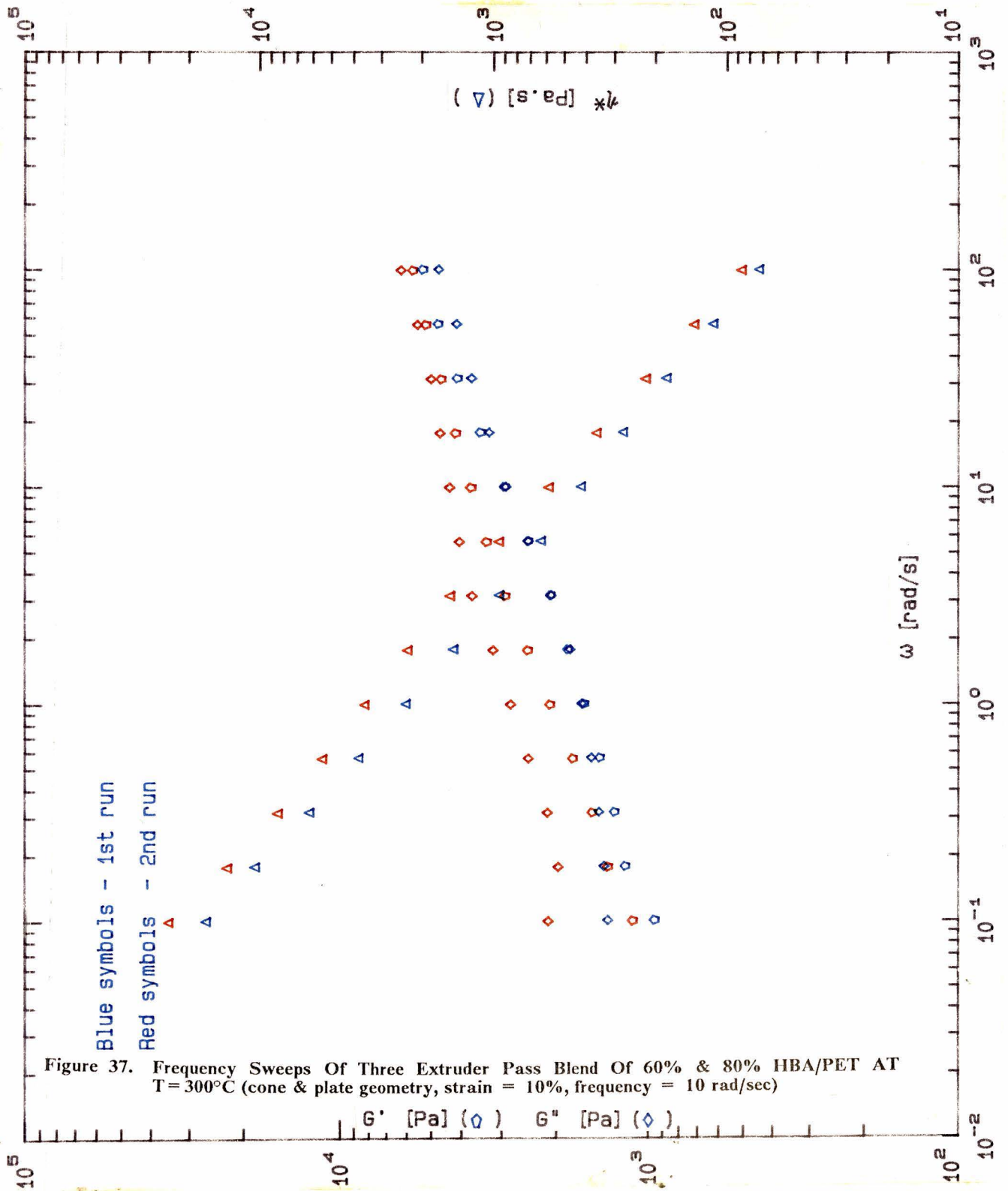


Figure 34. Strain sweep of the one extrusion pass blend at 290°C after the material had been subjected to a time sweep (frequency = 10 rad/sec, strain = 2%, time = 60 sec., 290°C)







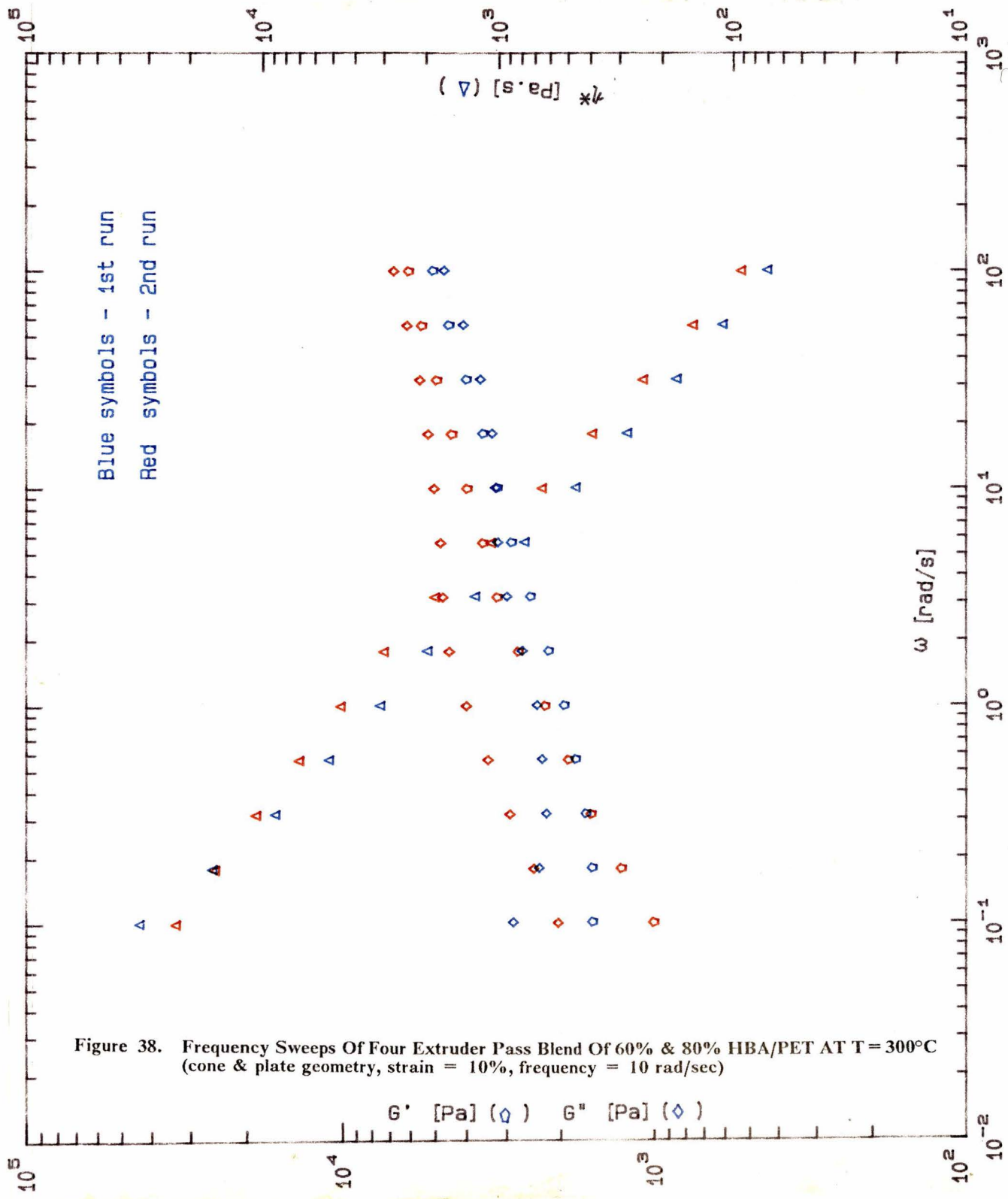


Figure 38. Frequency Sweeps Of Four Extruder Pass Blend Of 60% & 80% HBA/PET AT T = 300°C (cone & plate geometry, strain = 10%, frequency = 10 rad/sec)

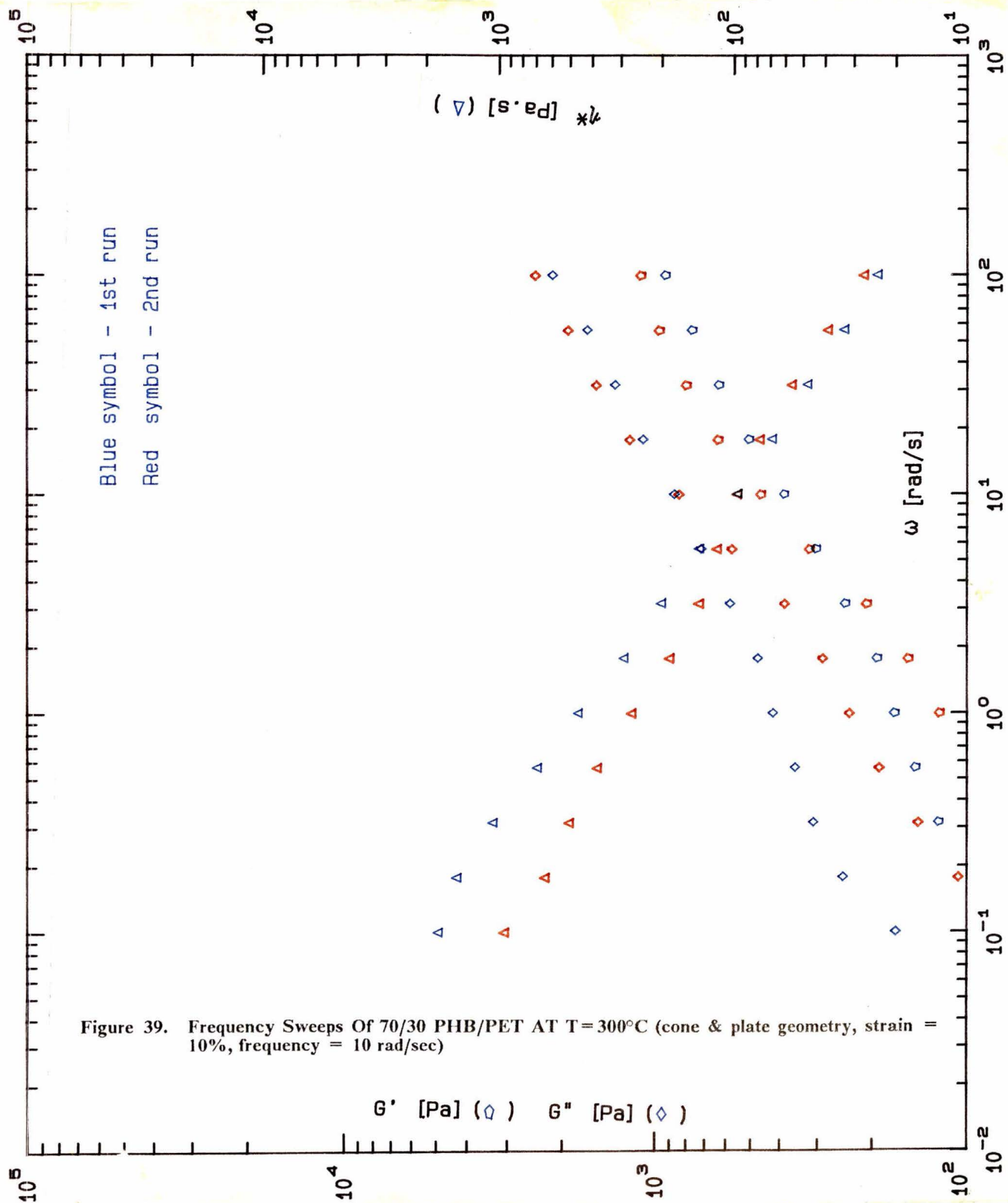


Figure 39. Frequency Sweeps Of 70/30 PHB/PET AT T=300°C (cone & plate geometry, strain = 10%, frequency = 10 rad/sec)

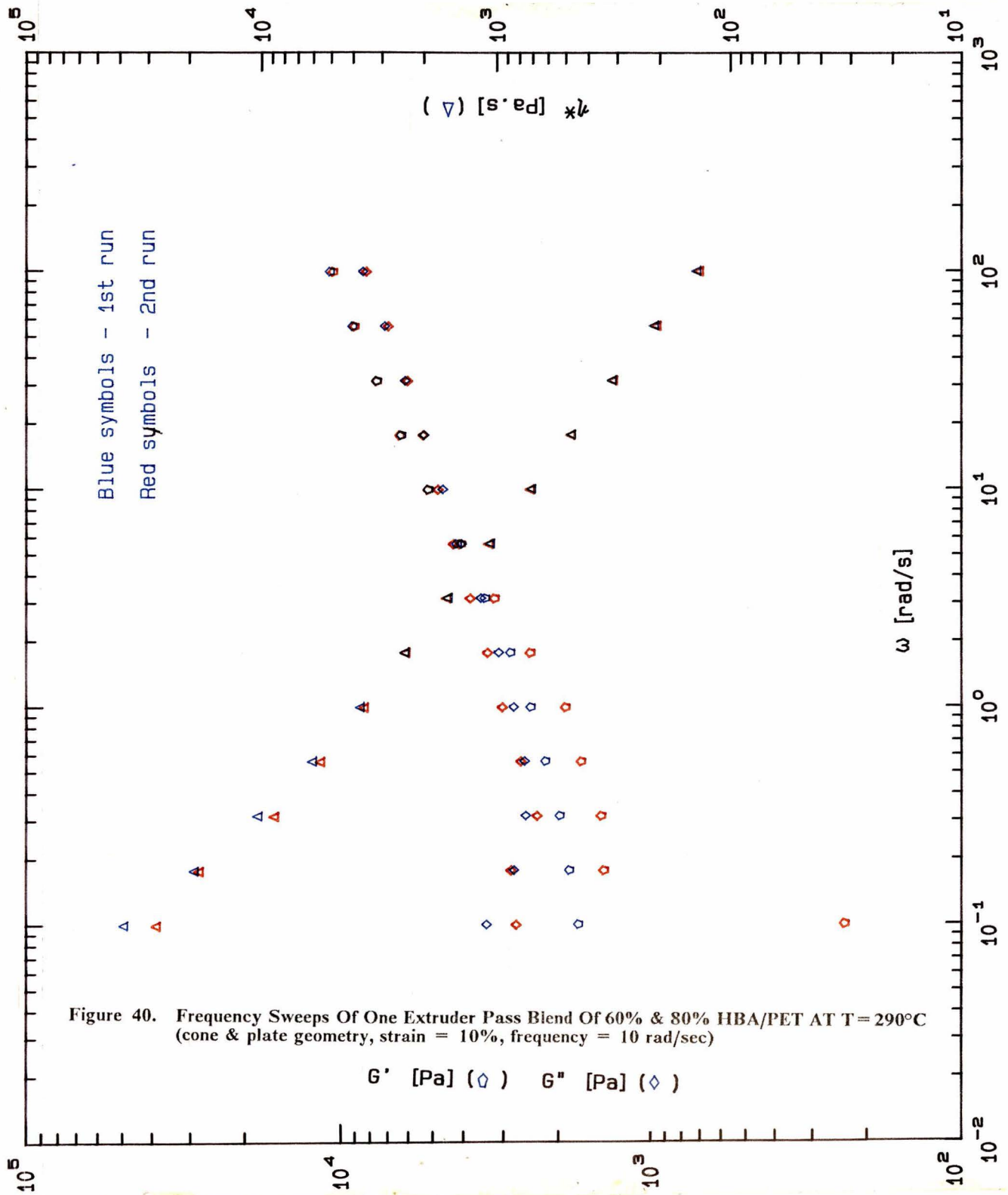


Figure 40. Frequency Sweeps Of One Extruder Pass Blend Of 60% & 80% HBA/PET AT T=290°C (cone & plate geometry, strain = 10%, frequency = 10 rad/sec)

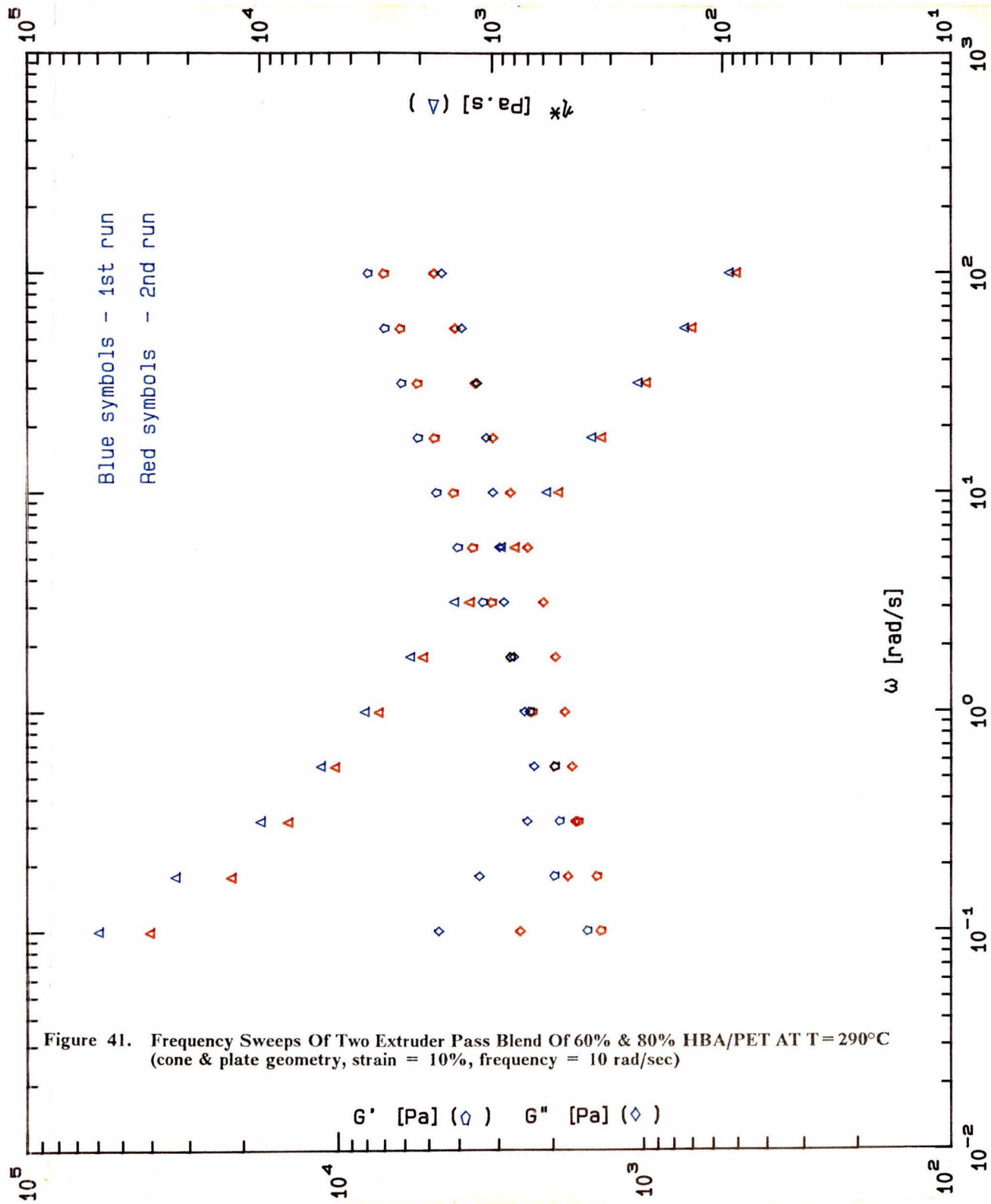


Figure 41. Frequency Sweeps Of Two Extruder Pass Blend Of 60% & 80% HBA/PET AT T = 290°C (cone & plate geometry, strain = 10%, frequency = 10 rad/sec)

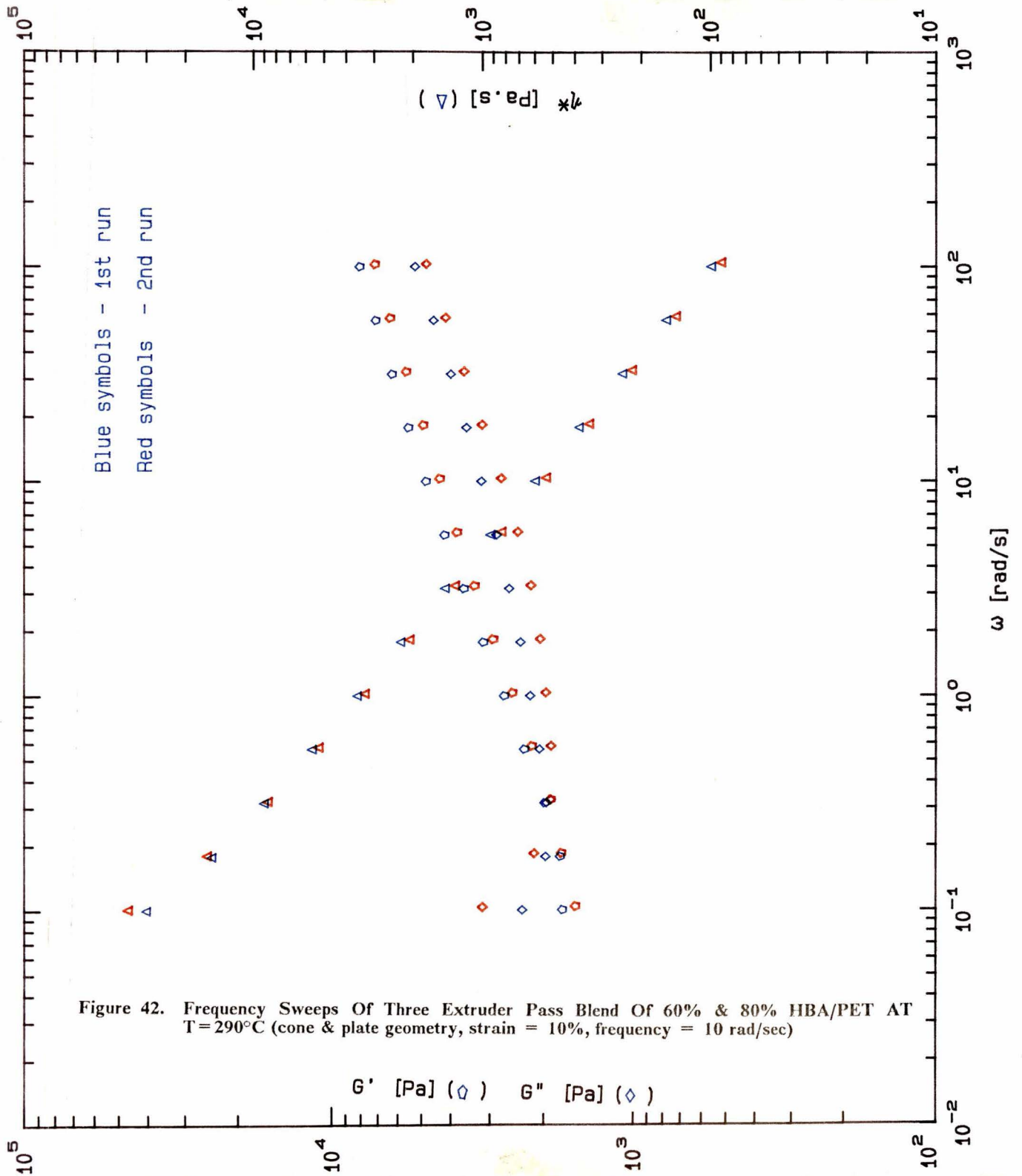


Figure 42. Frequency Sweeps Of Three Extruder Pass Blend Of 60% & 80% HBA/PET AT $T=290^{\circ}\text{C}$ (cone & plate geometry, strain = 10%, frequency = 10 rad/sec)

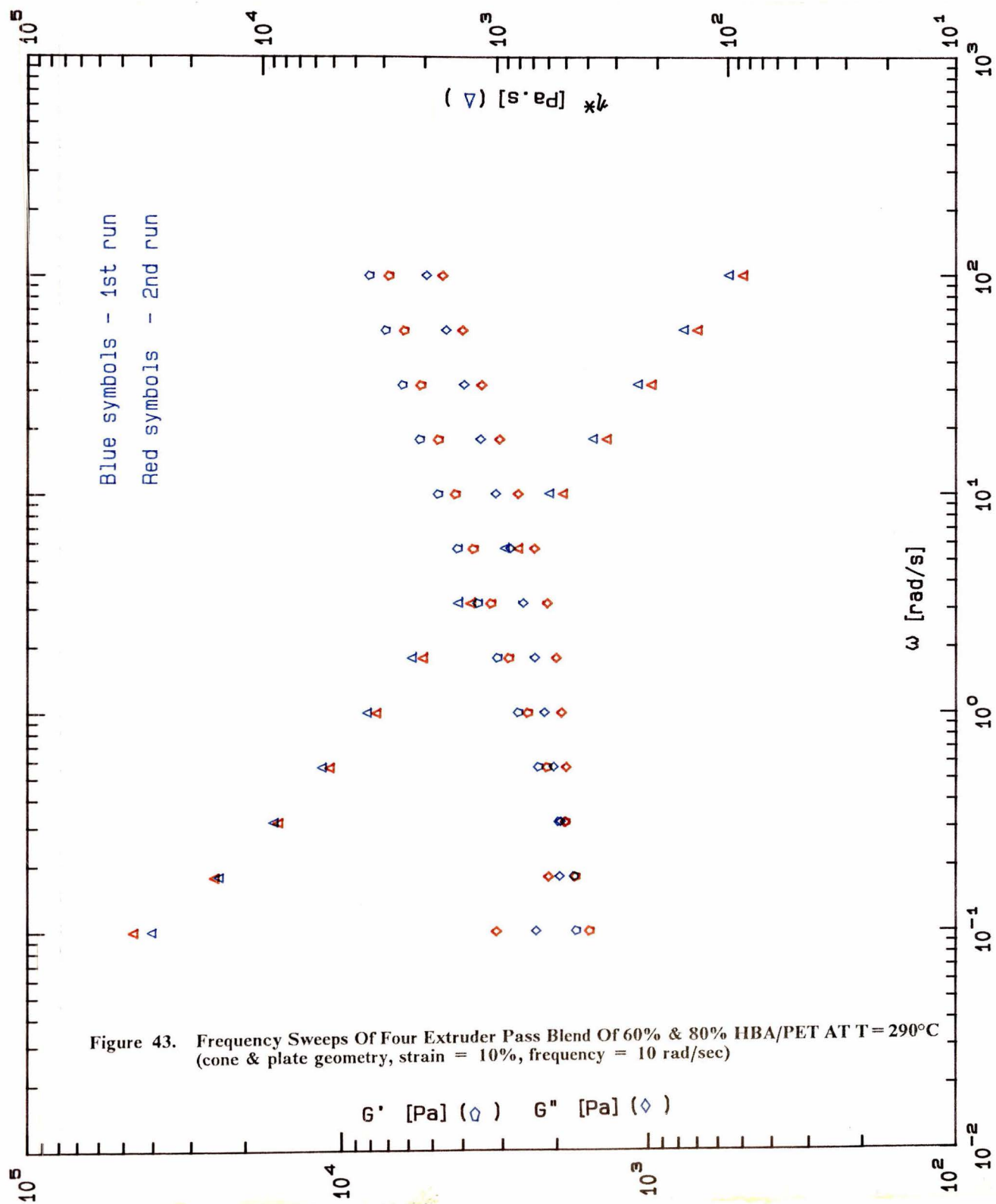


Figure 43. Frequency Sweeps Of Four Extruder Pass Blend Of 60% & 80% HBA/PET AT T = 290°C (cone & plate geometry, strain = 10%, frequency = 10 rad/sec)

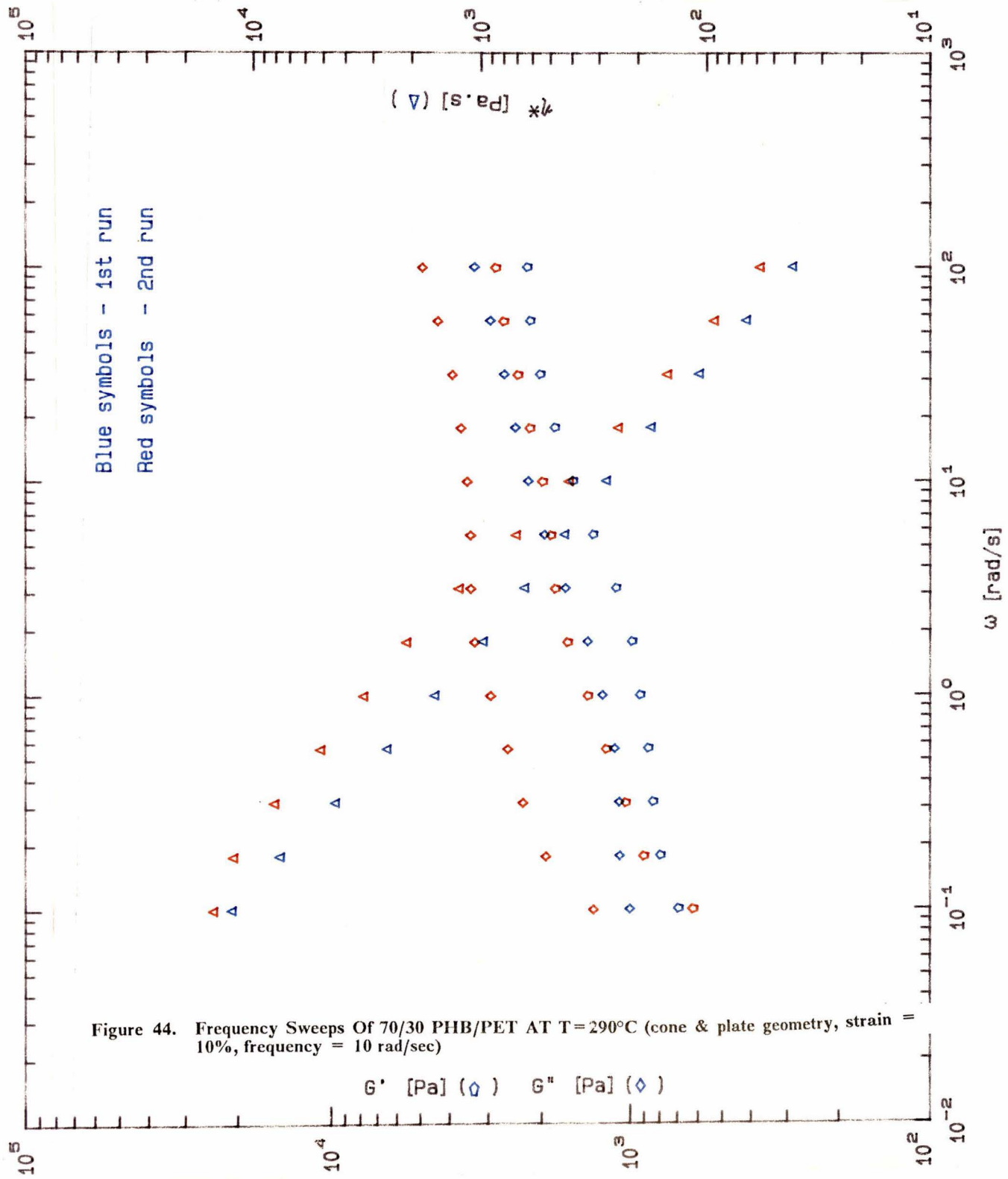


Figure 44. Frequency Sweeps Of 70/30 PHB/PET AT $T = 290^\circ\text{C}$ (cone & plate geometry, strain = 10%, frequency = 10 rad/sec)

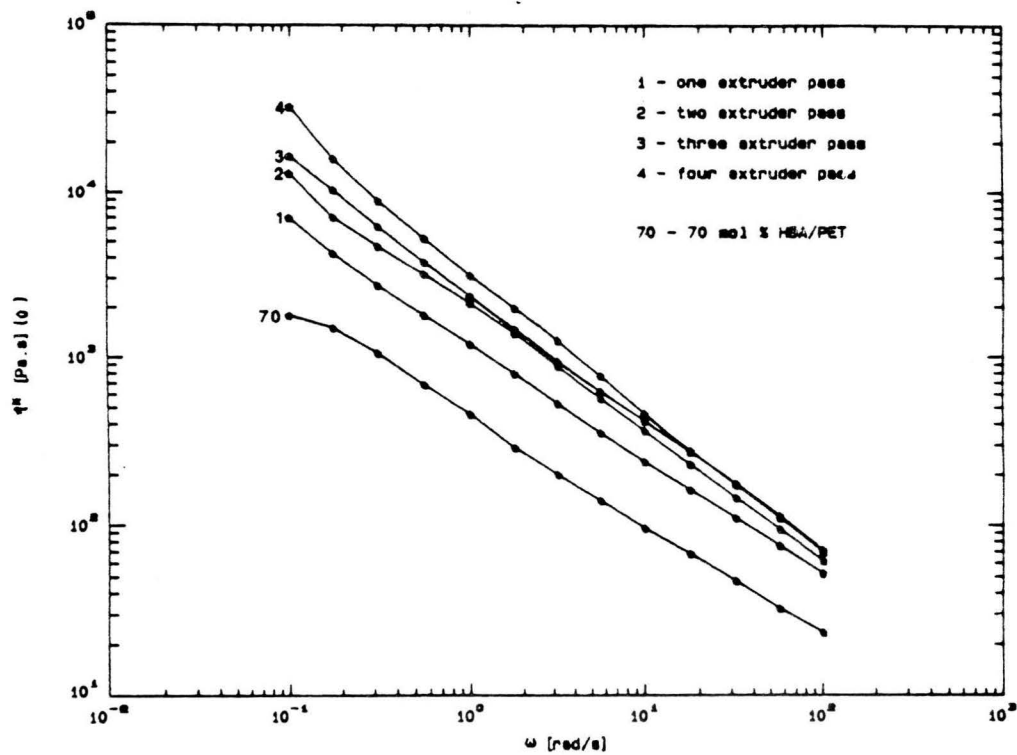


Figure 45. Dynamic Viscosity Of The Multiple Extrusion Pass Blends And 70/30 PHB/PET AT $T = 300^{\circ}\text{C}$ (cone & plate geometry, strain = 10%, frequency = 10 rad/sec)

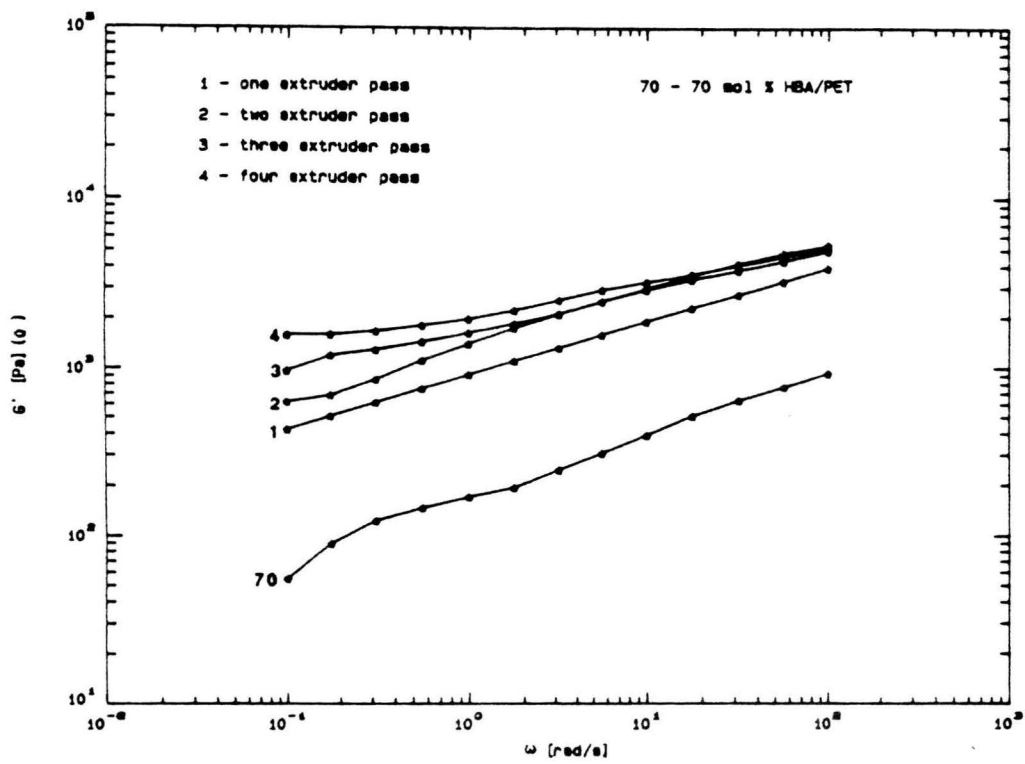


Figure 46. Storage Modulus Of The Multiple Extrusion Pass Blends And 70/30 PHB/PET AT T = 300°C (cone & plate geometry, strain = 10%, frequency = 10 rad/sec)

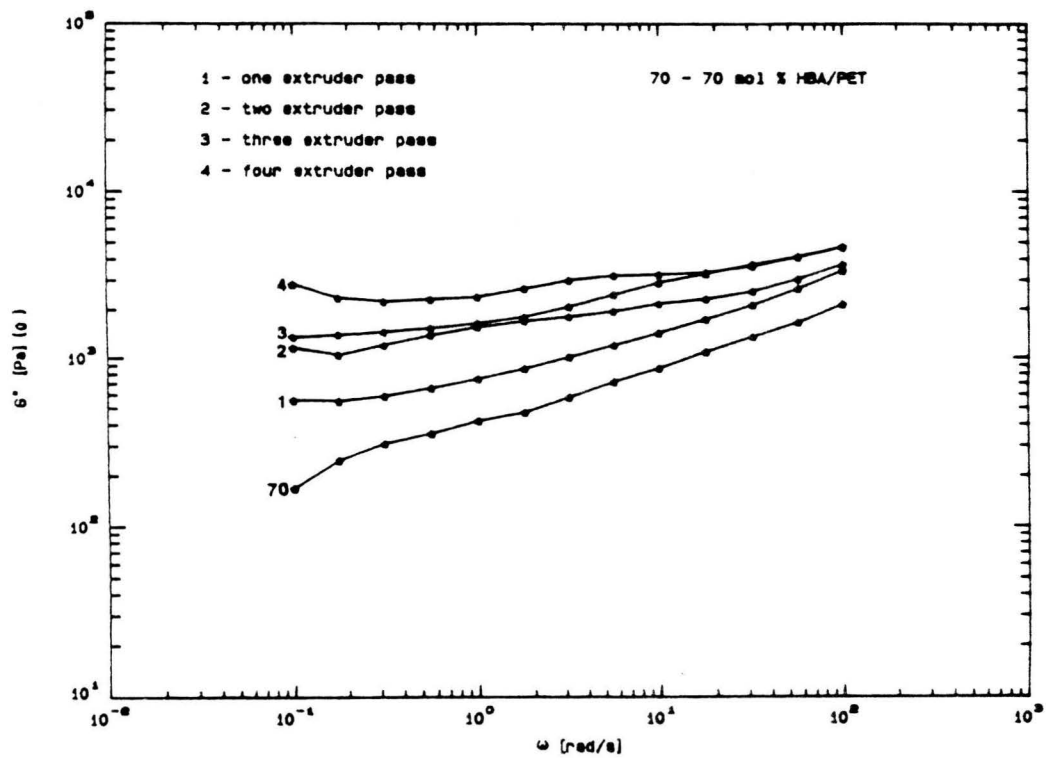


Figure 47. Loss Modulus Of The Multiple Extrusion Pass Blends And 70/30 PHB/PET AT T = 300°C (cone & plate geometry, strain = 10%, frequency = 10 rad/sec)

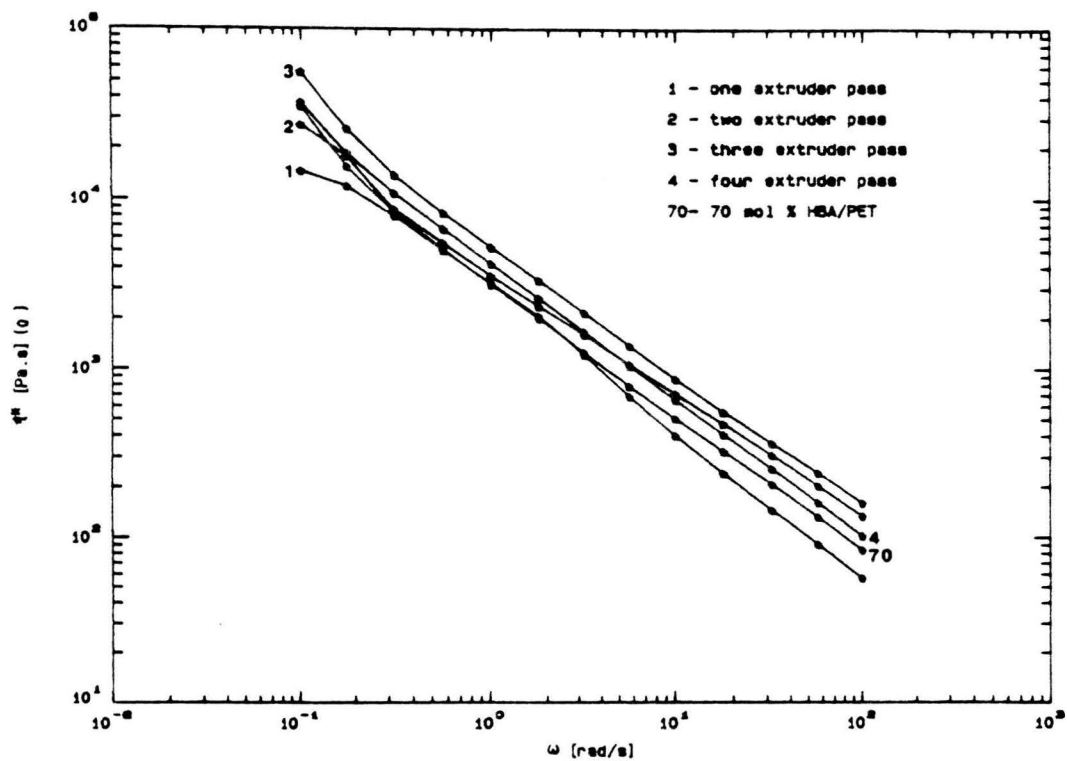


Figure 48. Dynamic Viscosity Of The Multiple Extrusion Pass Blends And 70/30 PHB/PET AT T=290°C (cone & plate geometry, strain = 10%, frequency = 10 rad/sec)

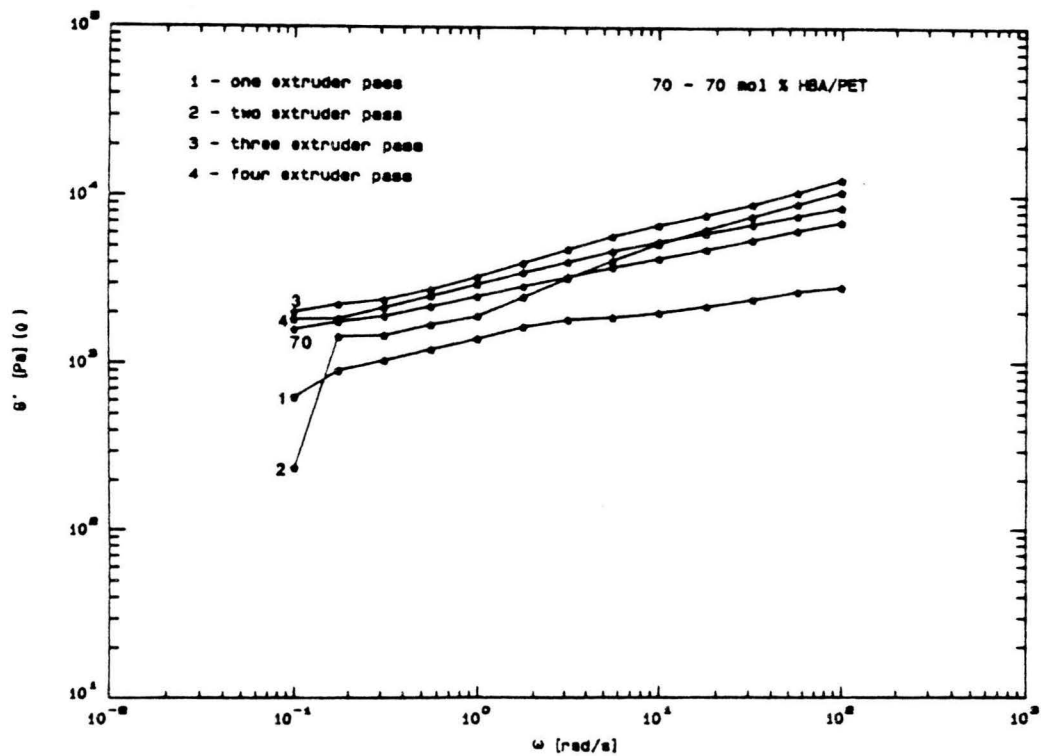


Figure 49. Storage Modulus Of The Multiple Extrusion Pass Blends And 70/30 PHB/PET AT T = 290°C (cone & plate geometry, strain = 10%, frequency = 10 rad/sec)

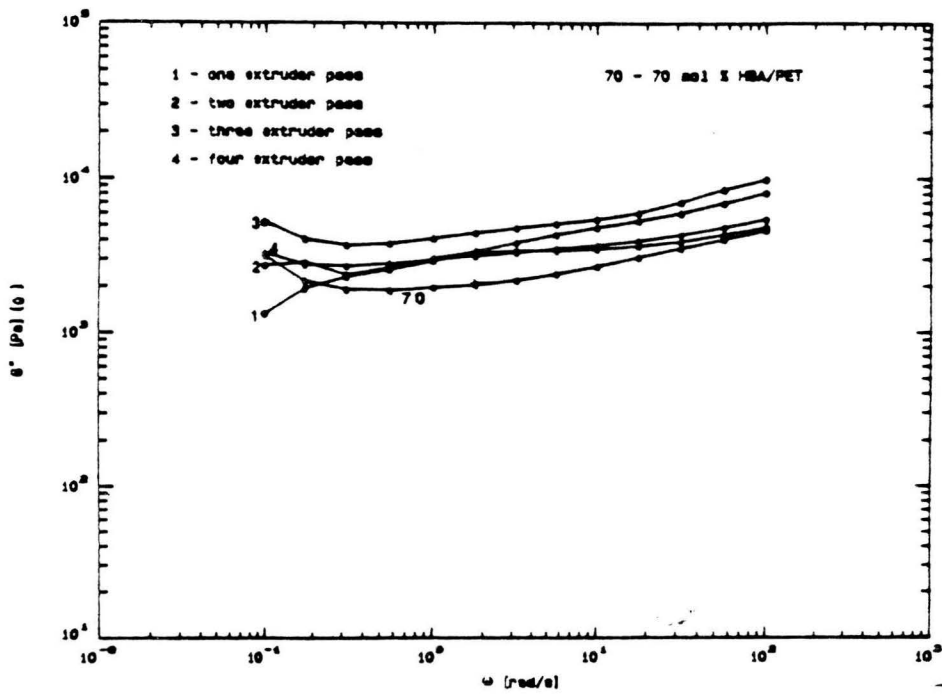


Figure 50. Loss modulus Of The Multiple Extrusion Pass Blends And 70/30 PHB/PET AT T = 290°C (cone & plate geometry, strain = 10%, frequency = 10 rad /sec)

garded as same for all the samples. However, the initial arrangement of the pellets on the plate would be different for each individual loading of the instrument. Thus, the initial texture at the start of the flow (lower frequencies) would be different for each run. This is so because of the extremely long relaxation time of the rigid chains. Another reason for the scatter might be that the composition of every pellet would not necessarily be the 50:50 weight% of the two copolyesters. Finally, the low values of the torque especially at low frequencies (which are near to the lowest limit of the transducer) would also contribute to the scattering of the data. Since the purpose of the rheological study was to find the changes in the rheology which might have been brought about by the occurrence of transesterification reaction, it was highly desirable that the thermal and shear history of all the multiple extrusion pass samples should be the same. However, as has been discussed above, the thermal and shear history effects can not be totally eliminated.

It was expected that at 290 and 300°C, the multiple extrusion pass samples will not completely melt. The DSC 'peak' temperature of the melting endotherm of the one extrusion pass sample is about 295°C. Additionally, the normal forces which develops when the gap of the cone & plate geometry is set, took a long time to relax. The DSC peak temperature of the melting endotherm of the 70/30 PHB/PET is about 270°C. For the 70/30 PHB/PET, the normal forces relaxed very quickly. Thus, in contrast to the 70/30 PHB/PET the multiple extrusion pass samples did not melt completely. Thus, no comparison between the extruded samples and the 70/30 PHB/PET is justifiable.

From Figs. 45-50, it can be seen that complex viscosity, storage modulus and loss modulus tend to increase with the increase in the number of extrusion passes. For the dynamic tests carried out at 290°C, this trend is observed for one, two and three extrusion pass samples. At 300°C, the complex viscosity increase from one extrusion pass samples to four extrusion pass sample. The increase in viscosity is unexpected. It is known that transesterification leads to a reduction in the average chain length, and thus a decrease in weight average molecular weight (49) and viscosity (38, 46, 47, 49, 52). One explanation for the observed increase in viscosity might be that since the difference in viscosity, storage modulus and loss modulus is significant only at lower shear rates, the difference in the initial polydomain structure might be responsible for this behavior. However, the

individual pellets are loaded on the plate in an essentially random fashion. Also the processing history of the multiple extrusion pass samples is nearly the same. Thus, the difference in the initial polydomain structure should lead to a random rather than the observed systematic increase in the rheological properties with the increase in the number of extrusion passes.

The second explanation might be that crystallization occurs in the extruder (formation of a more perfect crystal with the consequent increase in the rheological properties at near melt temperatures has been reported for a thermotropic liquid crystalline polymer (65, 66)). As has been discussed in detail in the literature review (section 2.5) the crystallization can occur in the extruder. Since the extrusion temperature is too low to completely melt out the PHB crystallinity, some residual crystallinity would be present in the melt during the extrusion. Thus the crystallization induced reaction proposed by Lenz et al. (25, 26) can theoretically take place in the melt, though at an extremely slow rate. This should lead to an increase in the melting temperature, degree of crystallinity and blockiness in the blend. The presence of some split peaks at temperature higher than 296°C was observed for the samples annealed at 310 and 300°C (Figs. 23 & 24). This would indicate that HBA crystallization might occur in the blend in the melt state. The crystalline solid can act as physical cross-links, tying the molecular chains together in a three-dimensional network, and therefore lead to an increase in the rheological functions (65, 66). However, for the four extrusion pass samples (Figs. 19 & 20) the split peaks were observed at a lower temperature than the high temperature peak temperature of the one extrusion pass samples. Also, the sheared blend (Figs. 25 & 26) exhibited a lowering of the melting point and degree of crystallinity with the increase in the reaction time. These effects are indicative of transesterification reaction. Thus, both crystallization-induced-reaction and transesterification reaction will occur in the blend in the melt state.

The third explanation might be that transesterification disturbs the two-dimensional mesophase order and thus the viscosity would increase (anisotropic phase, in general, has a lower viscosity than the isotropic phase due to the two-dimensional order (7, 8, 9, 10, 12, 13)). This explanation is supported by the study of Paci et al. (61) in which it was found that transesterification leads to a progressive reduction in the enthalpy of isotropization (smectic to isotropic transition).

It was proposed by the authors that the transesterification leads to a disruption of the chain periodicity and therefore, of the lamellar organization of the mesophase. This would also explain why the mechanical properties decrease on increase in the residence time in the extruder. This is so because as discussed in the literature review, it is the ability of the PHB/PET copolyesters to maintain a two dimensional mesophase order in the melt state (the ability of the rigid chains to orient easily and to maintain the induced orientation) which is responsible for their higher mechanical properties in comparison to those of PET. Thus if the mesophase order is affected by the transesterification reaction, it would follow that the mechanical properties will decrease with an increase in the residence time in the extruder. The evidence that the blend does exhibit the mesophase character is discussed in the next section.

From this work, we can conclude that the flexural properties of the injection-molded parts from the blend are higher than those of the 60/40 PHB/PET, 70/30 PHB/PET and 80/20 PHB/PET, and that it approaches the equilibrium composition of 70/30 PHB/PET due to the transesterification reaction.

4.6 Optical microscopy results

It was of interest to know if the thermal transitions observed by means of DSC corresponds to a change in the optical texture of these materials. The multiple extrusion pass samples were examined in a polarized light under the cross polarizers at a magnification of 350. The extruded pellets were hand pressed into thin films between the glass slides at 305°C and then cooled rapidly in a stream of nitrogen. No change in the optical texture could be observed as a function of temperature (from room temperature to 305°C) for any of the extruded materials. Also, similar optical texture was observed for all the multiple extrusion pass samples. A typical optical micrograph is shown in Fig. 51. From the micrograph, it is clear that the blend exhibits the mesophase order in the melt state. Also, since this texture is also observed at temperatures below the melt temperature, it follows that the mesophase can be largely quenched in the blend.



Figure 51. Optical Microstructure Of The 'One Extrusion Pass' blend (Magnification = 350) between the cross polars at 305°C

5. Conclusions and Recommendations

In this final chapter the conclusions and the recommendations for the future work are given. The purpose of this research was to find out if the mechanical properties of the blend are superior to those of 70/30 PHB/PET copolyester. The second question which was sought to be answered is whether a single pass through the extruder gives us an equilibrium composition blend. In addition to answering these questions, additional experiments were carried out in the RMS to give us a better understanding of the non-equilibrium nature of the blend. In section 5.1, conclusions regarding the mechanical properties of the blend are given. In section 5.2, conclusions about the equilibrium nature of the blend are summarized. In the process of answering these two questions, this work generated a whole new array of interesting questions. These questions along with the need for future work to further justify the assumptions and to supplement the conclusions made in this work are discussed in section 5.3.

5.1 Mechanical properties

1. The flexural modulus of the injection-molded plaques of a 50/50 blend of 60/40 PHB/PET and 80/20 PHB/PET mixed only in the injection-molding unit was 2.2×10^6 psi which is 40% higher

than that reported for the 60/40 PHB/PET, 100% higher than reported for either 80/20 PHB/PET or 70/30 PHB/PET compositions.

2. The tensile strength of the same composition was not significantly different from that of the 60/40 PHB/PET composition.

3. The tensile properties (tensile strength, modulus and elongation at break in the machine direction) of the blend (as a function of temperature) exhibit a maxima at 320°C. The properties of the blend increase with an increase in the injection-molding temperature (from 300 to 320°C) and then decrease.

4. The flexural modulus and strength of the blend decrease with an increase in the residence time in the extruder. For example, the flexural modulus decreased from 15,781 MPa for the 'zero extrusion pass' blend to only 8,847 MPa for the 'four extrusion pass' blend.

5. There was no significant change in the tensile strength and modulus of the blend with an increase in the residence time in the extruder.

6. The modulus versus temperature profile (softening profile) of the blend was independent of the residence time in the extruder for a residence time of less than about 4.5 minutes. The TMA results showed that the softening profiles of one, two and three extrusion pass blends were the same but that of the four extrusion pass blend was different and was closer to the softening profile of the 70/30 PHB/PET composition.

the observed changes in the thermal behavior of the blend with an increase in the reaction time are indicative of transesterification reaction. For example, multiple peaks were observed in the DSC thermograms of the 'four extrusion pass' blend and also for the blend heated above the melting temperature for different lengths of time. The multiple peaks can be considered to be indicative of an incomplete transesterification reaction. Similarly, the DMA results showed a decrease in the melting temperature of the blend with an increase in the residence time in the extruder. Similar decrease in the melting temperature with an increase in the reaction time was observed for the blend which had been subjected to a simple shear field for different lengths of time. The decrease in the melting temperature is indicative of transesterification reaction.

2. The 'induction time' (i.e. the time before which significant reaction has not taken place) for the transesterification reaction in the blend depends on both the reaction conditions and the sensitivity of the measuring instrument. For the 'multiple extrusion pass' blends, no significant change in the thermal behavior of the one, two and three extrusion pass blend was observed. However, the DSC thermograms of the 'four extrusion pass' blend showed multiple peaks which are indicative of transesterification reaction. Thus, an induction time of 4.5 minutes (residence time of 'three extrusion pass' blend) to 6.0 minutes (residence time of 'four extrusion pass' blend) would be indicated by the DSC results of the 'multiple extrusion pass' blend. Similarly, the TMA results would imply an induction time of about 4.5-6.0 minutes since the softening profiles of the one, two and three extrusion pass blends were the same. In contrast to the DSC and TMA results, the DMA results showed that the melting temperatures of all the 'multiple extrusion pass' blends were different. Thus, the DMA results would point to an absence of any induction time (or an induction time of less than 1.5 minutes which is the the average residence time of the 'one extrusion pass' blend). For the transesterification reaction in the blend outside the extruder (in the RMS), there was an induction time of 3-5 minutes (at 300°C) and 10-15 minutes (at 310°C) as indicated by the appearance of multiple peaks in the corresponding DSC thermograms.

3. The transesterification reaction leads the blend towards the equilibrium composition of 70/30 PHB/PET. The DMA results showed that the melting temperature of the 'four extrusion pass' blend was approximately equal to that of the 70/30 PHB/PET copolyester. Also, the DSC study indicated that the structure of the blend which has been subjected to a shearing environment (in the RMS) for 18 minutes was close to that of the 70/30 PHB/PET composition.

4. The transesterification reaction proceeds faster in the presence of deformation such as occurs in the extruder or in a simple shear flow and with an increase in temperature. These results are based on a comparison of the thermal behavior of the blend (as a function of temperature) in different environments. It was found that the formation of multiple peaks is observed in the DSC thermograms of the samples which had been annealed for 5 minutes (at 310°C) and 15 minutes (at 300°C). In contrast to this, multiple peak formation in the 'multiple extrusion pass' blend was observed for the 'four extrusion pass' blend (the residence time of the 'four extrusion pass' blend is only 6 minutes and the melt temperature at the exit of the extruder was about 290°C). Also, a decrease in the melting temperature and the corresponding enthalpy was observed with an increase in the reaction time for the blend which had been subjected to a simple shear field. The conclusion that the transesterification reaction rate increase with an increase in temperature is based on the DSC results of the blend annealed at 310°C and 300°C. It was observed that the splitting of the higher temperature peak not only starts earlier for the blend annealed at 310°C but also is much more pronounced.

5.3 Recommendations

1. It was observed that the flexural properties of the blend decrease to a greater extent as compared to the tensile properties with the increase in the number of extrusion passes. The proposed explanation which links this to the transesterification reaction in the blend was that the chemical reaction affects the two-dimensional mesophase order in the blend. This would in turn affect the skin layer

which affects the flexural properties to a greater extent in comparison to the tensile properties. Thus, a study to check this explanation should be done. Specifically, the study should target the following two questions:

1. Does the formation of a highly oriented skin layer occur in the injection-molded parts of the blend (which would affect the flexural properties to a greater extent than the tensile properties)?
2. Does transesterification reaction affect the skin layer?

To answer the first question, mechanical properties of the injection-molded plaques of different thickness should be determined. The skin-core morphology should lead to a decrease in the mechanical properties with an increase in the sample thickness. Also, wide-angle x-ray scattering and scanning electron microscopy study on the microtomed layers (33) can indicate the oriented skin and a less oriented core morphology. To answer the second question, a suitable transesterification reaction catalyst should be found (typically, heavy metals catalyze the transesterification reaction). A comparison of the mechanical properties and the morphology of the plaques obtained from the blends (with and without the catalyst in the injection-molder) should clearly show whether the transesterification reaction affects the skin layer.

2. It was found that there is no significant change in the flexural properties of the zero extrusion pass and one extrusion pass samples of pure 60/40 PHB/PET and pure 80/20 PHB/PET. It was proposed that compared to the blend, the transesterification reaction in the extruder for pure 60/40 and 80/20 PHB/PET compositions is not significant. Thus, further studies on the occurrence of transesterification reaction in pure 60/40 and pure 80/20 PHB/PET compositions should be done. The pure compositions should be passed a number of times through the extruder. The extruded products should be sufficiently dried before the next extrusion pass. The extruded products should then be examined by means of the DSC to detect the changes in their thermal behavior. Also, as was done in this study, the extruded products can also be examined by means of the DMA, TMA, SEM and RMS. Additionally, transesterification studies can also be done on the pure 60/40 and 80/20 PHB/PET polyesters which have been annealed above their melting points outside the extruder environment.

3. Transesterification studies should also be carried out in the as received 70/30 PHB/PET copolyester. In this work, this non-random 70/30 PHB/PET was regarded as the equilibrium composition. The true equilibrium composition towards which the transesterification reaction would cause the blend to approach should be a totally random 70/30 PHB/PET. It would be of interest to know when the transesterification reaction is 'complete' in the blend. To accomplish this, the blend should be annealed above its melting point for different lengths of time. The annealed products can be examined by means of the DSC. When no change in the thermal behavior with the reaction time occurs, it can be concluded that transesterification reaction is 'complete' in the blend. The thermal behavior of the fully transesterified blend should be same as that of the fully transesterified as received 70/30 PHB/PET polyester.

4. Degradation studies should be carried out in the blend. Also, it would be interesting to know the effect of transesterification on the molecular weight and the molecular weight distribution. Transesterification reaction leads to a reduction in the molecular weight and in the ratio of the weight-average molecular weight and number-average molecular weight. The molecular weights, molecular weights distributions and the ratio of weight-average molecular weight and number-average molecular weight for transesterified condensation polyesters have been theoretically computed by Kotliar, A. M. (78). A comparison of the results should be made with the results of Kotliar (78).

5. Transesterification in the blend can be even further confirmed by a solubility test. A solvent should be chosen in which only one of the copolyesters (60/40 or 80/20 PHB/PET) is soluble. The solubility of either the blend transesterified to varying degrees (i.e. the multiple extrusion pass blends) or of the one extrusion pass samples above the melt temperature as a function of time should then be monitored. Care should be taken to select the right solvent. A solvent like deuterated trifluoroacetic acid can not be recommended as a solvent (even though it only dissolves 60/40 PHB/PET), since it is likely to catalyze the transesterification reaction.

Bibliography

1. Jackson, W.J., Jr. and Kuhfuss, H.F., *Journal Of Polymer Science; Polymer Chemistry Edition*, Vol 14, 2043-2058, 1976
2. Zachariades, A.E., Economy, J. and Logan, J.A., *Journal Of Applied Polymer Science*, Vol 27, 2009-2014, 1982
3. Viney, C., Windle, A.H., *Journal Of Materials Science*, 17, 2661-2670, 1982
4. Meesiri, W., Menczel, J., Gaur, U. and Wunderlich, B., *Journal Of Polymer Science: Polymer Physics Edition*, Vol. 20, 719-728, 1982
5. Zachariades, A.E. and Logan, J.A, *Polymer Engineering And Science*, October, 1983, Vol.23, No.15
6. Menczel, J. and Wunderlich, B., *Journal Of Polymer Science: Polymer Physics Edition*, Vol.18, 1433-1438, 1980
7. Papkov, S.P., Kulichikhin, V.G., Kalmykova, V.A. and Malkin, A.Y., *Journal Of Polymer Science: Polymer Physics Edition*, 12, 1753, 1974
8. Baird, D.G., *Journal Of Rheology*, 24(4), 465-482, 1982
9. Wissbrun, K.F., *Journal Of Rheology*, 25(6), 619-692, 1981
10. Simoff, D.A. and Porter, R.S., *Mol. Cryst. Liq. Cryst.*, 110, 1, 19 84
11. Viney, C., Mitchell, G.R., and Windle, A.H., *Polymer Communication* s, 1983, vol.24, 145
12. Suto, S, White, J.L., and Fellers, J.F., *Rheological Acta*, 21, 62, 1982
13. Wissbrun, K.F. and Griffin, A.C., *Journal Of Polymer Science: Polymer Physics Edition*, Vol 20, 1835-1845, 1982

14. Joseph, E.G., Wilkes, G.L., and Baird, D.G., *Polymer Engineering And Science*, May 1985, Vol 18, No. 7
15. Tadmor, G., *Journal Of Applied Polymer Science*, Vol 18, 1753-1772, 1974
16. Ophir, Z. and Ide, Y., *Polymer Engineering And Science*, Mid October, 1983, Vol 23, No. 14
17. Acierno, D., La Mantia, F.P., Polzotti, G., Ciferri, A., and Valenti, B., *Macromolecules*, Vol 15, 1455, 1982
18. Baird, D.G., Sun, T., Done, D.S., and Ramanathan, R., To Be Published
19. Muramatsu, H. and Krigbaum, W.R., *Journal Of Polymer Science: Polymer Physics Edition*, Vol 25, 2303-2314, 1987
20. Muramatsu, H. and Krigbaum, W.R., *Journal Of Polymer Science: Polymer Physics Edition*, Vol 24, 1695, 1986
21. Muramatsu, H. and Krigbaum, W.R., *Journal Of Polymer Science: Polymer Physics Edition*, 25, 803, 1987
22. Viola, G.G., Done, D.S., and Baird, D.G., *SPE ANTEC Technical Papers*, 31, 619, 1985
23. Cogswell, F.N., *The British Polymer Journal*, Dec., 1980
24. Wissbrun, K.F., *The British Polymer Journal*, 12, 163, 1980
25. Lenz, R.W., and Schuler, A.N., *Journal Of Polymer Science: Polymer Symposium*, 63,343, 1978
26. Lenz, R.W., Jin, J., and Feichtinger, K.A., *Polymer*, 1983, Vol 24, March
27. Sugiyama, H., Lewis, D.N., White, J.L., Fellers, J.F., *Journal Of Applied Polymer Science*, Vol 30, 2329, 1985
28. McFarlane, F.E., Nicely, V.A., and Davis, T.G., *Contemporary Topics In Polymer Science*, Vol 2, Pearce, E.M. and Schafgen, J.R., EDS., Plenum, New York, 1976
29. Wunderlich, B., *Macromolecular physics*, Vol 3, Crystal melting, Academic, New York, 1980
30. Krigbaum, W.R. and Salaris, F., *Journal of Polymer Science: Polymer physics Edition*, Vol 16, 8835, 1978
31. Zhou, C. and Clough, S.B., *Polymer Engineering And Science*, Jan., 1988, Vol. 28, No.2
32. Wunderlich, B., *Macromolecular Physics*, Vol 1, Crystal Structure, Morphology, Defects, Academic, NY, 1973
33. Joseph, E., Wilkes, G.L., and Baird, D.G., *Polymer*, 1985, Vol 26, May
34. Nicely, V.A., Dougherty, J.T., and Renfro, L.W., *Macromolecules*, 1987, 20, 573-576
35. Sun, T., and Porter, R.S., To Be Published.

36. Done, D and Baird, D.G., *Polymer Engineering And Science*, 27, 816, 1987
37. Ramanathan, R., Mehta, R., Done, D., and Baird, D.G., *SPE ANTEC Technical Papers*, 1989
38. Flory, P.J., *J. Am. Chem. Soc.*, 62, 2255(1940)
39. Korshak, V.V., and Vinogradova, S.V., *Izv. Akad. Nauk sssr Old. Khim. Nauk*, 1951, 756; *Chem. Abstr.*, 46, 7527d(1952)
40. Korshak, V.V., Bekasova, N.I., and Zamyatina, V.A., *Izv. Akad. Nauk. SSSR Old. Khim. Nauk*, 1958, 614, *Chem. Abstr.*, 52, 20028d(1958)
41. Vereinigte Glanzstoff-Fabriken A.G, *British Patent* 755,071, Aug. 15, 1956; *Chem. Abstr.*, 51, 7057h (1957)
42. Zeidler, I.I., and Shkolman, E.E., *Zh. Prikl. Khim.*, 26, 410(1953); *Chem. Abstract.* 48, 7587a(1954)
43. Korshak, V.V., and Vinogradova, S.V., *Izv. Akad. Nauk SSSR Old. Khim. Nauk*, 1953, 951; *Bull. Acad. Sci. USSR, Div. Chem. Sci.*, (English Transl.) 1953, 125; *Chem. Abstr.*, 49, 866d(1955)
44. Kursonov, V.N., Korshak, V.V. and Vinogradova, S.V., *Chem. Abstr.* 48, 3912g(1954)
45. Kimura M., Salee G., and Porter R., *J. of App. Polymer Sci.*, Vol 29, 1629-1638(1984)
46. Kimura M., Porter R.S., *J. of Poly. Sci. : Polymer physics edition*, Vol. 21, 367-378(1983)
47. Kresse, P., *Faserforsch. Textiltech.*, 11, 353(1960); *Chem. Abstr.*, 54, 23340c(1960)
48. Wahrmund D.C., Paul D.R., and Barlow J.W., *J. of Applied Polymer Science*, Vol. 22, 2155-2164(1978)
49. Flory, P.J., *J. of Am. Chem. Soc.*, 62, 1057(1940)
50. Rafikov, S.R., Korshak, V.V., and Chelnokova, G.N., *Chem. Abstr.* 48, 12674g(1954)
51. Devaux, J., Godard, P., and Mercier, J.P., *Polymer Engineering Science*, March 1982, Vol. 22, No. 4
52. Griel, W. and Schnock, G., *Faserforsch. Textiltech.*, 8, 408(1957); *Chem. Abstr.*, 52, 11781b(1958)
53. Korshak, V.V., Bekasova, N.I., and Zamyatina, V.A., *Chem. Abstr.*, 52, 17167f(1958)
54. Skwarski, T., *Chem. Abstr.* 51, 1704e(1957)
55. Korshak, V.V. and Vinogradova, S.V., *Chem. Abstr.*, 48, 9919d(1954)
56. Griel, W., and Forster, P.F., *Chem. Abstr.*, 51, 3179b(1957)
57. Reimschuessel, H.K., *Ind. Eng. Chem. Prod. Res. Dev.*, 1980, 19, 117-125
58. Allport, D.C. and Mohajer, A.A., *Block copolymers* 265-270

59. Droscher, M., and Schmidt, F.G., *Polymer Bull.*,4,261(1981)
60. Imperial Chemical Industries, Ltd., British Patent 760,125 (by Burton, W.R. and Davies, D.S.), Oct. 31, 1956; *Chem. Abstracts*, 51, 7733a, 1957
61. Paci, M., Barone, C., and Luigi, P., *Journal Of Polymer Science: Part B: Polymer Physics*, Vol 25, 1595, 1987
62. Yamudra, R. and Murano, M., *Jouranal Of Polymer Science: Part A-1*, Vol.5, 2259, 1967
63. Odian, G., *Principles of Polymerization*, p.24, Wiley Interscience, 1981
64. Flory, P.J., *Journal Of Chemical Society*, 2261, 1940
65. Lin, Y.G., and Winter, H.H., To Be Published
66. Lin, Y.G., and Winter, H.H., To Be published
67. *Polymeric Liquid Crystals*, Blumstein, Pa.21, Noel, C.
68. Turi, E.A., 'Thermal characterization of Polymeric materials', Academic Press, 1981
69. Macknight, W.J., and Karasz, F.E., Chapter 5, 'Polymer Blends, Paul, R., and Newman, S., Vol.1, Academic press, 1978'
70. Wendlandt, W.W., 'Thermal methods of Analysis, John Wiley and Sons, 1974
71. Rheometrics Mechanical Spectrometer, Operation Manual
72. Rheometrics Mechanical Spectrometer, Reference Manual
73. Tadmor, Z. and Gogos, C.C., 'Principles of Polymer Processing', John Wiley and Sons, 1979
74. Arburg Injection-molder, Operation Manual
75. Antwerpen, F.N., and Krevelen, D.W.N., *Journal Of Polymer Science, Polymer Physics Edition*, Vol.10, 2423-2435, 1972
76. Bassett, D. C., Olley, R. H., and Raheil, I. A. M., *Polymer*, Vol.29 , 1745, 1988
77. *Treatise on solid state chemistry*, Plenum 1976, Ed. Hannay, N. B., Vol. III, Chapter 7
78. Kotliar, A. M., *Journal Of Polymer Science, Polymer Chemistry Edition*, 6, 1157, 1973

**Appendix A. The rheological data of 'multiple
extrusion pass' blends And 70/30 PHB/PET
copolyester**

Table A1. Strain sweep of the one extrusion pass blend at 290°C (cone & plate geometry, frequency = 10 rad/sec)

| NO. | *STRAIN | G' Pa | G'' Pa | ETA* Pa. s |
|-----|-----------|-----------|-----------|---------------|
| 1 | 1.995e+00 | 2.782e+03 | 1.787e+03 | 3.307e+02 |
| 2 | 3.904e+00 | 2.386e+03 | 1.572e+03 | 2.858e+02 |
| 3 | 5.806e+00 | 2.153e+03 | 1.482e+03 | 2.614e+02 |
| 4 | 7.706e+00 | 1.972e+03 | 1.412e+03 | 2.425e+02 |
| 5 | 9.598e+00 | 1.839e+03 | 1.363e+03 | 2.290e+02 |
| 6 | 1.150e+01 | 1.730e+03 | 1.334e+03 | 2.184e+02 |
| 7 | 1.339e+01 | 1.642e+03 | 1.336e+03 | 2.117e+02 |
| 8 | 1.529e+01 | 1.552e+03 | 1.325e+03 | 2.041e+02 |
| 9 | 1.719e+01 | 1.466e+03 | 1.295e+03 | 1.956e+02 |
| 10 | 1.908e+01 | 1.422e+03 | 1.295e+03 | 1.924e+02 |
| 11 | 2.098e+01 | 1.342e+03 | 1.255e+03 | 1.837e+02 |
| 12 | 2.287e+01 | 1.249e+03 | 1.203e+03 | 1.734e+02 |
| 13 | 2.477e+01 | 1.170e+03 | 1.156e+03 | 1.645e+02 |
| 14 | 2.667e+01 | 1.093e+03 | 1.101e+03 | 1.552e+02 |
| 15 | 2.856e+01 | 1.021e+03 | 1.057e+03 | 1.469e+02 |
| 16 | 3.046e+01 | 9.631e+02 | 1.032e+03 | 1.412e+02 |
| 17 | 3.236e+01 | 9.096e+02 | 9.991e+02 | 1.351e+02 |
| 18 | 3.425e+01 | 8.627e+02 | 9.771e+02 | 1.303e+02 |
| 19 | 3.615e+01 | 8.190e+02 | 9.546e+02 | 1.258e+02 |
| 20 | 3.806e+01 | 7.782e+02 | 9.310e+02 | 1.213e+02 |

Table A2. Strain sweep of the one extrusion pass blend at 290°C after the material had been subjected to a time sweep (frequency = 10 rad/sec, strain = 2%, time = 60 sec., 290°C)

| NO. | %STRAIN | G' Pa | G'' Pa | ETA* Pa.s |
|-----|-----------|-----------|-----------|--------------|
| 1 | 1.995e+00 | 3.067e+03 | 1.830e+03 | 3.571e+02 |
| 2 | 3.904e+00 | 2.569e+03 | 1.635e+03 | 3.045e+02 |
| 3 | 5.806e+00 | 2.382e+03 | 1.582e+03 | 2.860e+02 |
| 4 | 7.706e+00 | 2.303e+03 | 1.557e+03 | 2.780e+02 |
| 5 | 9.598e+00 | 2.236e+03 | 1.532e+03 | 2.710e+02 |
| 6 | 1.150e+01 | 2.171e+03 | 1.514e+03 | 2.647e+02 |
| 7 | 1.339e+01 | 2.115e+03 | 1.493e+03 | 2.589e+02 |
| 8 | 1.529e+01 | 2.052e+03 | 1.483e+03 | 2.531e+02 |
| 9 | 1.719e+01 | 1.996e+03 | 1.477e+03 | 2.483e+02 |
| 10 | 1.908e+01 | 1.942e+03 | 1.479e+03 | 2.441e+02 |
| 11 | 2.098e+01 | 1.871e+03 | 1.445e+03 | 2.364e+02 |
| 12 | 2.287e+01 | 1.813e+03 | 1.441e+03 | 2.316e+02 |
| 13 | 2.477e+01 | 1.765e+03 | 1.450e+03 | 2.284e+02 |
| 14 | 2.667e+01 | 1.715e+03 | 1.449e+03 | 2.245e+02 |
| 15 | 2.856e+01 | 1.666e+03 | 1.431e+03 | 2.196e+02 |
| 16 | 3.046e+01 | 1.619e+03 | 1.424e+03 | 2.156e+02 |
| 17 | 3.236e+01 | 1.567e+03 | 1.413e+03 | 2.110e+02 |
| 18 | 3.425e+01 | 1.524e+03 | 1.400e+03 | 2.069e+02 |
| 19 | 3.615e+01 | 1.487e+03 | 1.382e+03 | 2.030e+02 |
| 20 | 3.806e+01 | 1.442e+03 | 1.350e+03 | 1.975e+02 |

Table A3. Frequency Sweeps Of One Extruder Pass Blend Of 60% & 80% HBA/PET AT T = 300°C
(cone & plate geometry, strain = 10%, frequency = 10 rad/sec)

| NO. | FREQ rad/s | G' Pa | G'' Pa | ETA* Pa.s |
|-----|---------------|-----------|-----------|--------------|
| 1 | 1.000e-01 | 4.242e+02 | 5.593e+02 | 7.020e+03 |
| 2 | 1.778e-01 | 5.095e+02 | 5.552e+02 | 4.237e+03 |
| 3 | 3.162e-01 | 6.210e+02 | 5.929e+02 | 2.715e+03 |
| 4 | 5.623e-01 | 7.591e+02 | 6.636e+02 | 1.793e+03 |
| 5 | 1.000e+00 | 9.239e+02 | 7.549e+02 | 1.193e+03 |
| 6 | 1.778e+00 | 1.120e+03 | 8.690e+02 | 7.974e+02 |
| 7 | 3.162e+00 | 1.339e+03 | 1.022e+03 | 5.328e+02 |
| 8 | 5.623e+00 | 1.604e+03 | 1.204e+03 | 3.567e+02 |
| 9 | 9.999e+00 | 1.920e+03 | 1.440e+03 | 2.400e+02 |
| 10 | 1.778e+01 | 2.302e+03 | 1.747e+03 | 1.625e+02 |
| 11 | 3.162e+01 | 2.754e+03 | 2.144e+03 | 1.104e+02 |
| 12 | 5.623e+01 | 3.306e+03 | 2.693e+03 | 7.584e+01 |
| 13 | 1.000e+02 | 3.971e+03 | 3.432e+03 | 5.248e+01 |

| NO. | FREQ rad/s | G' Pa | G'' Pa | ETA* Pa.s |
|-----|---------------|-----------|-----------|--------------|
| 1 | 1.000e-01 | 4.669e+02 | 8.978e+02 | 1.012e+04 |
| 2 | 1.778e-01 | 3.767e+02 | 5.092e+02 | 3.562e+03 |
| 3 | 3.162e-01 | 6.151e+02 | 5.736e+02 | 2.659e+03 |
| 4 | 5.623e-01 | 6.728e+02 | 5.479e+02 | 1.543e+03 |
| 5 | 1.000e+00 | 8.185e+02 | 6.482e+02 | 1.044e+03 |
| 6 | 1.778e+00 | 9.327e+02 | 7.407e+02 | 6.698e+02 |
| 7 | 3.162e+00 | 1.113e+03 | 8.587e+02 | 4.445e+02 |
| 8 | 5.623e+00 | 1.332e+03 | 1.016e+03 | 2.979e+02 |
| 9 | 9.999e+00 | 1.579e+03 | 1.206e+03 | 1.987e+02 |
| 10 | 1.778e+01 | 1.882e+03 | 1.446e+03 | 1.335e+02 |
| 11 | 3.162e+01 | 2.236e+03 | 1.781e+03 | 9.040e+01 |
| 12 | 5.623e+01 | 2.658e+03 | 2.220e+03 | 6.159e+01 |
| 13 | 1.000e+02 | 3.166e+03 | 2.852e+03 | 4.261e+01 |

Table A4. Frequency Sweeps Of two Extruder Pass Blend Of 60% & 80% HBA/PET AT T = 300°C
(cone & plate geometry, strain = 10%, frequency = 10 rad/sec)

| NO. | FREQ rad/s | G' Pa | G'' Pa | ETA* Pa. s |
|-----|---------------|-----------|-----------|---------------|
| 1 | 1.000e-01 | 6.206e+02 | 1.155e+03 | 1.312e+04 |
| 2 | 1.778e-01 | 6.859e+02 | 1.047e+03 | 7.041e+03 |
| 3 | 3.162e-01 | 8.615e+02 | 1.204e+03 | 4.683e+03 |
| 4 | 5.623e-01 | 1.126e+03 | 1.391e+03 | 3.182e+03 |
| 5 | 1.000e+00 | 1.420e+03 | 1.565e+03 | 2.113e+03 |
| 6 | 1.778e+00 | 1.753e+03 | 1.701e+03 | 1.374e+03 |
| 7 | 3.162e+00 | 2.122e+03 | 1.815e+03 | 8.831e+02 |
| 8 | 5.623e+00 | 2.526e+03 | 1.969e+03 | 5.696e+02 |
| 9 | 9.999e+00 | 2.941e+03 | 2.192e+03 | 3.668e+02 |
| 10 | 1.778e+01 | 3.367e+03 | 2.335e+03 | 2.304e+02 |
| 11 | 3.162e+01 | 3.809e+03 | 2.596e+03 | 1.458e+02 |
| 12 | 5.623e+01 | 4.344e+03 | 3.073e+03 | 9.464e+01 |
| 13 | 1.000e+02 | 4.962e+03 | 3.740e+03 | 6.213e+01 |

| NO. | FREQ rad/s | G' Pa | G'' Pa | ETA* Pa. s |
|-----|---------------|-----------|-----------|---------------|
| 1 | 1.000e-01 | 4.834e+02 | 7.773e+02 | 9.153e+03 |
| 2 | 1.778e-01 | 5.498e+02 | 7.462e+02 | 5.212e+03 |
| 3 | 3.162e-01 | 7.370e+02 | 8.980e+02 | 3.674e+03 |
| 4 | 5.623e-01 | 9.477e+02 | 1.040e+03 | 2.502e+03 |
| 5 | 1.000e+00 | 1.159e+03 | 1.187e+03 | 1.659e+03 |
| 6 | 1.778e+00 | 1.412e+03 | 1.312e+03 | 1.084e+03 |
| 7 | 3.162e+00 | 1.694e+03 | 1.434e+03 | 7.019e+02 |
| 8 | 5.623e+00 | 2.018e+03 | 1.594e+03 | 4.574e+02 |
| 9 | 9.999e+00 | 2.387e+03 | 1.779e+03 | 2.978e+02 |
| 10 | 1.778e+01 | 2.736e+03 | 2.268e+03 | 1.999e+02 |
| 11 | 3.162e+01 | 3.126e+03 | 2.557e+03 | 1.277e+02 |
| 12 | 5.623e+01 | 3.545e+03 | 2.850e+03 | 8.090e+01 |
| 13 | 1.000e+02 | 3.972e+03 | 3.335e+03 | 5.187e+01 |

Table A5. Frequency Sweeps Of Three Extruder Pass Blend Of 60% & 80% HBA/PET AT T = 300°C
(cone & plate geometry, strain = 10%, frequency = 10 rad/sec)

| NO. | FREQ rad/s | G' Pa | G'' Pa | ETA* Pa.s |
|-----|---------------|-----------|-----------|--------------|
| 1 | 1.000e-01 | 9.668e+02 | 1.354e+03 | 1.664e+04 |
| 2 | 1.778e-01 | 1.203e+03 | 1.397e+03 | 1.037e+04 |
| 3 | 3.162e-01 | 1.309e+03 | 1.453e+03 | 6.183e+03 |
| 4 | 5.623e-01 | 1.461e+03 | 1.542e+03 | 3.777e+03 |
| 5 | 1.000e+00 | 1.647e+03 | 1.659e+03 | 2.338e+03 |
| 6 | 1.778e+00 | 1.866e+03 | 1.815e+03 | 1.464e+03 |
| 7 | 3.162e+00 | 2.132e+03 | 2.098e+03 | 9.460e+02 |
| 8 | 5.623e+00 | 2.516e+03 | 2.484e+03 | 6.288e+02 |
| 9 | 9.999e+00 | 2.993e+03 | 2.931e+03 | 4.189e+02 |
| 10 | 1.778e+01 | 3.558e+03 | 3.308e+03 | 2.732e+02 |
| 11 | 3.162e+01 | 4.189e+03 | 3.748e+03 | 1.778e+02 |
| 12 | 5.623e+01 | 4.819e+03 | 4.165e+03 | 1.133e+02 |
| 13 | 1.000e+02 | 5.387e+03 | 4.747e+03 | 7.180e+01 |

| NO. | FREQ rad/s | G' Pa | G'' Pa | ETA* Pa.s |
|-----|---------------|-----------|-----------|--------------|
| 1 | 1.000e-01 | 1.132e+03 | 2.126e+03 | 2.408e+04 |
| 2 | 1.778e-01 | 1.366e+03 | 1.977e+03 | 1.351e+04 |
| 3 | 3.162e-01 | 1.544e+03 | 2.149e+03 | 8.369e+03 |
| 4 | 5.623e-01 | 1.791e+03 | 2.472e+03 | 5.429e+03 |
| 5 | 1.000e+00 | 2.129e+03 | 2.822e+03 | 3.536e+03 |
| 6 | 1.778e+00 | 2.514e+03 | 3.211e+03 | 2.293e+03 |
| 7 | 3.162e+00 | 2.974e+03 | 3.729e+03 | 1.508e+03 |
| 8 | 5.623e+00 | 3.405e+03 | 4.082e+03 | 9.452e+02 |
| 9 | 9.999e+00 | 3.797e+03 | 4.380e+03 | 5.798e+02 |
| 10 | 1.778e+01 | 4.232e+03 | 4.693e+03 | 3.554e+02 |
| 11 | 3.162e+01 | 4.700e+03 | 5.012e+03 | 2.173e+02 |
| 12 | 5.623e+01 | 5.258e+03 | 5.537e+03 | 1.358e+02 |
| 13 | 1.000e+02 | 5.789e+03 | 6.263e+03 | 8.528e+01 |

Table A6. Frequency Sweeps Of Four Extruder Pass Blend Of 60% & 80% HBA/PET AT T = 300°C
(cone & plate geometry, strain = 10%, frequency = 10 rad/sec)

| NO. | FREQ rad/s | G' Pa | G'' Pa | ETA* Pa. s |
|-----|---------------|-----------|-----------|---------------|
| 1 | 1.000e-01 | 1.593e+03 | 2.860e+03 | 3.274e+04 |
| 2 | 1.778e-01 | 1.602e+03 | 2.367e+03 | 1.607e+04 |
| 3 | 3.162e-01 | 1.682e+03 | 2.248e+03 | 8.879e+03 |
| 4 | 5.623e-01 | 1.816e+03 | 2.325e+03 | 5.246e+03 |
| 5 | 1.000e+00 | 1.985e+03 | 2.414e+03 | 3.125e+03 |
| 6 | 1.778e+00 | 2.234e+03 | 2.696e+03 | 1.969e+03 |
| 7 | 3.162e+00 | 2.564e+03 | 3.021e+03 | 1.253e+03 |
| 8 | 5.623e+00 | 2.944e+03 | 3.225e+03 | 7.766e+02 |
| 9 | 9.999e+00 | 3.265e+03 | 3.278e+03 | 4.627e+02 |
| 10 | 1.778e+01 | 3.621e+03 | 3.363e+03 | 2.779e+02 |
| 11 | 3.162e+01 | 4.086e+03 | 3.653e+03 | 1.733e+02 |
| 12 | 5.623e+01 | 4.619e+03 | 4.135e+03 | 1.103e+02 |
| 13 | 1.000e+02 | 5.160e+03 | 4.725e+03 | 6.996e+01 |

| NO. | FREQ rad/s | G' Pa | G'' Pa | ETA* Pa. s |
|-----|---------------|-----------|-----------|---------------|
| 1 | 1.000e-01 | 1.015e+03 | 2.043e+03 | 2.282e+04 |
| 2 | 1.778e-01 | 1.288e+03 | 2.465e+03 | 1.564e+04 |
| 3 | 3.162e-01 | 1.617e+03 | 2.945e+03 | 1.063e+04 |
| 4 | 5.623e-01 | 1.921e+03 | 3.451e+03 | 7.023e+03 |
| 5 | 1.000e+00 | 2.293e+03 | 4.039e+03 | 4.644e+03 |
| 6 | 1.778e+00 | 2.798e+03 | 4.554e+03 | 3.006e+03 |
| 7 | 3.162e+00 | 3.269e+03 | 4.771e+03 | 1.829e+03 |
| 8 | 5.623e+00 | 3.624e+03 | 4.843e+03 | 1.076e+03 |
| 9 | 9.999e+00 | 4.062e+03 | 5.072e+03 | 6.499e+02 |
| 10 | 1.778e+01 | 4.520e+03 | 5.294e+03 | 3.915e+02 |
| 11 | 3.162e+01 | 5.021e+03 | 5.612e+03 | 2.381e+02 |
| 12 | 5.623e+01 | 5.588e+03 | 6.152e+03 | 1.478e+02 |
| 13 | 1.000e+02 | 6.130e+03 | 6.772e+03 | 9.134e+01 |

Table A7. Frequency Sweeps Of 70/30 PHB/PET AT T = 300°C (cone & plate geometry, strain = 10%, frequency = 10 rad/sec)

| NO. | FREQ rad/s | G' Pa | G'' Pa | ETA* Pa.s |
|-----|---------------|-----------|-----------|--------------|
| 1 | 1.000e-01 | 2.099e+01 | 9.214e+01 | 9.450e+02 |
| 2 | 1.778e-01 | 3.668e+01 | 1.071e+02 | 6.368e+02 |
| 3 | 3.162e-01 | 6.697e+01 | 1.442e+02 | 5.027e+02 |
| 4 | 5.623e-01 | 9.335e+01 | 1.910e+02 | 3.780e+02 |
| 5 | 1.000e+00 | 1.243e+02 | 2.373e+02 | 2.679e+02 |
| 6 | 1.778e+00 | 1.565e+02 | 2.902e+02 | 1.854e+02 |
| 7 | 3.162e+00 | 2.114e+02 | 3.885e+02 | 1.399e+02 |
| 8 | 5.623e+00 | 3.242e+02 | 5.767e+02 | 1.176e+02 |
| 9 | 9.999e+00 | 4.703e+02 | 8.448e+02 | 9.670e+01 |
| 10 | 1.778e+01 | 6.436e+02 | 1.212e+03 | 7.715e+01 |
| 11 | 3.162e+01 | 8.093e+02 | 1.558e+03 | 5.553e+01 |
| 12 | 5.623e+01 | 9.833e+02 | 1.929e+03 | 3.851e+01 |
| 13 | 1.000e+02 | 1.124e+03 | 2.455e+03 | 2.700e+01 |

| NO. | FREQ rad/s | G' Pa | G'' Pa | ETA* Pa.s |
|-----|---------------|-----------|-----------|--------------|
| 1 | 1.000e-01 | 5.515e+01 | 1.694e+02 | 1.781e+03 |
| 2 | 1.778e-01 | 9.017e+01 | 2.488e+02 | 1.488e+03 |
| 3 | 3.162e-01 | 1.250e+02 | 3.114e+02 | 1.061e+03 |
| 4 | 5.623e-01 | 1.486e+02 | 3.577e+02 | 6.888e+02 |
| 5 | 1.000e+00 | 1.728e+02 | 4.247e+02 | 4.585e+02 |
| 6 | 1.778e+00 | 1.958e+02 | 4.764e+02 | 2.897e+02 |
| 7 | 3.162e+00 | 2.476e+02 | 5.850e+02 | 2.009e+02 |
| 8 | 5.623e+00 | 3.083e+02 | 7.228e+02 | 1.397e+02 |
| 9 | 9.999e+00 | 3.937e+02 | 8.746e+02 | 9.592e+01 |
| 10 | 1.778e+01 | 5.136e+02 | 1.097e+03 | 6.814e+01 |
| 11 | 3.162e+01 | 6.392e+02 | 1.354e+03 | 4.734e+01 |
| 12 | 5.623e+01 | 7.759e+02 | 1.667e+03 | 3.270e+01 |
| 13 | 1.000e+02 | 9.389e+02 | 2.164e+03 | 2.359e+01 |

Table A8. Frequency Sweeps Of One Extruder Pass Blend Of 60% & 80% HBA/PET AT T = 290°C
(cone & plate geometry, strain = 10%, frequency = 10 rad/sec)

| NO. | FREQ rad/s | G' Pa | G'' Pa | ETA* Pa. s |
|-----|---------------|-----------|-----------|---------------|
| 1 | 1.000e-01 | 1.735e+03 | 3.396e+03 | 3.814e+04 |
| 2 | 1.778e-01 | 1.863e+03 | 2.789e+03 | 1.886e+04 |
| 3 | 3.162e-01 | 2.007e+03 | 2.564e+03 | 1.030e+04 |
| 4 | 5.623e-01 | 2.242e+03 | 2.589e+03 | 6.090e+03 |
| 5 | 1.000e+00 | 2.506e+03 | 2.809e+03 | 3.764e+03 |
| 6 | 1.778e+00 | 2.911e+03 | 3.143e+03 | 2.409e+03 |
| 7 | 3.162e+00 | 3.511e+03 | 3.584e+03 | 1.587e+03 |
| 8 | 5.623e+00 | 4.298e+03 | 4.122e+03 | 1.059e+03 |
| 9 | 9.999e+00 | 5.269e+03 | 4.702e+03 | 7.062e+02 |
| 10 | 1.778e+01 | 6.404e+03 | 5.370e+03 | 4.700e+02 |
| 11 | 3.162e+01 | 7.710e+03 | 6.165e+03 | 3.122e+02 |
| 12 | 5.623e+01 | 9.231e+03 | 7.162e+03 | 2.078e+02 |
| 13 | 1.000e+02 | 1.093e+04 | 8.397e+03 | 1.378e+02 |

| NO. | FREQ rad/s | G' Pa | G'' Pa | ETA* Pa. s |
|-----|---------------|-----------|-----------|---------------|
| 1 | 1.000e-01 | 2.385e+02 | 2.731e+03 | 2.742e+04 |
| 2 | 1.778e-01 | 1.432e+03 | 2.846e+03 | 1.792e+04 |
| 3 | 3.162e-01 | 1.465e+03 | 2.359e+03 | 8.780e+03 |
| 4 | 5.623e-01 | 1.705e+03 | 2.658e+03 | 5.615e+03 |
| 5 | 1.000e+00 | 1.922e+03 | 3.052e+03 | 3.607e+03 |
| 6 | 1.778e+00 | 2.514e+03 | 3.402e+03 | 2.379e+03 |
| 7 | 3.162e+00 | 3.272e+03 | 3.861e+03 | 1.601e+03 |
| 8 | 5.623e+00 | 4.187e+03 | 4.348e+03 | 1.074e+03 |
| 9 | 9.999e+00 | 5.266e+03 | 4.864e+03 | 7.169e+02 |
| 10 | 1.778e+01 | 6.463e+03 | 5.404e+03 | 4.738e+02 |
| 11 | 3.162e+01 | 7.672e+03 | 6.052e+03 | 3.091e+02 |
| 12 | 5.623e+01 | 9.076e+03 | 6.969e+03 | 2.035e+02 |
| 13 | 1.000e+02 | 1.067e+04 | 8.180e+03 | 1.344e+02 |

Table A9. Frequency Sweeps Of Two Extruder Pass Blend Of 60% & 80% HBA/PET AT T = 290°C
(cone & plate geometry, strain = 10%, frequency = 10 rad/sec)

| NO. | FREQ rad/s | G' Pa | G'' Pa | ETA* Pa. s |
|-----|---------------|-----------|-----------|---------------|
| 1 | 1.000e-01 | 1.598e+03 | 3.542e+03 | 3.886e+04 |
| 2 | 1.778e-01 | 1.916e+03 | 3.079e+03 | 2.039e+04 |
| 3 | 3.162e-01 | 2.217e+03 | 2.958e+03 | 1.169e+04 |
| 4 | 5.623e-01 | 2.608e+03 | 3.142e+03 | 7.261e+03 |
| 5 | 1.000e+00 | 3.118e+03 | 3.420e+03 | 4.628e+03 |
| 6 | 1.778e+00 | 3.799e+03 | 3.795e+03 | 3.020e+03 |
| 7 | 3.162e+00 | 4.635e+03 | 4.190e+03 | 1.976e+03 |
| 8 | 5.623e+00 | 5.643e+03 | 4.540e+03 | 1.288e+03 |
| 9 | 9.999e+00 | 6.776e+03 | 4.846e+03 | 8.331e+02 |
| 10 | 1.778e+01 | 7.959e+03 | 5.163e+03 | 5.335e+02 |
| 11 | 3.162e+01 | 9.175e+03 | 5.557e+03 | 3.392e+02 |
| 12 | 5.623e+01 | 1.050e+04 | 6.117e+03 | 2.161e+02 |
| 13 | 1.000e+02 | 1.192e+04 | 6.817e+03 | 1.373e+02 |

| NO. | FREQ rad/s | G' Pa | G'' Pa | ETA* Pa. s |
|-----|---------------|-----------|-----------|---------------|
| 1 | 1.000e-01 | 2.007e+03 | 5.246e+03 | 5.617e+04 |
| 2 | 1.778e-01 | 2.241e+03 | 4.036e+03 | 2.596e+04 |
| 3 | 3.162e-01 | 2.403e+03 | 3.676e+03 | 1.389e+04 |
| 4 | 5.623e-01 | 2.792e+03 | 3.805e+03 | 8.392e+03 |
| 5 | 1.000e+00 | 3.331e+03 | 4.113e+03 | 5.293e+03 |
| 6 | 1.778e+00 | 4.052e+03 | 4.469e+03 | 3.392e+03 |
| 7 | 3.162e+00 | 4.911e+03 | 4.814e+03 | 2.175e+03 |
| 8 | 5.623e+00 | 5.835e+03 | 5.117e+03 | 1.380e+03 |
| 9 | 9.999e+00 | 6.792e+03 | 5.497e+03 | 8.738e+02 |
| 10 | 1.778e+01 | 7.819e+03 | 6.092e+03 | 5.575e+02 |
| 11 | 3.162e+01 | 9.024e+03 | 7.097e+03 | 3.631e+02 |
| 12 | 5.623e+01 | 1.063e+04 | 8.542e+03 | 2.425e+02 |
| 13 | 1.000e+02 | 1.262e+04 | 9.987e+03 | 1.609e+02 |

Table A10. Frequency Sweeps Of Three Extruder Pass Blend Of 60% & 80% HBA/PET AT T=290°C (cone & plate geometry, strain = 10%, frequency = 10 rad/sec)

| NO. | FREQ rad/s | G' Pa | G'' Pa | ETA* Pa.s |
|-----|---------------|-----------|-----------|--------------|
| 1 | 1.000e-01 | 1.552e+03 | 4.648e+03 | 4.900e+04 |
| 2 | 1.778e-01 | 2.006e+03 | 3.475e+03 | 2.256e+04 |
| 3 | 3.162e-01 | 1.934e+03 | 2.441e+03 | 9.848e+03 |
| 4 | 5.623e-01 | 2.009e+03 | 2.322e+03 | 5.461e+03 |
| 5 | 1.000e+00 | 2.426e+03 | 2.497e+03 | 3.482e+03 |
| 6 | 1.778e+00 | 2.802e+03 | 2.712e+03 | 2.193e+03 |
| 7 | 3.162e+00 | 3.446e+03 | 2.923e+03 | 1.429e+03 |
| 8 | 5.623e+00 | 4.130e+03 | 3.015e+03 | 9.094e+02 |
| 9 | 9.999e+00 | 4.816e+03 | 3.169e+03 | 5.765e+02 |
| 10 | 1.778e+01 | 5.516e+03 | 3.327e+03 | 3.623e+02 |
| 11 | 3.162e+01 | 6.237e+03 | 3.559e+03 | 2.271e+02 |
| 12 | 5.623e+01 | 7.082e+03 | 3.971e+03 | 1.444e+02 |
| 13 | 1.000e+02 | 8.027e+03 | 4.574e+03 | 9.239e+01 |

| NO. | FREQ rad/s | G' Pa | G'' Pa | ETA* Pa.s |
|-----|---------------|-----------|-----------|--------------|
| 1 | 1.000e-01 | 1.395e+03 | 2.553e+03 | 2.910e+04 |
| 2 | 1.778e-01 | 1.439e+03 | 1.781e+03 | 1.287e+04 |
| 3 | 3.162e-01 | 1.664e+03 | 1.682e+03 | 7.481e+03 |
| 4 | 5.623e-01 | 1.998e+03 | 1.729e+03 | 4.699e+03 |
| 5 | 1.000e+00 | 2.366e+03 | 1.829e+03 | 2.991e+03 |
| 6 | 1.778e+00 | 2.782e+03 | 1.967e+03 | 1.916e+03 |
| 7 | 3.162e+00 | 3.201e+03 | 2.158e+03 | 1.221e+03 |
| 8 | 5.623e+00 | 3.681e+03 | 2.425e+03 | 7.839e+02 |
| 9 | 9.999e+00 | 4.219e+03 | 2.762e+03 | 5.043e+02 |
| 10 | 1.778e+01 | 4.841e+03 | 3.138e+03 | 3.244e+02 |
| 11 | 3.162e+01 | 5.486e+03 | 3.568e+03 | 2.070e+02 |
| 12 | 5.623e+01 | 6.224e+03 | 4.117e+03 | 1.327e+02 |
| 13 | 1.000e+02 | 7.027e+03 | 4.785e+03 | 8.502e+01 |

Table A11. Frequency Sweeps Of Four Extruder Pass Blend Of 60% & 80% HBA/PET AT T = 290°C
(cone & plate geometry, strain = 10%, frequency = 10 rad/sec)

| NO. | FREQ rad/s | G' Pa | G'' Pa | ETA* Pa.s |
|-----|---------------|-----------|-----------|--------------|
| 1 | 1.000e-01 | 1.748e+03 | 2.343e+03 | 2.923e+04 |
| 2 | 1.778e-01 | 1.780e+03 | 1.966e+03 | 1.492e+04 |
| 3 | 3.162e-01 | 2.006e+03 | 1.958e+03 | 8.865e+03 |
| 4 | 5.623e-01 | 2.345e+03 | 2.069e+03 | 5.561e+03 |
| 5 | 1.000e+00 | 2.727e+03 | 2.221e+03 | 3.517e+03 |
| 6 | 1.778e+00 | 3.184e+03 | 2.392e+03 | 2.239e+03 |
| 7 | 3.162e+00 | 3.680e+03 | 2.608e+03 | 1.426e+03 |
| 8 | 5.623e+00 | 4.253e+03 | 2.869e+03 | 9.123e+02 |
| 9 | 9.999e+00 | 4.899e+03 | 3.201e+03 | 5.852e+02 |
| 10 | 1.778e+01 | 5.608e+03 | 3.575e+03 | 3.740e+02 |
| 11 | 3.162e+01 | 6.378e+03 | 4.019e+03 | 2.384e+02 |
| 12 | 5.623e+01 | 7.249e+03 | 4.571e+03 | 1.524e+02 |
| 13 | 1.000e+02 | 8.191e+03 | 5.266e+03 | 9.738e+01 |

| NO. | FREQ rad/s | G' Pa | G'' Pa | ETA* Pa.s |
|-----|---------------|-----------|-----------|--------------|
| 1 | 1.000e-01 | 1.575e+03 | 3.138e+03 | 3.511e+04 |
| 2 | 1.778e-01 | 1.757e+03 | 2.137e+03 | 1.556e+04 |
| 3 | 3.162e-01 | 1.907e+03 | 1.886e+03 | 8.481e+03 |
| 4 | 5.623e-01 | 2.196e+03 | 1.878e+03 | 5.138e+03 |
| 5 | 1.000e+00 | 2.536e+03 | 1.949e+03 | 3.198e+03 |
| 6 | 1.778e+00 | 2.922e+03 | 2.030e+03 | 2.001e+03 |
| 7 | 3.162e+00 | 3.340e+03 | 2.178e+03 | 1.261e+03 |
| 8 | 5.623e+00 | 3.797e+03 | 2.397e+03 | 7.985e+02 |
| 9 | 9.999e+00 | 4.311e+03 | 2.708e+03 | 5.091e+02 |
| 10 | 1.778e+01 | 4.882e+03 | 3.105e+03 | 3.254e+02 |
| 11 | 3.162e+01 | 5.551e+03 | 3.540e+03 | 2.082e+02 |
| 12 | 5.623e+01 | 6.278e+03 | 4.054e+03 | 1.329e+02 |
| 13 | 1.000e+02 | 7.042e+03 | 4.672e+03 | 8.451e+01 |

Table A12. Frequency Sweeps Of 70/30 PHB/PET AT T = 290°C (cone & plate geometry, strain = 10%, frequency = 10 rad/sec)

| NO. | FREQ rad/s | G' Pa | G'' Pa | ETA* Pa.s |
|-----|---------------|-----------|-----------|--------------|
| 1 | 1.000e-01 | 6.974e+02 | 9.994e+02 | 1.219e+04 |
| 2 | 1.778e-01 | 8.006e+02 | 1.084e+03 | 7.578e+03 |
| 3 | 3.162e-01 | 8.477e+02 | 1.091e+03 | 4.369e+03 |
| 4 | 5.623e-01 | 8.804e+02 | 1.131e+03 | 2.549e+03 |
| 5 | 1.000e+00 | 9.361e+02 | 1.243e+03 | 1.556e+03 |
| 6 | 1.778e+00 | 9.976e+02 | 1.400e+03 | 9.667e+02 |
| 7 | 3.162e+00 | 1.132e+03 | 1.671e+03 | 6.382e+02 |
| 8 | 5.623e+00 | 1.356e+03 | 1.964e+03 | 4.245e+02 |
| 9 | 9.999e+00 | 1.591e+03 | 2.226e+03 | 2.736e+02 |
| 10 | 1.778e+01 | 1.835e+03 | 2.456e+03 | 1.724e+02 |
| 11 | 3.162e+01 | 2.051e+03 | 2.671e+03 | 1.065e+02 |
| 12 | 5.623e+01 | 2.215e+03 | 2.965e+03 | 6.582e+01 |
| 13 | 1.000e+02 | 2.263e+03 | 3.327e+03 | 4.024e+01 |

| NO. | FREQ rad/s | G' Pa | G'' Pa | ETA* Pa.s |
|-----|---------------|-----------|-----------|--------------|
| 1 | 1.000e-01 | 6.265e+02 | 1.327e+03 | 1.468e+04 |
| 2 | 1.778e-01 | 9.073e+02 | 1.928e+03 | 1.198e+04 |
| 3 | 3.162e-01 | 1.044e+03 | 2.300e+03 | 7.988e+03 |
| 4 | 5.623e-01 | 1.216e+03 | 2.583e+03 | 5.077e+03 |
| 5 | 1.000e+00 | 1.407e+03 | 2.941e+03 | 3.261e+03 |
| 6 | 1.778e+00 | 1.654e+03 | 3.309e+03 | 2.080e+03 |
| 7 | 3.162e+00 | 1.823e+03 | 3.412e+03 | 1.223e+03 |
| 8 | 5.623e+00 | 1.886e+03 | 3.421e+03 | 6.948e+02 |
| 9 | 9.999e+00 | 2.013e+03 | 3.509e+03 | 4.046e+02 |
| 10 | 1.778e+01 | 2.216e+03 | 3.679e+03 | 2.415e+02 |
| 11 | 3.162e+01 | 2.432e+03 | 3.928e+03 | 1.461e+02 |
| 12 | 5.623e+01 | 2.706e+03 | 4.380e+03 | 9.157e+01 |
| 13 | 1.000e+02 | 2.874e+03 | 4.928e+03 | 5.705e+01 |

Appendix B. Source listing of the Fortran Program

Table B1. Source listing of a Fortran program which calculates the tensile properties from the raw Instron data

```

sdebug
c      This program needs the following input parameters
c      name - any identification number
c      temp - any identification number (temperature of injection-molding)
c      mw - maximum load in kgs.
c      x and y - coordinates of any point in the linear region
c      of the curve (both x and y in cms.)
c      cd - chart displacement at the maximum stress point
c      l - gauge length
c      The output contains the following information:
c      The tensile strength (MPa), modulus (MPa) and elongation(%)
c      preceded by the two identifications - name and temp.
c      Also it outputs the standard deviation for each of these parameters:
c      (ref. ASTM D 638M).
c      This program has the limitation that exactly five values
c      must be input for each parameters
      program instron
      integer temp,i
      real t,mw,x,y,cd,l,mts,stp,ym,a1,a2,a3,sq1,
+      sq2,av1,av2,av3,s1,s2,s3,sqrt,a,b,c
      real*8 z
      character *3 name
      open (9,file='pl.dat',status='old')
      open (10,file='pl.rst',status='new')
      write (10,90)
90     format('1',6x,'RESULTS')
      i=0
13     a1=0.0
          a2=0.0
          a3=0.0
          sq1=0.0
          sq2=0.0
          sq3=0.0
95     read(9,100,end=999)name,temp,t,mw,x,y,cd,l
100    format(a3,i3,5f4.1,f4.2)
      i=i+1
      mts = (154.43 * mw)/t
      a1 = a1 + mts
      sq1= sq1 + mts**2
      stp =(0.5*cd)/l
      a2 = a2 + stp
      sq2 =sq2 + stp**2
      ym =(30886 *x*l)/(y*t)
      a3 = a3 + ym
      z=ym**2
      sq3= sq3 +z
      if(i.eq.5)then
          av1=(0.2 * a1)
          av2=(0.2 * a2)
          av3=(0.2*a3)
          a=(sq1-5.0*av1**2)/4.0
          if(a.lt.0.0)a=a*(-1)
          s1=sqrt(a)
          b=(sq2-5.0*av2**2)/4.0
          if(b.lt.0.0)b=b*(-1)
          s2=sqrt(b)
          c=(sq3-5.0*av3**2)/4.0
          if(c.lt.0.0)c=c*(-1)
          s3=sqrt(c)
          i=0
          write(10,400) temp,name
400    format('0','temperature = ',i3,5x,a3)
          write(10,500)av1,s1,av2,s2,av3,s3
500    format(1x,f7.3,2x,f5.2,3x,f5.2,2x,f5.2,5x,f9.3,2x,f8.2)
          go to 13
      else
          go to 95
      endif
999    stop
      end

```

**The vita has been removed from
the scanned document**